



Biochemical and pharmacological
modulation of scarring, axon regeneration
and long-term functional improvement
after spinal cord injury in rat

Inaugural-Dissertation

zur Erlangung des Doktorgrades
der Mathematisch-Naturwissenschaftlichen Fakultät
der Heinrich-Heine-Universität Düsseldorf

vorgelegt von

Brigitte König
aus Rottweil

Düsseldorf, Juli 2014

aus dem Labor für Molekulare Neurobiologie der Neurologischen Klinik
der Heinrich-Heine Universität Düsseldorf

Gedruckt mit der Genehmigung
der Mathematisch-Naturwissenschaftlichen Fakultät der
Heinrich-Heine Universität Düsseldorf

Referent: Prof. Dr. Hans Werner Müller
Korreferent: Prof. Dr. Christine Rose

Tag der mündlichen Prüfung: 23.09.2014

To my family.

Table of contents

SUMMARY	8
ZUSAMMENFASSUNG	10
1 INTRODUCTION	12
1.1 Pathophysiology of spinal cord injury	12
1.2 Neural response to injury	13
1.3 The lesion scar.....	14
1.3.1 Characteristics of the glial scar.....	15
1.3.2 Characteristics of the fibrous scar	16
1.4 Experimental strategies for spinal cord repair after injury	17
1.4.1 Suppression of the collagenous scar using iron chelators	19
1.4.1.1 Deferoxamine mesylate (DFO).....	21
1.4.2 Stimulation of axonal sprouting	23
1.4.2.1 Stromal cell-derived factor 1 (SDF-1).....	24
1.5 Recovery of locomotion – an important factor for evaluating treatment efficacy.....	25
1.5.1 Topographical organisation of the rat spinal cord	26
1.5.2 Role of CST and RST in motor control	28
1.5.3 Behavioural testing of spinal cord injured rats	29
1.6 Aim of this thesis	30
2 MATERIALS AND METHODS	32
2.1 Buffers, solutions and antibodies.....	32
2.1.1 Buffers and solutions.....	32
2.1.2 Antibodies	33
2.1.2.1 Primary antibodies	33
2.1.2.2 Secondary antibodies.....	33
2.1.3 Tracer substances and reagents	33
2.2 Animals	34
2.3 Surgical procedures	35

2.3.1	Filling and priming of osmotic minipumps	35
2.3.2	Dorsal hemisection.....	35
2.3.3	Intrathecal catheter application.....	36
2.3.4	Testing of catheter functionality over time (<i>in vivo</i>)	37
2.3.4.1	Catheter fixation	37
2.3.4.2	Analysis of catheter-induced compression	37
2.3.4.3	Testing of catheter patency	37
2.3.5	Anterograde labelling of corticospinal tract axons.....	38
2.3.6	Anterograde labelling of sciatic afferents.....	39
2.3.7	Post-operative care	40
2.3.8	Animal sacrifice.....	40
2.4	Tissue preparation	40
2.4.1	Freezing-Microtome sections	40
2.4.2	Paraffin sections.....	40
2.4.3	Gelatine sections.....	41
2.5	Histological staining protocols	41
2.5.1	Masson trichrome staining (without nucleus labelling).....	41
2.5.2	Immunohistochemical staining of Coll IV / vWF	42
2.5.3	Immunohistochemical staining of axons	42
2.6	Analysis of tissue sections.....	43
2.6.1	Coll IV quantification in the scar	43
2.6.1.1	Manual removal of blood vessels from Coll IV images	43
2.6.1.2	vWF pixel subtraction.....	44
2.6.2	Analysis of blood vessel density in the Coll IV positive scar area	46
2.6.3	Evaluation of lesion depth, lesion area and tissue sparing	46
2.6.4	Axon quantification.....	46
2.7	Behavioural testing.....	47
2.7.1	Open field Basso, Beattie and Bresnahan (BBB) locomotor test	47
2.7.2	Horizontal ladder walking test (Gridwalk).....	48

2.7.3	CatWalk gait analysis	48
2.8	Statistics.....	50
3	RESULTS	51
3.1	Intrathecal catheter infusion	51
3.1.1	Catheter fixation and compression	51
3.1.2	Catheter patency.....	53
3.2	Coll IV reduction in the scar using iron chelators	53
3.2.1	Coll IV quantification method.....	54
3.2.2	Coll IV reduction via BPY-DCA infusion	55
3.2.3	Coll IV reduction via BPY infusion	56
3.2.4	Coll IV reduction via DFO infusion or systemic application	57
3.3	Effect of DFO on blood vessel density.....	59
3.4	Analysis of functional recovery after DFO intrathecal infusion	60
3.4.1	Autotomy.....	61
3.4.2	Horizontal ladder walking test (Gridwalk).....	61
3.4.3	CatWalk gait analysis	63
3.4.4	Open field BBB locomotor scoring.....	66
3.5	Tissue sparing.....	68
3.6	Axonal regeneration into the lesion area and beyond	69
3.6.1	Quantitative analysis of CGRP-positive axons.....	70
3.6.2	Quantitative analysis of CTB-traced axons.....	70
3.6.3	Quantitative analysis of BDA-traced CST axons.....	71
4	DISCUSSION.....	73
4.1	Intrathecal infusion in a rat spinal cord injury model	73
4.2	Intrathecally infused iron chelators reduce collagenous lesion scarring	74
4.2.1	BPY-DCA (2,2'-bipyridine-5,5'-dicarboxylic acid)	74
4.2.2	BPY (2,2'-bipyridine)	76
4.2.3	DFO (deferrioxamine mesylate)	78
4.3	DFO enhances blood vessel density in the scar area	80

4.4	Effect of DFO on functional recovery and its synergy with SDF-1 α	81
4.4.1	A 2-week intrathecal DFO infusion temporarily and marginally improves functional outcome	82
4.4.2	Synergistic effect of DFO+SDF-1 α enables long-term regeneration of precise limb control (horizontal ladder)	83
4.4.3	A 2-week intrathecal infusion of SDF-1 α induces moderate unilateral improvements in precise limb control	84
4.4.4	BSA treatment promotes long-lasting functional recovery	85
4.5	Tissue preservation as a possible reason for functional recovery	87
4.6	Observed functional recovery is associated with modest axon regeneration	89
4.7	Concluding remarks and further considerations.....	90
5	REFERENCES.....	93
6	ABBREVIATIONS.....	115
7	DANKSAGUNG	118

Summary

Traumatic injuries of the spinal cord result in the formation of a collagenous fibrous scar in the lesion centre. Characterised by a dense extracellular matrix network, which accumulates a variety of growth-inhibitory molecules, the fibrous scar is regarded as a barrier for regenerating axons. Previously, our group has developed an anti-scarring treatment (AST), consisting of the injection of the iron chelator 2,2'-bipyridine-5,5'-dicarboxylic acid (BPY-DCA) to inhibit the enzyme prolyl-4-hydroxylase and 8-bromoadenosine 3',5'-cyclic monophosphate (8-Br-cAMP) to inhibit CTGF expression into the injured spinal cord. AST transiently suppressed fibrous scar formation and promoted axonal regeneration through the lesion site as well as partial improvements of motor functions. Despite these promising results, a medical application in humans is very unlikely due to the chelator-solvent Tris and the method of application, which includes injections into the intact spinal cord. In this study, the injection protocol has been replaced by intrathecal catheter infusion, which is widely accepted in clinical use, and which has been connected to an osmotic minipump, that allows continuous drug infusion. Due to the very narrow subdural and subarachnoid space in rats, chronic intrathecal tubing is often discussed to induce extensive scarring and compressions in the rat spinal cord. In this work, an intrathecal catheter application method is presented that allows unrestricted intrathecal drug infusion over a period of at least two weeks without provoking further damage to the spinal cord. In comparison to BPY-DCA, the potency of the iron chelators 2,2'-bipyridine (BPY) and deferoxamine mesylate (DFO) to reduce collagenous scarring was investigated after a dorsal hemisection at thoracic level Th8. The quantification of the Coll IV pixel percentage in the scar area revealed that all three iron chelators, intrathecally infused for 7 days, were able to reduce collagenous scarring significantly. In previous studies addressing the local AST injection, however, a combination with 8-Br-cAMP was indispensable for effective collagen reduction. Since DFO shows a higher potential in reducing the collagenous scar than BPY and has additionally the advantage of being an approved drug, DFO has been selected for further studies. Moreover, DFO can also be applied systemically. A comparison between intrathecal DFO infusion and daily systemic (i.p.) DFO injections for 14 days showed that systemically applied DFO was just as effective in reducing collagenous scarring as intrathecally infused DFO. Further, the quantitative analysis of the blood vessel density in the scar area confirmed DFO's potential to promote angiogenesis. However, the investigation of functional regeneration over a period of 16 weeks revealed that a 2-week intrathecal infusion of DFO in spinal cord injured rats is ineffective to induce long-lasting functional recovery. As moderate functional improvements were seen in the early phase of behavioural testing, it indicates that DFO has regenerative

potential but probably longer treatment periods are necessary to promote long-lasting functional recovery. Furthermore, there was no evidence of axonal regeneration through the lesion site. Only a trend towards reduced lesion size and improved tissue preservation has been found in DFO-treated animals. Due to the generally limited axon regeneration in the adult CNS, DFO was combined in an additional group with the chemokine stromal cell-derived factor 1 α (SDF-1 α /CXCL12), which is known to stimulate axonal sprouting. In contrast to the modest effect of DFO or SDF alone on locomotor recovery, simultaneous treatment with DFO and SDF-1 α induced significant long-term regeneration of skilled walking. Normal overground locomotion evaluated by gait analysis was, however, not improved by the treatment. In addition, histological analyses revealed that DFO+SDF-1 α improves neither tissue protection nor regeneration of CST axons, but it enhanced axon densities of ascending sensory fibres in the lesion scar, which may have contributed to the observed functional improvements. The most surprising finding of this study was that BSA, which was included as vehicle control for SDF-1 α , seems to have a more potent effect on functional recovery than DFO and SDF-1 α together. In all functional analyses (except BBB), BSA treatment resulted in the largest functional recovery, which was already evident from the very first moment of post-injury testing. An early onset of functional recovery is indicative for a neuroprotective function of BSA, which was supported by significantly reduced lesion areas and a tendency towards better tissue preservation in BSA-treated animals. Furthermore, the histological investigation of different fibre populations showed that BSA treatment enhanced only axon ingrowth of sensory sciatic afferents into the lesion scar.

In summary, the present thesis identifies two functionally effective treatment approaches for acute spinal cord injury. Based on the existing data, BSA treatment seems to be more promising than DFO+SDF-1 α . However, the results also indicate, that the best treatment condition of DFO and SDF-1 α has not been reached. Further investigations on dosage and treatment duration will clarify whether the observed functional recovery can still be improved. Furthermore, the aspect of spinal plasticity should be addressed in future studies to examine the contribution of axonal sprouting in the observed functional recovery.

Zusammenfassung

Traumatische Verletzungen des Rückenmarks führen zur Ausbildung einer kollagenhaltigen fibrösen Narbe im Läsionszentrum. Diese Narbe zeichnet sich durch eine dichte Extrazellulärmatrix aus, die aufgrund der Akkumulation verschiedener wachstumshemmender Moleküle als Barriere für regenerierende Nervenfasern angesehen wird. In unserer Arbeitsgruppe wurde eine Therapie zur Unterdrückung dieser Narbenbildung (anti-scarring treatment, AST) bestehend aus dem Eisenchelator 2,2'-Bipyridin-5,5'-dicarbonsäure (BPY-DCA) zur Hemmung der Prolyl-4-Hydroxylase und 8-Brom-zyklisches Adenosin-Monophosphat (8-Br-cAMP) zur Hemmung der CTGF-Expression im verletzten Rückenmark entwickelt. Die lokalen Injektionen des ASTs ins verletzte Rückenmark bewirkten axonale Regeneration und partiell funktionelle Erholung. Trotz dieser vielversprechenden Ergebnisse ist eine medizinische Anwendung im Menschen aufgrund des Lösungsmittels (Tris) für den Eisenchelator und der Applikationsweise, die auch Injektionen ins intakte Rückenmark beinhaltet, sehr unwahrscheinlich. In der vorliegenden Arbeit wurde das Injektionsverfahren durch die klinisch weit verbreitete intrathekale Katheter-Infusion ersetzt. Aufgrund des sehr engen Subarachnoidalraumes in der Ratte wird bei einer langfristigen intrathekalen Katheterisierung oft eine starke Narbenbildung und Kompression des Rückenmarks beobachtet. Die vorliegende Arbeit, hingegen, beschreibt eine intrathekale Katheterapplikationsweise in Kombination mit einer osmotischen Minipumpe, die eine uneingeschränkte Wirkstoffapplikation über mindestens 2 Wochen ermöglicht ohne weitere Beeinträchtigungen des Rückenmarks hervorzurufen. Im Vergleich zu BPY-DCA wurde die Reduktionsstärke der Eisenchelatoren 2,2'-Bipyridin (BPY) und Deferoxaminmesilat (DFO) auf die kollagene Narbenbildung nach einer dorsalen thorakalen Hemisektion auf Höhe Th8 untersucht. Die Quantifizierung des Prozents an Coll IV positiven Pixeln im Narbenareal ergab, dass alle 3 Eisenchelatoren, die für 7 Tage intrathekal infundiert wurden, signifikant die kollagene Narbenbildung reduzierten. In den früheren AST-Injektionsstudien hingegen war eine zusätzliche Injektion von 8-Br-cAMP für eine effektive Kollagenreduktion unerlässlich. Da DFO insgesamt ein breiteres Kollagen-Reduktionspotential aufweist als BPY und zusätzlich den Status eines geprüften Medikaments hat, wurde für die weiteren Untersuchungen DFO ausgewählt. Darüber hinaus könnte DFO auch systemisch appliziert werden. Ein Vergleich zwischen intrathekal infundiertem und täglich systemisch (i.p.) appliziertem DFO über 14 Tage zeigte, dass systemisch verabreichtes DFO ebenso effektiv die Narbe reduzieren kann wie intrathekal infundiertes DFO. Ferner konnte durch die quantitative Auswertung der Blutgefäßdichte in der Narbe die Angiogenese fördernde Wirkung von DFO bestätigt werden. Die Untersuchung der funktionellen Regeneration im Offenfeld-Test (BBB), Gridwalk sowie im CatWalk über einen

Zeitraum von 16 Wochen offenbarte jedoch, dass eine 2-wöchige intrathekale DFO-Infusion nicht ausreichend ist, um eine langanhaltende funktionelle Erholung zu bewirken. Da allerdings in den ersten Wochen der Verhaltensanalysen funktionelle Verbesserungen in der feinmotorischen Lokomotion beobachtet werden konnten, scheint DFO ein gewisses regeneratives Potential zu besitzen, aber vermutlich sind längere Behandlungszeiträume notwendig um langanhaltende Regeneration auszulösen. Bei der histologischen Untersuchung wurde kein Unterschied bezüglich regenerierter Axone zwischen DFO und der Kontrollgruppe festgestellt. Lediglich ein Trend zu reduzierten Läsionsgrößen und verbessertem Gewebeerhalt war erkennbar. Aufgrund der generell nur begrenzt auftretenden axonalen Regeneration im adulten ZNS wurde zusätzlich eine Kombinationstherapie mit dem Chemokin Stromal Cell-Derived Factor 1 α (SDF-1 α /CXCL12), das axonales Aussprossen fördert, untersucht. Im Gegensatz zu den moderaten Einzelwirkungen induzierte die gleichzeitige Verabreichung von DFO und SDF-1 α signifikant langanhaltende Verbesserung feinmotorischer Bewegung. Die allgemeine Lokomotion und dessen Gangeigenschaften wurden jedoch durch die kombinatorische Behandlung nicht markant verbessert. Die histologischen Analysen ergaben weiterhin, dass DFO+SDF-1 α weder den Gewebeerhalt noch die Regeneration des für die Lokomotorik wichtigen Kortikospinaltraktes (CST) verbessert, allerdings erhöhte es die Axondichte von aufsteigenden sensorischen Fasern in der Läsionsnarbe. Dies könnte zu den beobachteten funktionellen Verbesserungen beigetragen haben. Das Überraschendste dieser Studie war allerdings, dass BSA, das als Vehikel-Kontrolle für SDF-1 α eingesetzt wurde, wirksamer die funktionelle Regeneration förderte als DFO und SDF-1 α zusammen. In allen funktionellen Analysen (Ausnahme BBB) hatte die BSA-Behandlung immer die stärkste funktionelle Erholung zur Folge und war bereits ab dem ersten Testzeitpunkt offensichtlich. Früh auftretende funktionelle Erholung ist ein Hinweis auf eine neuroprotektive Wirkung, die durch die signifikant reduzierte Läsionsgröße sowie tendenziell verbesserte Gewebeerhaltung bekräftigt wird. Bei der histologischen Untersuchung verschiedener Fasertrakte wurde festgestellt, dass lediglich sensorische Afferenzen des Ischiasnervs verstärkt in die Läsionsnarbe eingewachsen sind.

Zusammenfassend beschreibt diese Arbeit zwei funktionell wirksame Ansätze zur Behandlung von akuten Rückenmarksverletzungen. Basierend auf den vorliegenden Daten scheint eine Behandlungsstrategie mit BSA vielversprechender zu sein als mit DFO+SDF-1 α . Allerdings deuten die Ergebnisse ebenso an, dass das Optimum von DFO und SDF-1 α hier nicht erreicht wurde. Weitere Untersuchungen zu Dosierung und Behandlungszeitraum werden darüber Aufschluss geben können. Des Weiteren sollte in zukünftigen Studien beider Ansätze der Aspekt der spinalen Plastizität thematisiert werden, um Aufschluss über den zugrundeliegenden Mechanismus der beobachteten funktionellen Erholung zu erhalten.

1 Introduction

1.1 Pathophysiology of spinal cord injury

Traumatic spinal cord injury (SCI) causes immediate damage of nervous tissue leading to devastating motor, sensory and autonomic dysfunctions below the injury. At the beginning of the 20th century, a cervical spinal cord injury implied in 80 % of cases death within the first two weeks. It was the work by Sir Ludwig Guttmann starting in 1943 with the opening of the first spinal centre that led to a modern era of rehabilitation after spinal cord injury (Anderberg et al., 2007). Today, the life expectancy of spinal cord injured patients is close to uninjured people and the quality of life has substantially improved compared to earlier years, but by now there is no curative therapy available. For a long time, it was even believed that, in contrast to the peripheral nervous system (PNS), the central nervous system (CNS) is incapable of regeneration (Ramón y Cajal, 1928), which was refuted in 1981 by the work of David and Aguayo (David and Aguayo, 1981). They were the first who provided the proof that CNS axons have the intrinsic capacity to regenerate. Since then much effort is spend to understand the pathophysiological mechanisms ongoing after spinal cord injury and to identify potential therapy strategies.

The disruption of neuro-glial tissue and vasculature through the primary mechanical injury activates a complex set of pathophysiologic processes, leading to haemorrhage and edema, demyelination, axon swelling/degeneration, cell death of neurons and oligodendrocytes and scar formation (Tator, 1995; Dumont et al., 2001; Bareyre and Schwab, 2003; Kwon et al., 2004; Mann and Kwon, 2007). By this 'secondary injury', which takes place over a time course of minutes to weeks after injury (Tator, 1995; Bareyre and Schwab, 2003), adjacent healthy spinal cord tissue will be affected and further destruction of neuronal and glial cells will expand the lesion area. The mechanisms, which are thought to contribute to this secondary damage, are vascular alterations leading to haemorrhage and ischemia (Tator and Fehlings, 1991; Mautes et al., 2000; Oudega, 2012), excitotoxicity (mediated by glutamate and aspartate) and electrolyte imbalance (Choi, 1992; Stichel and Müller, 1998b; Li and Stys, 2000), oxidative stress (free radicals and lipid peroxidation) (Hall, 1989; Facchinetti et al., 1998; Lewén et al., 2000), inflammation (Jones et al., 2005) and necrotic and apoptotic cell death (Crowe et al., 1997; Beattie et al., 2000).

1.2 Neural response to injury

Although many CNS neurons can survive for years after axotomy (Dusart and Sotelo, 1994; Schwab and Bartholdi, 1996), they finally fail to regenerate beyond the lesion site in contrast to the axons of the PNS or the embryonic nervous system, where long-distance axon regeneration can occur. This contrary ability to regenerate is mainly based on several intrinsic and environmental differences. While axonal injury is leading in both, PNS and CNS, to Wallerian degeneration (Waller, 1850) in the distal axon stump, the responses are quite different (Fenrich and Gordon, 2004; Vargas and Barres, 2007; Huebner and Strittmatter, 2009). In the PNS, myelinating Schwann cells respond rapidly to axonal injury by dedifferentiation into a non-myelinating phenotype, breakdown of myelin sheaths, clearance of its debris and recruiting of haematogenous macrophages, which will phagocytose the complete myelin debris within two weeks (George and Griffin, 1994; Stoll and Müller, 1999; Fenrich and Gordon, 2004; Vargas and Barres, 2007; Bosse, 2012). In the CNS, however, myelin debris persists years after axon degeneration due to the reduced ability of oligodendrocytes and CNS microglia to phagocytose myelin debris (Becerra et al., 1995; Buss et al., 2004; Vargas and Barres, 2007). As oligodendrocytes expresses myelin-associated inhibitors including NogoA (Chen et al., 2000; GrandPre et al., 2000; Prinjha et al., 2000), myelin-associated glycoprotein (MAG) (McKerracher et al., 1994; Mukhopadhyay et al., 1994), oligodendrocyte-myelin glycoprotein (OMgp) (Wang et al., 2002), semaphorin 4D (Sema4D) (Moreau-Fauvarque et al., 2003) and ephrin B3 (Benson et al., 2005) as components of the CNS myelin, the failure to clear CNS myelin debris leads to a growth inhibitory environment for axons. The fast clearance of myelin debris in the PNS, however, enables a growth permissive area, which is supported by Schwann cell proliferation and their longitudinally alignment within the basal lamina tube to form the bands of Büngner (Büngner, 1891; Ramón y Cajal, 1928; Mumenthaler et al., 2003). These nerve guides support injured axons to regenerate from the proximal into the distal nerve stump. In the CNS, such a guiding for regenerating axons is missing, because oligodendrocytes fail to dedifferentiate into growth supportive cells and, in addition, proliferation of reactive astrocytes is promoted by the growth-inhibitory molecules of the CNS myelin leading to the creation of the glial scar (Fenrich and Gordon, 2004). In this scar, growth inhibitory molecules accumulate and form a physical and chemical barrier for regenerating axons. Furthermore, injured CNS axons do not upregulate regeneration associated genes (RAGs) to the same extent as it occurs in the PNS. Whereas e.g. c-Jun (Raivich et al., 2004), activating transcription factor-3 (ATF-3) (Seiffers et al., 2006), growth-associated protein-43 (GAP-43) and Cap-23 (Bomze et al., 2001) are upregulated after a peripheral axotomy, no activation of these genes is found in

the CNS (Rossi et al., 2001). Hence, the ability of CNS axons to regenerate remains limited even in the absence of growth inhibitors.

1.3 The lesion scar

The complex molecular and cellular interactions occurring after CNS damage, as described before, are leading to the formation of a lesion scar (Fawcett and Asher, 1999; Hermanns et al., 2001a; Silver and Miller, 2004; Kawano et al., 2012), which represents a general wound healing response after injury (Gurtner et al., 2008). This wound healing process (mainly based on reactive astrocytes) repairs the damaged blood-brain barrier and restricts further cellular degeneration by preventing an overwhelming inflammatory response (Bush et al., 1999; Faulkner et al., 2004), but simultaneously it acts as a physical and chemical barrier to regenerating axons (Afshari et al., 2009). Scar formation starts already within hours after CNS injury by infiltration of blood proteins such as thrombin (Nishino et al., 1993) and fibrinogen (Ryu et al., 2009; Schachtrup et al., 2010) through the disrupted blood-brain barrier and/or damaged blood vessels. Schachtrup et al. (2010) showed that fibrinogen induces reactive astrocytosis and deposition of inhibitory proteoglycans via the TGF- β /Smad signalling pathway. Additionally to the blood proteins, the lesion site is also invaded by hematogenous cells including macrophages, leukocytes and lymphocytes leading to activation of astrocytes, microglia and oligodendrocyte precursors through secretion of various cytokines and chemokines (Donnelly and Popovich, 2008). This gliotic response, predominantly of astrocytic structure, results in the formation of the glial scar (Fig. 1.1), which is located at the penumbra of the lesion and characterized by strong expression of the glial fibrillary acidic protein (GFAP) (Fawcett and Asher, 1999; Silver and Miller, 2004). The lesion centre – the fibrous scar (Fig. 1.1) – consists of a dense extracellular matrix (ECM) including collagen type IV (Coll IV), fibronectin and laminin and is formed by invading fibroblasts (Hermanns et al., 2001a; Brazda and Müller, 2009; Kawano et al., 2012). It is thought that these fibroblasts intrude mainly from the damaged meninges into the lesion site (Carbonell and Boya, 1988; Shearer and Fawcett, 2001), but a recently published paper by Soderblom et al. (2013) identified a perivascular origin as the main source. At the area where reactive astrocytes of the glial scar contact meningeal cells of the fibrotic scar, a glia limitans-like structure is formed as it exists in the uninjured CNS between the pia mater layer of the meninges and the cells of the CNS (Shearer and Fawcett, 2001).

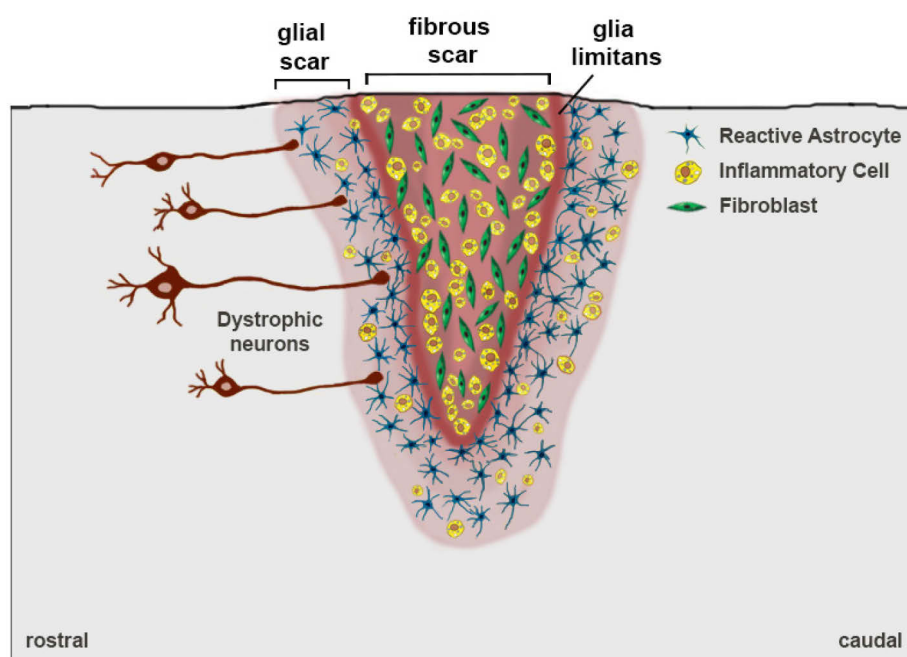


Fig. 1.1: Schematic representation of the lesion scar after spinal cord injury [based on Fitch and Silver (2008)]. A traumatic injury to the spinal cord induces the formation of a fibrous scar which consists of a dense extracellular matrix (ECM) network and invading cells such as fibroblasts (meningeal and perivascular) and inflammatory cells. The fibrous scar is surrounded mainly by reactive astrocytes forming the glial scar. At the contact area of reactive astrocytes and meningeal cells a dense glia limitans arises and together with the fibrotic scar it appears as a barrier to regenerating axons.

1.3.1 Characteristics of the glial scar

Glial scars consist mainly of reactive astrocytes, which are hallmarked by upregulation of intermediate filament proteins such as glial fibrillary acidic protein (GFAP) and vimentin (Silver and Miller, 2004; Pekny and Nilsson, 2005; Busch and Silver, 2007). Immediately after CNS injury, resident astrocytes become hypertrophic and form with their processes a tightly interwoven meshwork (Stichel and Müller, 1998a; Fawcett and Asher, 1999; Grimpe and Silver, 2002). The processes are attached to one another and to other cell types (oligodendrocytes, microglia, macrophages, meningeal cells and endothelial cells) by many tight and gap junctions (Fawcett and Asher, 1999; Klapka et al., 2002). The activation of astrocytes (as well oligodendrocyte precursors and microglia) leads to rapid upregulation of inhibitory extracellular matrix (ECM) molecules like, e.g., tenascin and proteoglycans (Fawcett and Asher, 1999; Silver and Miller, 2004; Yiu and He, 2006; Busch and Silver, 2007). Especially, chondroitin sulphate proteoglycans (CSPGs) have been shown to be the most important class of growth inhibitory molecules associated with CNS scar tissue (Fawcett and Asher, 1999; Morgenstern et al., 2002; Rolls et al., 2009; Leal-Filho, 2011). Although reactive astrocytes act as a potent physical and chemical barrier for regenerating

axons by releasing various inhibitory ECM molecules, reactive astrocytes are also important cells in the wound healing and blood-brain barrier repair response, in prevention of an overwhelming inflammatory response and in protection of neurons and oligodendrocytes (Bush et al., 1999; Faulkner et al., 2004). The fact that axons succeed in entering dense glial scar tissue (Stichel and Müller, 1994; Li and Raisman, 1995; Davies et al., 1999; Camand et al., 2004; Klapka et al., 2005) demonstrates that the glial scar is not an absolute barrier for regenerating axons. Additional to inhibitory ECM molecules, many growth promoting molecules such as laminin or fibronectin are also upregulated in the lesion scar (Condic and Lemons, 2002). Hence, the glial scar components promote and inhibit axonal regeneration at the same time (Fehlings and Hawryluk, 2010).

1.3.2 Characteristics of the fibrous scar

The fibrous scar located in the lesion core is characterised by a dense extracellular matrix (ECM) network (Stichel and Müller, 1998a; Klapka and Müller, 2006; Brazda and Müller, 2009) resembling the molecular structure of a basement membrane (Fig. 1.2) (Yurchenco and Schittny, 1990; Timpl and Brown, 1996; Hermanns et al., 2006). The backbone of the fibrous scar tissue is mainly built by Coll IV which assembles to a sheet-like network (Yurchenco and Schittny, 1990; Timpl and Brown, 1996) and is synthesized by different cell types of the CNS such as meningeal fibroblasts (Berry et al., 1983), astrocytes (Liesi and Kauppila, 2002) and endothelial cells (Schwab et al., 2001). The formation of the collagenous scar starts within 4-5 days and is immunohistochemically well detectable at 7 days post lesion (Hermanns et al., 2001a). A second network in the basement membrane is formed by laminin and is linked to the Coll IV network via nidogen/entactin (Berry et al., 1983; Stichel and Müller, 1998a; Klapka and Müller, 2006). Coll IV is not per se inhibitory to axonal outgrowth (Tonge et al., 1997), but the variety of anchored inhibitory molecules, e.g. CSPGs, tenascin, semaphorins (Condic and Lemons, 2002), creates a barrier for regenerating axons (Hermanns et al., 2006; Klapka and Müller, 2006; Brazda and Müller, 2009). Hence, Coll IV serves as an adhesive scaffold for the accumulation of numerous ECM components and growth-inhibitory molecules with the aim to seal off the lesion site (Klapka and Müller, 2006).

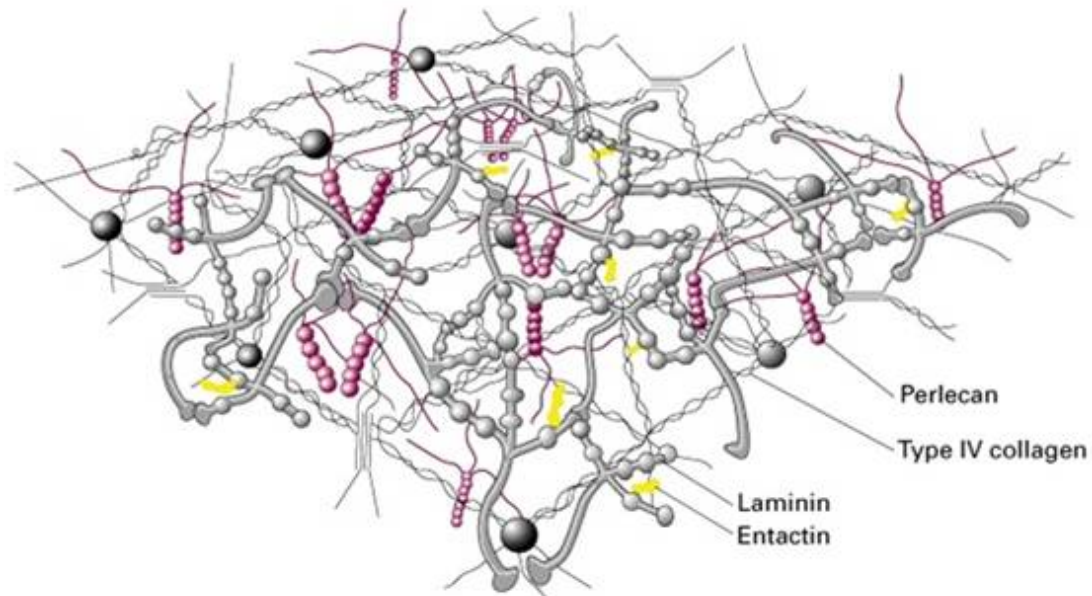


Fig. 1.2: Schematic illustration of a basement membrane. The sheet-like network of Coll IV connected via entactin/nidogen to the laminin network forms the structural backbone of a basement membrane (<http://jpkc.pumc.edu.cn/images/2.jpg>).

1.4 Experimental strategies for spinal cord repair after injury

Since it has been shown that CNS axons have the intrinsic capacity to regenerate (David and Aguayo, 1981), many research groups have focused on identifying the factors and mechanisms which are responsible for the failure of axonal regeneration. In theory, there are two determinants leading to the inhibition of axonal regrowth: on the one hand, most CNS axons have a low intrinsic regenerative capacity, and on the other hand, the CNS environment is inhibitory to axonal growth (Fawcett, 1998) as described in the previous chapters. Due to these findings various experimental strategies for spinal cord repair have been established. The use of growth factors such as brain-derived neurotrophic factor (BDNF) or neurotrophin-3 (NT-3) in injured spinal cords has shown that trophic factors are able to stimulate axonal growth and neuronal survival (Houle and Ziegler, 1994; McTigue et al., 1998; Jones et al., 2001; Lu and Tuszynski, 2008). Cell transplantations of autologous Schwann cells, olfactory ensheathing glia (OEG), neural precursor or stem cells into the lesioned spinal cord have the potential to support axon regeneration by replacing lost cells, by guiding regenerating axons and/or by providing trophic factors to enhance the regenerative capacity (Fisher, 1997; Bunge, 2001; Santos-Benito and Ramon-Cueto, 2003; Raisman, 2004; Coutts and Keirstead, 2008; Li and Lepski, 2013). The elimination of growth inhibitory factors within the lesion area by immunological neutralization of myelin inhibitors (e.g. antibody IN-1) (Fouad et al., 2001; Buchli and Schwab, 2005), by inhibition of the intracellular Rho signalling pathway (Fournier et al., 2003; McKerracher and Higuchi, 2006), by degradation of inhibitors associated with the lesion scar, e.g. chondroitinase ABC

(ChABC), (Bradbury et al., 2002; Barritt et al., 2006; Garcia-Alias et al., 2008) or suppression of fibrous scarring to prevent accumulation of inhibitors at the lesion site, e.g. iron chelator 2,2'-bipyridine-5,5'-dicarboxylic acid (BPY-DCA), (Stichel et al., 1999a; Klapka et al., 2005; Schiwy et al., 2009) enables axon regrowth through the scar area. In summary, the main targets of spinal cord repair strategies, as illustrated in Fig. 1.3, are (i) to limit the progression of secondary damage (neuroprotection), (ii) to replace perished cells (neuroreconstruction), (iii) to stimulate and guide axonal growth (neuroregeneration/plasticity), (iv) to promote axonal conduction (neurorestoration) and (v) to create a growth permissive environment (Schwab et al., 2006). Each of these repair strategies have been shown to improve axonal regeneration and to some extent functional recovery but mainly with modest effectivity. Therefore, it is likely that effective treatments for spinal cord injured patients will require combinations of the mentioned repair strategies. Several studies have demonstrated that the combination of two or more repair strategies have synergistic potential. For example, Fouad et al. (2005) combined in completely transected rat spinal cords ChABC, to reduce inhibitory cues in the glial scar, with a Schwann cell bridge, to provide a growth-supportive substrate for axonal regeneration, and with OEG to enable regenerated axons to re-enter the spinal cord at the Schwann cell bridge/host interface. They showed that only the group receiving both cell grafts and ChABC have significantly improved in locomotor performance compared to the controls. By translating the acquired knowledge from single and combinatorial therapies into future studies will lead to refined and more efficacious treatments. In the present study, the suppression of the collagenous lesion scar via iron chelator treatment (to prevent the accumulation of inhibitors at the lesion site) will be tested in combination with a chemokine enhancing axonal sprouting to examine their combinatorial potential to improve functional recovery.

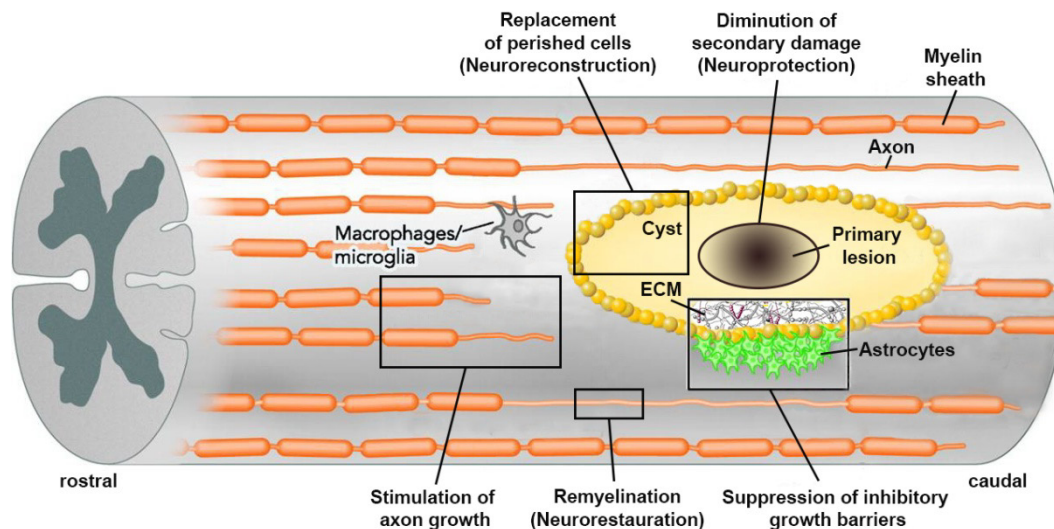


Fig. 1.3: Schematic drawing of a lesioned spinal cord illustrating the target areas of therapeutic repair strategies [according to Schwab et al. (2006)]. Precise regeneration of lesioned axons after spinal cord injury needs to overcome several barriers. Assuming that the neuron survives the disruption of its axon, it has to activate the regrowth of the damaged axon. The regenerating axon has to pass the lesion site and elongate target-oriented to reinnervate its former target area. Finally, the electrophysiological conduction of the axon has to be re-established. This gives rise to the following repair strategies: (i) neuroprotection: reduction of the secondary damage, (ii) neuroreconstruction: transplantation of cells and tissues to replace dead cells, (iii) neuroregeneration/plasticity: stimulation of axon growth, (iv) neurorestoration: remyelination to re-establish axonal conductivity and (v) suppression of growth inhibitors. [Spinal cord modified from Obermair et al. (2008)].

1.4.1 Suppression of the collagenous scar using iron chelators

As previously described, the fibrous scar is considered as a barrier for regrowing axons. The backbone of the fibrous scar, a sheet-like Coll IV network, is not per se inhibitory to axonal growth (Tonge et al., 1997), but the accumulation of numerous growth-inhibitory molecules such as CSPGs in the Coll IV network creates a non-permissive environment (Klapka and Müller, 2006; Brazda and Müller, 2009). To overcome this axon growth barrier, experimental strategies are focussing either on inhibition, degradation and/or neutralization of these individual growth inhibitors, as for example the enzymatic digestion of CSPGs by ChABC treatment (Bradbury et al., 2002), or prevention of the formation/deposition of the collagenous basement membrane, which serves normally as an adhesive scaffold for these growth-inhibitory molecules (Klapka and Müller, 2006; Brazda and Müller, 2009; Fawcett et al., 2012). The latter strategy has the advantage that the deprivation of the ECM structure reduces the accumulation possibility of all inhibitory molecules associated with the fibrous scar. Early attempts to suppress the collagenous scar by enzymatic digestion were ineffective as it caused massive bleeding into the lesion due to concomitant destruction of the basement membranes around intact blood vessels (Feringa et al., 1979; Guth et al., 1980). Recent work by Stichel et al. (1999a) has demonstrated a possibility to inhibit the *de novo* biosynthesis of collagen in the lesion area after a postcommissural fornix transection.

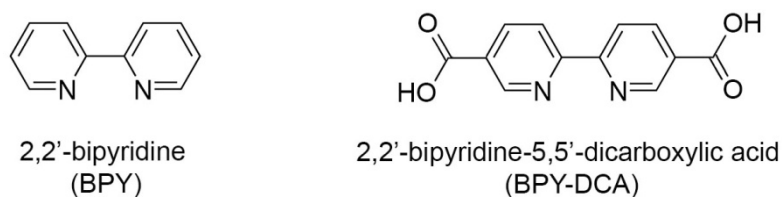


Fig. 1.4: Chemical structure of the ferrous iron chelator 2,2'-bipyridine (BPY) and its dicarboxylated derivative 2,2'-bipyridine-5,5'-dicarboxylic acid (BPY-DCA). BPY and BPY-DCA chelate ferrous iron at a 3:1 mole ratio.

They injected locally the ferrous iron chelator 2,2'-bipyridine (BPY, Fig. 1.4), a competitive inhibitor of prolyl-4-hydroxylase (Hales and Beattie, 1993), which is a key enzyme in collagen biosynthesis and catalyzes the hydroxylation of procollagen chains (Fig. 1.5). This hydroxylation reaction requires 2-oxoglutarate, O_2 , ascorbate and Fe^{2+} as cofactors (Kivirikko et al., 1989). Hence, iron deprivation will transiently inhibit the formation of stable collagen triple helices and consequently also the spontaneous network formation. With this scar-suppressing idea Stichel et al. were the first who showed that inhibition of Coll IV biosynthesis reduced transiently lesion-induced basement membrane deposition and resulted in regeneration of postcommissural fornix axons (Stichel et al., 1999a; Stichel et al., 1999b). The local application of BPY into the lesioned rat spinal cord, however, failed to reduce the basement membrane deposition, which is more extensive in the spinal cord than in the postcommissural fornix (Hermanns et al., 2001b). The larger extension of the lesion-induced basement membrane in the injured spinal cord is probably due to the close proximity of the lesion site to the meninges, an area rich of collagen-producing fibroblasts which infiltrate the CNS lesion site (Carbonell and Boya, 1988). Only after a combined application of the far more potent BPY derivative 2,2'-bipyridine-5,5'-dicarboxylic acid (BPY-DCA, Fig. 1.4) (Hales and Beattie, 1993) and 8-bromoadenosine 3',5'-cyclic monophosphate (8-Br-cAMP), an inhibitor of TGF- β induced activation of connective tissue growth factor (CTGF), which causes fibroblast proliferation (Duncan et al., 1999), the fibrous scar formation was transiently suppressed in the injured spinal cord and resulted in axonal regeneration, neuroprotection and partial recovery of motor function (Hermanns et al., 2001b; Klapka et al., 2005; Schiwy et al., 2009). In conclusion, this anti-scarring treatment (AST) is a promising strategy in treating spinal cord injury.

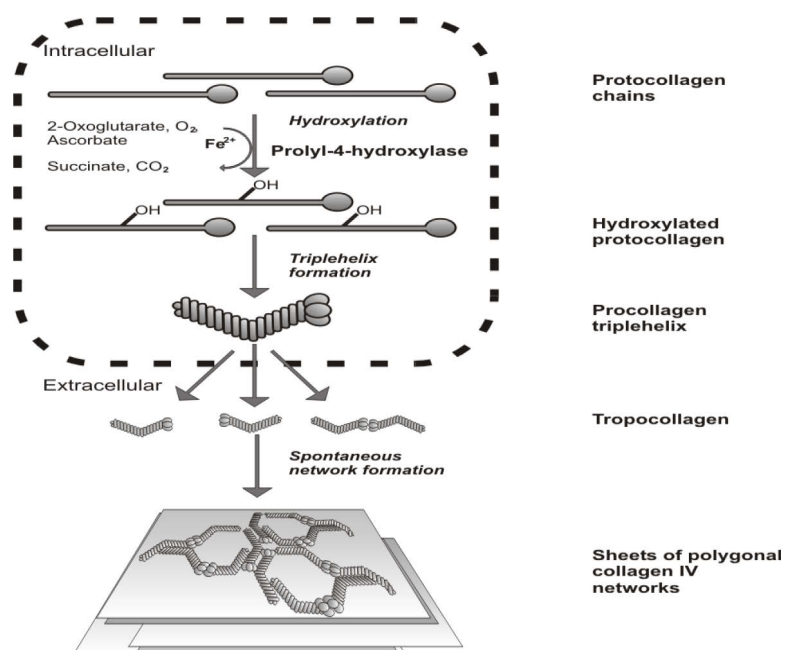


Fig. 1.5: Schematic representation of collagen biosynthesis. Essential co-substrates for hydroxylation of procollagen chains are 2-oxoglutarate, O₂, ascorbate and Fe²⁺ (Klapka et al., 2002).

However, one major disadvantage of the anti-scarring treatment (AST) regarding medical application consists in the solvent tris(hydroxymethyl)-aminomethane (Tris) of the clinically not approved iron chelator BPY-DCA. Tris can penetrate biological membranes in its un-ionized form and causes cytotoxicity (ANGUS chemical company technology review). Due to this cytotoxicity potential of Tris, the application of BPY-DCA, which is insoluble in water and PBS buffer, in spinal cord injured patients is very unlikely. Considering this issue, the approved water-soluble iron chelator deferoxamine mesylate (DFO), trade name Desferal[®], has been tested in the present work for its potential to reduce Coll IV scarring and to improve axonal and functional recovery.

1.4.1.1 Deferoxamine mesylate (DFO)

DFO is a bacteria-derived siderophore produced by actinobacter *Streptomyces pilosus* (Keberle, 1964) and is clinically used as an iron-chelating drug to treat acute iron intoxication and chronic iron overload due to repeated blood transfusions. DFO is a water-soluble hexadentate chelator with a terminal elimination half-life of approximately 6 h and it binds iron 1:1 stoichiometrically (Hershko et al., 1998; Howland, 2006). It chelates predominantly ferric iron (Fe³⁺) by twining its initially straight-chained form (Fig. 1.6) around the ion and becoming attached via its three hydroxamic acid groups (Keberle, 1964). The resultant ferrioxamine (Fig. 1.6) is a very stable octahedral iron complex (Howland, 2006), preventing the participation of iron in harmful chemical reactions as for example the hydroxyl radical formation through the Haber-Weiss reaction (Gutteridge et al., 1979).

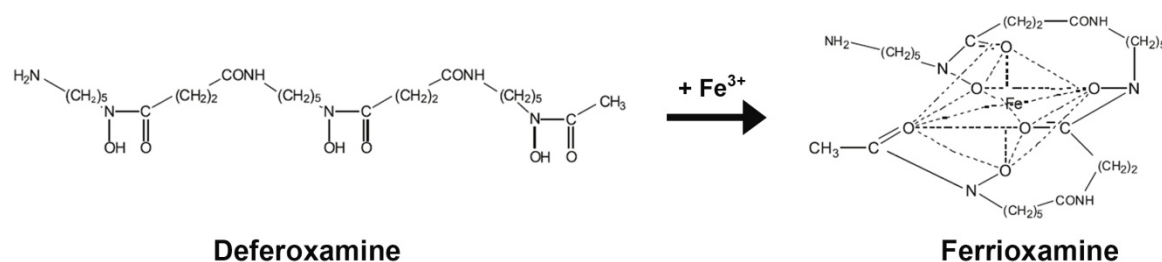


Fig. 1.6: Chemical structure of deferoxamine and its ferric chelate ferrioxamine [modified from Beyer and Cornejo (2012)].

DFO has also binding affinity to zinc, copper, nickel, magnesium or calcium, but with a far less affinity constant (10^2 - 10^{14} vs. 10^{31} for iron), i.e. at physiologic pH values DFO chelates almost exclusively ferric iron (Keberle, 1964; Howland, 2006). As DFO is hydrophilic, in contrast to BPY and BPY-DCA, it cannot permeate through most cell membranes easily, thus chelating mainly free non-transferrin-bound iron in the plasma. However, it is by now widely accepted that DFO is able to deplete also intracellular iron, which is in transit between transferrin (extracellular transport protein) and ferritin (major intracellular storage protein), the so-called chelatable labile iron pool, as different cell culture studies have shown (Rothman et al., 1992; Hoyes and Porter, 1993; Emerit et al., 2001; Kicic et al., 2001). The efficiency in depleting the cellular labile iron pool depends on the length of DFO incubation. Short incubations (≤ 2 h) with DFO were far less effective than incubations over longer periods. Additionally, iron from ferritin or hemosiderin can be slowly mobilized by DFO, but iron once bound to transferrin cannot be removed (Keberle, 1964; Balcerzak et al., 1966).

Due to the highly reactive nature of iron, the amount of free (unbound) iron is tightly regulated under physiological conditions by transferrin and ferritin maintaining reactive iron at extremely low levels to avoid the catalysation of free radical reactions (Emerit et al., 2001; Lee et al., 2006; Bains and Hall, 2012). Free iron reacts with hydrogen peroxide (H_2O_2) and superoxide anion ($\text{O}_2^{\bullet-}$) to form hydroxyl radicals (OH^{\bullet}) (Haber-Weiss reaction). Together with further free radicals they are significantly involved in peroxidation of lipids, DNA strand breaks, and degradation of biomolecules, which can lead to cell death (Emerit et al., 2001; Petrat et al., 2002; Lee et al., 2006). After spinal cord injury, the extracellular iron concentration increases extensively (Liu et al., 2003; Liu et al., 2011), presumably as a result from leaking cells damaged by the injury and haemorrhage followed by degradation of haemoglobin (Moos and Morgan, 2004; Lee et al., 2010). As the pH value is declining after injury in the spinal cord tissue, catalytically active iron is released from transferrin and ferritin initiating the production of oxygen radicals (Halliwell and Gutteridge, 2008; Hall, 2011; Bains and Hall, 2012). The resulting lipid peroxidation and oxidative damage to spinal neurons, glia and microvascular cells have a significant role in the pathophysiology of spinal cord injury

(Hall, 2011; Jia et al., 2012). There is evidence suggesting that lowering tissue iron level by DFO treatment results in attenuation of the expansion of secondary cellular damage. In several studies DFO has been shown to function as an antioxidant. It prevents free radical formation and lipid peroxidation leading to reduced cell death (Gutteridge et al., 1979; Almlı et al., 2001; Nowicki et al., 2009; Paterniti et al., 2010; Liu et al., 2011). In addition, DFO is able to inhibit iron-mediated glutamate excitotoxicity, thus protecting motor neurons against degeneration (Yu et al., 2009). This neuroprotective property of DFO seems to improve functional deficits as Liu et al. (2011) and Paterniti et al. (2010) have described in spinal cord injured rats and mice and is supported by similar findings from different CNS research areas, e.g. traumatic brain injury (Long et al., 1996), focal cerebral ischemia (Freret et al., 2006), intracerebral haemorrhage (Nakamura et al., 2004). Furthermore, increased neurite outgrowth could also be involved in improving functional deficits, based on the *in vitro* observation by Nowicki et al. (2009) that DFO is able to mediate neurite outgrowth and enhance synapse formation in rat DRG neurons. However, this capability of DFO to promote axon growth has not yet been described *in vivo* and needs to be verified. Another important aspect that is well-recognized to support reparative events including impaired functions is the revascularization of damaged central nervous tissue (Fassbender et al., 2011; Oudega, 2012). As several studies have shown that DFO promotes angiogenesis through upregulation of the vascular endothelial growth factor (VEGF) (Gleadle et al., 1995; Beerepoot et al., 1996; Linden et al., 2003; Ikeda et al., 2011; Hertzberg et al., 2012), functional recovery could be supported by DFO-induced angiogenesis.

1.4.2 Stimulation of axonal sprouting

In recent years axonal sprouting has been recognized as an important recovery mechanism of locomotor functions via adaptive reorganization of the neural pathways (Bradbury and McMahon, 2006; Maier and Schwab, 2006; Fouad and Tse, 2008). As most experimental interventions that lead to functional improvements showed usually modest numbers of regenerated axons, the question was whether these regenerated axons can be considered as exclusively responsible for the observed functional recovery. Li et al. (1997) found that when as few as 1 – 2 % of the corticospinal tract (CST) was spared, performance in a forepaw reaching task recovered implying that regeneration of a small percentage of axons to its original target could potentially induce functional recovery (Bradbury and McMahon, 2006). But there is now also strong evidence that a further repair mechanism exists. Bareyre et al. (2004) demonstrated that the injured spinal cord has the capacity via anatomical plasticity to form new functional intraspinal circuits leading to spontaneous recovery of locomotor functions. Here, transected hindlimb CST axons sprouted into the cervical grey

matter to innervate long propriospinal neurons that bridge the lesion site and arborize on lumbar motoneurons. Supporting the endogenous capability of the adult CNS to reorganize by therapeutic interventions could be beneficial in promoting functional recovery. Indeed, various experimental strategies aiming to overcome inhibition of axonal regeneration such as neutralizing the myelin-associated growth inhibitor Nogo-A (Thallmair et al., 1998; Z'Graggen et al., 1998; Raineteau et al., 2002) and enzymatic degradation of CSPGs by ChABC (Barritt et al., 2006; Massey et al., 2006) have been shown to enhance axonal sprouting after spinal cord injury. Recently Opatz et al. (2009) observed that the chemokine stromal cell-derived factor 1 α (SDF-1 α), intrathecally infused into the spinal cord lesion area for 7 days, promotes extensive sprouting of CST axons indicating a regeneration supporting function of SDF-1 α after spinal cord injury.

1.4.2.1 Stromal cell-derived factor 1 (SDF-1)

SDF-1, also known as CXCL12, has been found to be a key regulator for early development of the CNS and is required for migration of neuronal progenitor cells, axon guidance and pathfinding (Li and Ransohoff, 2008; Jaerve et al., 2012a; Jaerve et al., 2012b). SDF-1 signals through two G-protein coupled receptors, CXCR4 (Oberlin et al., 1996) and CXCR7 (Balabanian et al., 2005), and their deficiency is perinatally lethal (Nagasawa et al., 1996; Zou et al., 1998; Siervo et al., 2007). In the adult uninjured spinal cord, SDF-1 is expressed mainly in the dorsal CST and the meninges (Tysseling et al., 2011). CXCR4 has been observed on ependymal cells surrounding the central canal (Jaerve et al., 2011; Tysseling et al., 2011) and in low levels on dorsal CST axons, which also express CXCR7 (Opatz et al., 2009; Jaerve et al., 2011). An injury to the spinal cord induces the upregulation of SDF-1, mostly associated with reactive astrocytes (Hill et al., 2004; Miller et al., 2005). Additional to the dorsal CST and the meninges, which already express SDF-1 in the intact spinal cord, SDF-1 expression is also found in endothelial cells (Graumann et al., 2010) and infiltrating macrophages (Sanchez-Martin et al., 2011; Tysseling et al., 2011). As the increased SDF-1 level forms a chemotactic gradient, CXCR4 expressing cells such as microglia/macrophages, ependymal stem cells, oligodendrocytes, bone marrow-derived stem cells, vascular precursors and presumably pericytes are attracted to the lesion site (Jaerve et al., 2012a). Hence, this cell recruiting via SDF-1/CXCR4 signalling is an important element in regulating spinal cord responses to injury.

Besides orchestrating cell migration, SDF-1 also promotes neurite outgrowth of postnatal dorsal root ganglion (DRG) neurons in the growth inhibitory environment of CNS myelin (Chalasani et al., 2003; Opatz et al., 2009) and local infusion of the SDF-1 α isoform into lesioned rat spinal cord stimulates axon outgrowth (Opatz et al., 2009). So far, enhanced rostral sprouting after SDF-1 α treatment have been reported in spinal cord injured rats for

axons of the dorsal CST and for serotonergic (5-HT) and tyrosine hydroxylase (TH)-positive fibres (Opatz et al., 2009; Jaerve et al., 2011). It has been described that SDF-1 acts through elevation of intracellular cAMP levels (Chalasan et al., 2003), which subsequently leads to an upregulation of regeneration-supporting genes such as Arginase I (Cai et al., 2002). Arginase I is a key enzyme in the synthesis of polyamines and the overexpression of one of them is sufficient to overcome regeneration inhibition by MAG and by myelin (Cai et al., 2002). The exact downstream mechanism of SDF-1 induced axonal sprouting, however, is not yet identified.

The capability of SDF-1 to promote neurite outgrowth in the presence of growth inhibitory CNS myelin and the stimulation of extensive axon sprouting make SDF-1 to a promising target for spinal cord repair. The first study on the impact of SDF-1 on functional recovery was very recently shown by Zendedel et al. (2012). They demonstrated that SDF-1 α , which was intrathecally infused for 28 days, improved locomotor deficits after spinal cord contusion. The functional improvement was correlated with higher numbers of neuronal cell bodies and lower numbers of apoptotic cells indicating a neuroprotective effect of SDF-1 α . Additionally they found that SDF-1 α induced angiogenesis and augmented microgliosis and astrocytosis, but they have not investigated whether axonal sprouting or regeneration was involved in functional recovery.

1.5 Recovery of locomotion – an important factor for evaluating treatment efficacy

The development of numerous behavioural testing methods for SCI animal models enables the understanding of mechanisms involved in motor control and the assessment of treatment efficacy. In the last years it has been generally accepted that locomotion depends on specialized networks of interneurons within the spinal cord termed central pattern generators (CPGs) (Majczynski and Slawinska, 2007; Rossignol and Frigon, 2011). These neuronal circuits are able to generate rhythmic movements, such as walking and swimming, even in absence of supraspinal and sensory inputs (MacKay-Lyons, 2002; Rossignol and Frigon, 2011). The main rhythmogenic capacity of the rat hindlimb locomotor CPG is believed to be localised in the ventral grey matter of the lumbar segments L1 – L2 with decreasing potential in rhythm generation in the caudal direction (Cazalets et al., 1995; Kiehn, 2006; Rossignol and Frigon, 2011). Hence, spinal cord injuries centred in these segments will induce more severe locomotor deficits than injuries centred in neighbouring spinal cord segments as it has been shown by Magnuson et al. (2005). The incoming inputs from descending supraspinal pathways (brainstem, basal ganglia and cortex) and ascending sensory afferents from the periphery modulate the locomotor CPG activity. While supraspinal structures are involved in

locomotion initiation, maintenance and coordination with other motor performance, sensory feedback is essential to adapt the locomotor pattern to changes in the internal and external environments (MacKay-Lyons, 2002; Majczynski and Slawinska, 2007). Additionally, it has been shown that neuromodulators, e.g. serotonin (5-HT), can considerably influence the locomotor CPG activity (Cazalets et al., 1992; Grillner et al., 1995) and can consequently improve locomotor movements in spinal cord injured animals (Feraboli-Lohnherr et al., 1999).

1.5.1 Topographical organisation of the rat spinal cord

The type and severity of locomotor impairments after spinal cord injury is mainly determined by the site of the impact and the extent of damage of the topographical organised spinal cord. In the white matter of the spinal cord millions of long axons are running longitudinally connecting the brain with the periphery (descending motor fibres) and vice versa (ascending sensory fibres). The location of the major ascending and descending fibre tracts in the rat spinal cord is illustrated in Fig. 1.7. Due to the lesion model (dorsal hemisection) used in this work, the CST and RST are of central importance and will therefore be described in detail. One important characteristic of the rat spinal cord anatomy is the location of the CST. In humans, the main component of the CST is located in the lateral column (Nathan et al., 1990; Martin, 2012), while in rats it is primarily located in the ventral most part of the dorsal column and only a few CST axons descend within the lateral column (Brown, 1971; Brösamle and Schwab, 1997; Deumens et al., 2005). In both humans and rats, there is also a small population of CST axons that descend ventrally. The cells of origin of the dorsal/lateral CST lie in layer V of the contralateral cerebral cortex and their axons decussate at the spinomedullary junction (pyramidal decussation), whereas the ventral CST originates from the ipsilateral cortex (Brösamle and Schwab, 1997). CST axons of most mammals project primarily to the dorsal horn and to the intermediate gray matter (Rexed's laminae III-VI) (Watson, 2009). Functional cortico-motoneuronal connections are not present in the rat, they are a unique feature of primates and are believed to be largely responsible for the ability to make independent digit movements (Yang and Lemon, 2003; Alstermark et al., 2004; Lemon, 2008). The RST arises from the red nucleus in the midbrain, decussates at the level of the tegmental decussation and descends within the dorsolateral funiculus (Brown, 1974; Deumens et al., 2005). RST axons terminate mostly on interneurons in Rexed's laminae V, VI and in the dorsal part of lamina VII at all levels of the spinal cord (Antal et al., 1992; Watson, 2009). Only a small proportion has been found to project directly onto motoneurons (lamina IX) (Küchler et al., 2002).

In addition to these long ascending and descending tracts, the spinal cord white matter also contains many intraspinal fibres that connect one spinal cord segment with another (Watson, 2009). These propriospinal (PS) fibres, whose cell bodies are located in the grey matter, can be subdivided into short- and long-distance axons. Short PS projections have been found in the limb segments of the spinal cord, i.e. in the cervical and lumbosacral enlargements (Watson, 2009). The neurons of cervical PS projections originate in the grey matter of the upper cervical segments (C3-C4) and terminate in the lower cervical segments (C6-Th1) (Alstermark et al., 1987a; Alstermark et al., 1990). They are key modulators of visually guided reaching and grasping movements of the forelimbs. Long PS projections originate in the cervical spinal cord segments C3-C5 and descend in the ventral and lateral funiculi (Giovannelli Barilari and Kuypers, 1969) to the ventral horn of the lumbosacral spinal cord (Alstermark et al., 1987b; Alstermark et al., 1987c), thus interconnecting both enlargements and their short PS projections (Reed et al., 2006; Watson, 2009). Long PS projections play an important role in mediating reflex control and in coordinating limb movements (Miller and Burg, 1973; Jankowska et al., 1974). Depending on the degree of spinal cord damage, long PS projections will be spared as for example in a mid-thoracic dorsal hemisection and can bridge the lesion site via new formed intraspinal circuits (Bareyre et al., 2004).

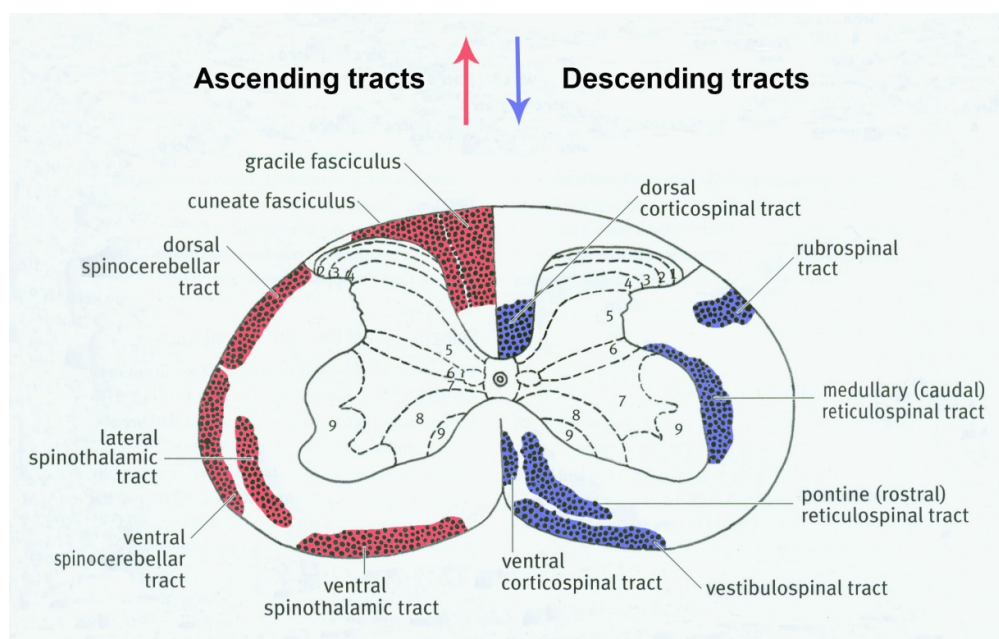


Fig. 1.7: Schematic cross-section of the rat spinal cord showing the position of the major ascending (red) and descending (blue) fibre tracts [modified from The Spinal Cord (Watson, 2009)]. To simplify the diagram, the fibre tracts are only depicted on one half of the spinal cord.

1.5.2 Role of CST and RST in motor control

The CST and RST play an important role in controlling skilled limb movements. However, their functional interaction or their behavioural contribution to skilled movements is not yet completely understood. In rats, it has been proposed, that the CST and RST collaborate closely in producing skilled forelimb movements (Whishaw et al., 1990; Whishaw et al., 1998) as lesions to either the corticospinal system (Schrimsher and Reier, 1993; Whishaw et al., 1993; Whishaw et al., 1998; Anderson et al., 2005; Kanagal and Muir, 2008) or the rubrospinal system (Whishaw et al., 1990; Schrimsher and Reier, 1993; Whishaw et al., 1998; Muir et al., 2007) impairs forelimb function during skilled movements. In addition, it has been also suggested, that the CST and RST can compensate for the loss of the other (Kennedy, 1990). The switch between these two systems is presumably assisted by the rubro-olivary projection, which is a collateral pathway of the RST in rats. It originates from the red nucleus and projects to the inferior olivary nucleus and then to the cerebellum. In the healthy animal, the rubro-olivary system is hypothesised to manage the transition of control from the CST to the RST when a new movement has been successfully learned and becomes automated (Kennedy, 1990). If an automated movement needs to be adapted, the RST control will be switched to the CST control.

Apart from this compensatory role of the CST and RST, there are other spinal tracts that could contribute to functional compensation after spinal cord injury. Kanagal and Muir (2009) reported recently that some fibre tracts of the dorsolateral funiculus (DLF), including the RST and the reticulospinal tract (ReST), do compensate for the loss of corticospinal input, but it is behavioural task specific. Rats with a bilateral pyramidotomy, followed by a bilateral DLF lesion after six weeks, were tested for skilled limb use during both horizontal ladder walking and pellet retrieval as well as for comparatively automated limb use during overground locomotion. Only in the skilled forelimb reaching task (single pellet retrieval) a compensatory response of the DLF could be determined. Since behavioural tasks address different aspects of locomotor behaviour, which are under control of different supraspinal inputs, one can assume that different compensation strategies are activated after injury according to the behavioural context. Lesion studies of the pyramidal tract have shown that the CST plays only a minor role in overground locomotion in rats (Metz et al., 1998; Muir and Whishaw, 1999; Kanagal and Muir, 2009), whereas it is essential for skilled limb use, such as skilled locomotion over a horizontal ladder or single pellet reaching (Whishaw et al., 1993; Whishaw et al., 1998; Metz and Whishaw, 2002; Kanagal and Muir, 2009). Although skilled walking over a horizontal ladder was impaired after bilateral pyramidal tract lesion, Kanagal and Muir (2009) could not find any compensation through the DLF as it was seen in the reaching task. This reflects the fact that the behavioural context determines the nature of compensation from spared fibre tracts after spinal cord injury. Lesion studies of the rubrospinal system have

shown that the RST is important in both normal overground locomotion (Muir and Whishaw, 2000; Webb and Muir, 2003) as well as in skilled movement in rats (Whishaw et al., 1998; Webb and Muir, 2003). Red nucleus lesions in rats induce persistent locomotor gait deficits (asymmetric gait), but the initiation of stepping movements is, however, not affected. Schucht et al. (2002) have demonstrated that the initiation of rhythmic stepping movements is caused by the ventrolaterally running reticulospinal tract, which activates the spinal cord central pattern generator for locomotion (Jordan, 1998). Sparing of a small percentage of the lateral funiculus enables already rhythmic limb activity. But to perform well on the horizontal ladder, sparing of the dorsolateral (RST) or dorsal (CST) column is additionally required. During skilled limb use, the RST is thought to be involved in a more general control of the limb musculature, because red nucleus lesions seem to induce no major deficits in precise paw reaching tasks. Lesions of the CST, in contrast, cause stronger and more permanent deficits resulting in decreasing success rates. Thus, the function of CST in skilled movements is the precise control of individual limb muscles (Küchler et al., 2002). Additionally, it has been shown, that direct rubro-motoneuronal projections are restricted to the distal and intermediate motor neuron pools of the spinal cord grey matter (Küchler et al., 2002).

1.5.3 Behavioural testing of spinal cord injured rats

Functional recovery after spinal cord injury is the ultimate goal of a therapeutic intervention. To evaluate experimentally treatment efficacy in spinal cord injury animal models, a diversity of different behavioural testing methods has been developed. As one single functional test addresses only a particular aspect of locomotor behaviour, a combination of several tests is necessary to assess functional recovery (Kunkel-Bagden et al., 1993; Muir and Webb, 2000). In addition, a functional impairment can be masked or compensated by intact functions. If only one functional test is performed, this impairment might not be detectable and a possible treatment effect might remain undiscovered. A complex task like the horizontal ladder walking test, e.g., can reveal deficits that are not apparent in open field locomotion (Kunkel-Bagden et al., 1993). For the assessment of functional recovery in thoracic lesion models, mainly behavioural tests focussing on locomotion like the Basso, Beattie and Bresnahan (BBB) open field locomotor test (Basso et al., 1995), horizontal ladder walking test (Metz and Whishaw, 2002; Metz and Whishaw, 2009), CatWalk gait analysis (Hamers et al., 2001), kinematic analysis (Metz et al., 1998), and narrow beam or rope test (Kim et al., 2001) are used. In this study, functional recovery after thoracic spinal cord hemisection in rats was monitored with the BBB open field test, horizontal ladder walking test and the CatWalk gait analysis. The BBB open field test is one of the most commonly used locomotor test in spinal cord injured rats and analyses the recovery of hindlimb movements during free overground

locomotion via a 21-point scale (see also Materials and Methods). Originally, the BBB score was developed for contusion injuries, but it is now also regarded as sensitive in hemisection injuries (Metz et al., 2000) and is therefore often used in thoracic hemisection lesion models (Schucht et al., 2002; Webb and Muir, 2002; Joosten et al., 2004; Klapka et al., 2005; Ballermann and Fouad, 2006; Schira et al., 2012; Redondo-Castro et al., 2013). Since overground locomotion is a stereotyped movement, which is controlled by the CPG network and its reticulospinal input (Jordan, 1998), lesions affecting the dorsal part of the spinal cord induce mainly minor deficits in normal overground locomotion (e.g. impaired toe clearance, internal or external paw rotation during locomotion). The horizontal ladder walking test, however, is a very sensitive test for evaluating the integrity of the dorsal spinal motor tracts, CST and RST. For a successful crossing of the horizontal ladder the laboratory animal requires sensory-motor coordination of the forelimbs and hindlimbs, mediated by ventrolateral tracts, an intact reticulospinal system to initiate rhythmic stepping, as well as voluntary movement control, which is predominantly mediated by the corticospinal and rubrospinal systems in rats (Metz et al., 2000). Consequently, transection of the CST and/or RST causes deficits in descending fine motor control and results in visible missteps due to the lost ability to place the hindlimb accurately on the grid bar. Detailed assessment of gait changes after spinal cord injury is another important measure of long-term functional recovery. The automated gait analysis using the CatWalk system enables the quantification of a large number of different locomotion parameters (e.g. interlimb coordination, duration of swing and stance phase, stride length, paw pressure) during walkway crossing by visualizing paw-floor contacts in time (Koopmans et al., 2005). The advantage of the CatWalk system is the ability to measure both static and dynamic gait parameters.

1.6 Aim of this thesis

Due to the limited capacity of the CNS to regenerate most spinal cord injuries lead to permanent functional deficits in the area below the lesion. In recent years, different therapeutic approaches that are able to promote regeneration in the adult CNS have been found. One promising approach was developed in the Molecular Neurobiology Laboratory of the Heinrich Heine University Düsseldorf. By applying the anti-scarring treatment (AST), composed of iron chelator BPY-DCA and 8-Br-cAMP, local into the lesion area of spinal cord injured rats, the fibrous scar formation was transiently suppressed and resulted in axonal regeneration, neuroprotection and partial recovery of motor function (Hermanns et al., 2001b; Klapka et al., 2005; Schiwy et al., 2009). However, despite promising results, a medical application of the current AST in humans is very unlikely due to two reasons: (1) Iron chelator BPY-DCA (not FDA approved) has to be solved in Tris, which can penetrate biological

membranes and causes cytotoxicity. As massive cell death is already occurring due to pathophysiologic processes activated by the injury, a treatment should avoid further cell death. (2) The injection method used for local application is not transferable into hospital as injections into the intact spinal cord are necessary to reduce scarring also at the rim of the lesion zone. Thus, there is a risk of further spinal cord damage. The aim of this thesis was to establish an anti-scarring treatment, which would be suitable for clinical use and would induce equivalent effects to the spinal cord. In particular, the following aspects are addressed in this work:

- Establishment of a local application method in the rat that would be accepted as drug delivery system in patients and that allows to draw reliable conclusions about the treatment efficacy. Due to the small dimensions of a rat, it is necessary to ensure that the application method does not induce adverse effects (e.g. spinal cord compression).
- Establishment of a Coll IV quantification method for histological spinal cord sections to measure lesion-induced Coll IV expression in the scar.
- Efficacy of intrathecally infused BPY-DCA to reduce Coll IV in the lesion area and comparison with two alternative iron chelators, BPY and DFO.
- Effect of DFO on induction of long-lasting locomotor recovery, stimulation of regenerative axon growth and prevention of tissue loss.
- Finally, the evaluation whether the effect of DFO on regeneration can be synergistically improved by simultaneous treatment with SDF-1 α .

2 Materials and Methods

2.1 Buffers, solutions and antibodies

2.1.1 Buffers and solutions

Table 2.1: Buffers and solutions

Buffers and solutions	Constituent parts/manufacturer
PB (phosphate buffer), 0.2 M, pH 7.4	28.8 g Na ₂ HPO ₄ (Merck) 5.2 g NaH ₂ PO ₄ (Merck) ad 1000 ml <i>aqua bidest</i>
PBS (phosphate buffer saline), 0.1 M, pH 7.4	50 ml 0.2 M PB 9 mg NaCl ad 1000ml <i>aqua bidest</i>
TRIS buffer, 20 mM, pH 7.4 or pH 7.9	0.242 g C ₄ H ₁₁ NO ₃ (Aldrich) ad 100 ml <i>aqua bidest</i> pH titration with HCl
BPY-DCA, 1.1 µg/d, 7.8 µg/d, 187.2 µg/d	for 187.2 µg/d: 78.14 mg BPY-DCA (Aldrich) ad 10 ml TRIS (20 mM)
BPY, 0.71 µg/d, 7.12 µg/d, 71.2 µg/d	for 71.2 µg/d: 29.68 mg BPY (Sigma-Aldrich) ad 10 ml PBS
DFO, 10 µg/d, 50 µg/d, 100 µg/d	for 100 µg/d: 1.25 mg DFO (Novartis) ad 3 ml PBS
8-Br-cAMP, 50 µg/d, 100 µg/d, 200µg/d	for 200 µg/d: 41.67 mg 8-Br-cAMP (Sigma) ad 5 ml PBS
SDF-1α (human), 10 µM	500 µg SDF-1α (1x Vial, R&D Systems) ad 6.279 ml 0.1 % BSA/PBS buffer
BSA (fraction V), 59.3 µg/d	31 mg BSA (Sigma) ad 6.279 ml PBS
Protease XXIV, 0.05 %	1.9 mg Protease XXIV (Sigma) ad 5 ml 20 mM TRIS buffer (pH 7.9)
DS (Donkey serum), 5 %	500 µl DS (Sigma) ad 10 ml PBS
Triton X-100, 0.3 %	30 µl Triton X-100 (Sigma) ad 10 ml PBS
PFA (Paraformaldehyde), 4 %, pH 7.4	40 g PFA powder (Merck) ad 1000 ml 0.1 M PB pH titration with 5 M NaOH
Gelatine, 10 %, for tissue embedding	10 g Difco™ gelatine (BD) ad 100 ml 0.1 M PB 60°C for solving, 37°C for embedding
Paraffin for tissue embedding	100 g paraffin (Merck) 5 g wax (Cera Alba, Caelo) 56°C
RotiHistol	Roth
Fluoromount G for tissue mounting	Southern Biotech
Immu-Mount for tissue mounting	Thermo Scientific

2.1.2 Antibodies

2.1.2.1 Primary antibodies

Table 2.2: Primary antibodies

Antibody	Class	Antigen	Dilution	Manufacturer
Coll IV (M3F7)	ms IgG ₁	collagen type IV	1:500	Developmental Studies Hybridoma Bank
vWF	rb	von Willebrand factor	1:500	Dako
CGRP	gt IgG	Calcitonin gene-related peptide	1:1500	Serotec
CTB	gt	Cholera Toxin B Subunit	1:80 000	List Biological Laboratories
GFAP	ms IgG ₁	glial fibrillary acidic protein	1:500	Chemicon

2.1.2.2 Secondary antibodies

Table 2.3: Secondary antibodies

Antibody	Class	Dilution	Manufacturer
anti-mouse Alexa Fluor® 488	dk	1:500	Molecular Probes
anti-rabbit Alexa Fluor® 488	dk	1:500	Molecular Probes
anti-rabbit Alexa Fluor® 594	dk	1:500	Molecular Probes
anti-goat Alexa Fluor® 594	dk	1:500	Molecular Probes
anti-mouse Alexa Fluor® 647	dk	1:500	Molecular Probes
Oregon Green® 488		1:1000	Molecular Probes

2.1.3 Tracer substances and reagents

Table 2.4: Tracer substances and reagents

Tracer substances/reagents	Dilution	Constituent parts/manufacturer
Biotinylated Dextran Amine (BDA) MW 10 000	10 %	Molecular Probes
Cholera Toxin B Subunit (CTB)	1 %	List Biological Laboratories
DAPI (4',6-Diamidino-2-phenylindole)	1:10 000	Roche
Sudan Black	0.3 %	Fluka

2.2 Animals

All experiments were performed using adult female Wistar rats (Wistar-Hannover) weighing 200-230 g. The animals were kept in groups in standard cages and in a specifically pathogen-free environment (21°C, 50 ± 5 % air humidity) with a 12h light/12h dark cycle. Individual caging was provided directly after surgery allowing the animal to recover from anaesthesia. Pelletized dry food and germ-free water were available *ad libitum*.

All surgical interventions and pre- and post-surgical animal care were conducted in compliance with the German Animal Protection law (State Office of Environmental and Consumer Protection of North Rhine-Westphalia, LANUV NRW). An overview of the experimental animal groups and animal numbers are given in table 2.5.

Table 2.5: Overview of the experimental animal groups

Analysis	Groups	Alzet osmotic minipump model	Survival time	n	
Intrathecal catheter application	Fixation and Compression	2001 (1 µl/h for 7d)	7d	8	
	Occlusion	2001 (1 µl/h for 7d)	7d	3	
		2002 (0.5 µl/h for 14d)	14d	2	
Coll IV reduction	BPY-DCA	lesion-only (control)	2001 (1 µl/h for 7d)	7d	6
		20 mM Tris (vehicle control)		6	
		1.1 µg/d BPY-DCA		6	
		7.8 µg/d BPY-DCA		6	
		187.2 µg/d BPY-DCA		4	
	BPY	lesion-only (control)	2001 (1 µl/h for 7d)	7d	6
		PBS (vehicle control)		6	
		0.71 µg/d BPY		6	
		7.12 µg/d BPY		6	
		71.2 µg/d BPY		6	
	DFO	lesion-only (control)	2001 (1 µl/h for 7d)	7d	7
		PBS (vehicle control)		7	
		10 µg/d DFO		5	
		50 µg/d DFO		6	
		100 µg/d DFO		7	
	DFO intrathecal vs. systemic	H ₂ O (vehicle control)	2002 (0.5 µl/h for 14d)	14d	6
		10 µg/d DFO		7d	6
		10 µg/d DFO		14d	6
		350 mg/kg/d DFO (systemic)	-	14d	5
	Functional recovery + tissue sparing + axon regeneration	PBS (vehicle control)	2002 (0.5 µl/h for 14d)	19w	8*
BSA (vehicle control)		6*			
DFO		2x 1007D (0.5 µl/h for 7d)	8*		
DFO+SDF-1α			8*		
SDF-1α			9*		

* animals showing autotomy are not listed

2.3 Surgical procedures

2.3.1 Filling and priming of osmotic minipumps

The osmotic minipumps (Alzet pump model 1007D, 2001, 2002) were filled and primed in advance to the surgery according to the instructions of Alzet. First of all, the empty pump together with its flow moderator was weighed. Using the supplied filling tube connected to a syringe, the minipump was slowly filled with the respective solution and it was avoided to introduce air bubbles. After insertion of the flow moderator the filled minipump was weighed again. The difference in the weights obtained before and after filling gives the net weight of the solution loaded and is a measurement for complete filling of the minipump.

Prior to *in vivo* implantation the filled minipumps were primed in sterile 0.9 % saline at 37°C *in vitro* for at least four to six hours to accomplish the 'start-up period'. Thus, a constant pumping rate was guaranteed at implantation time point. Due to a tight surgery timetable the minipumps for the functional recovery study were even primed overnight.

2.3.2 Dorsal hemisection

In all surgical interventions isoflurane anaesthesia [Forene (Abbott); 2-3 % in O₂ and NO₂ at a ratio of 1:2] was used. After checking the depth of anaesthesia by pinching a (hind)paw, the back of the animal was shaved and disinfected. Using a scalpel blade an incision from thoracic level Th6 – Th14 was made to expose the underlying paravertebral muscles. Adipose tissue between the shoulder blades was carefully detached from the muscles on one side so that it could be retracted with a clamp. Lateral to the vertebrae Th6 – Th12 the muscles were cut and forced apart by a muscle retractor. Then, a complete laminectomy was performed at Th8, Th9 and Th11. To allow a controlled operation procedure, the spinous processes of Th7 and Th10 were clamped and stabilized using a stereotactic device (Small Animal Adaptor, David Kopf Instruments). Using iridectomy scissors the *dura mater* was opened at thoracic level Th8 with a transverse cut and a dorsal hemisection lesion was induced with the Scouten wire knife (SWK, Bilaney): The knife was fixed on the stereotactic frame and aligned to the opening of the dura. On the right side of the spinal cord, the guidance canula of the unopened knife was stereotactically inserted 1.2 – 1.5 mm deep into the spinal cord tissue. To avoid compression of the spinal cord tissue when the knife is lifted up, the two remaining intact meninges, *arachnoidea* and *pia mater*, were also cut by iridectomy scissors. Then, the wire was opened and lifted up, transecting the axonal tracts of the dorsal spinal cord. Due to the asymmetry of the wire caused by the strain after multiple uses, only the dorsal corticospinal tract (CST), the left lateral rubrospinal tract (RST) and the dorsal columns were completely cut as illustrated in Fig. 2.1A. After transection of the dorsal axon tracts, the *dura mater* was sutured.

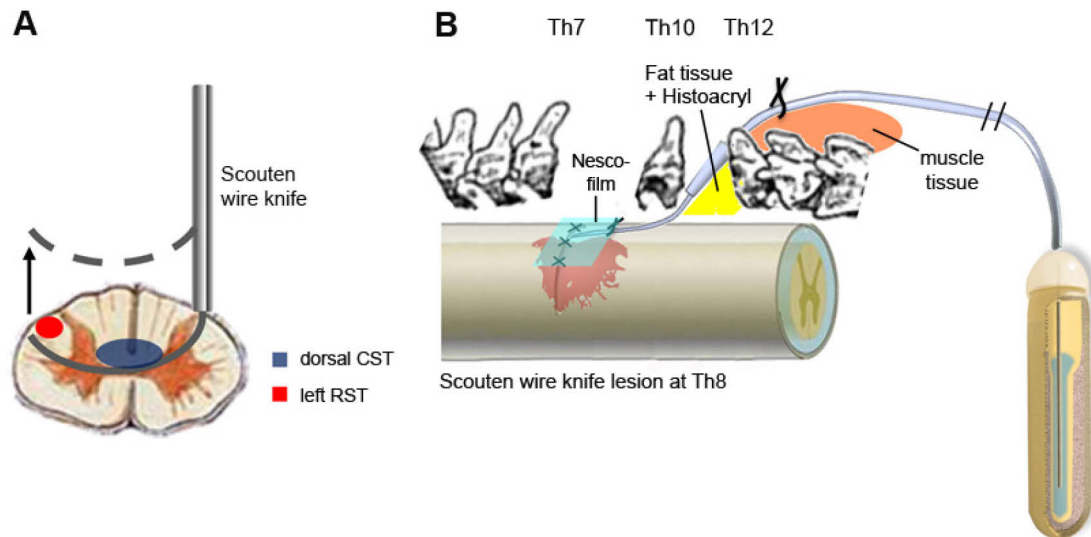


Fig. 2.1: Schematic illustration of the dorsal hemisection procedure with the Scouten wire knife (A) and the improved intrathecal catheter application (B). (A) The more the knife is used for transecting the spinal cord, the greater the asymmetry of the knife. Due to this occurring asymmetry only the dorsal corticospinal tract (CST), the dorsal columns and the left lateral rubrospinal tract (RST) were completely cut, whereas the right RST was presumably only partially affected. (B) The intrathecal catheter was guided epidurally as far as possible and was finally inserted into the subarachnoid space near the dura suture. The catheter was fixed on the dura and on the autologous fat cushion covering the exposed spinal cord area of Th11 (for detailed description see 2.3.3).

2.3.3 Intrathecal catheter application

In all studies addressing catheter functionality or scar reduction by infusing iron chelators the 28G polyurethane intrathecal catheter from Alzet (outer \varnothing : 0.36 mm; inner \varnothing : 0.18 mm) was used. For the animals in the functional recovery study the intrathecal catheters were self-made using 32G polyurethane from ReCathCo (outer \varnothing : 0.23 mm; inner \varnothing : 0.09 mm). As one group would receive two substances simultaneously, the catheter for this group was created as a Y to avoid mixing both substances in one osmotic minipump or placing two catheters on the spinal cord.

Following suture of the *dura mater*, the intrathecal catheter was guided in the epidural space from Th10 up to the lesion site. To keep the catheter in place, it was fixed on the muscles around Th12/13 by a stitch and it was additionally glued with Histoacryl® (Braun) tissue glue on a cushion of autologous fat tissue, which covered the exposed spinal cord area of Th11 (see Fig. 2.1B). The cushion itself was glued to surrounding tissue and bones. After adapting the catheter length to the transection area, the catheter was filled and inserted into the subarachnoid space towards the centre of the lesion through a small opening in the dura. The opening was made in close proximity to the dura suture to keep the catheter guidance within the subarachnoid space as short as possible. Subsequently, the catheter was also fixed by a stitch on the dura and connected to a filled and primed (37°C) osmotic minipump (Alzet pump model 1007D, 2001 or 2002) as illustrated in Fig. 2.1B. The osmotic minipump

was placed into a skin pocket on the back of the animal. Finally, the lesion area was covered with a piece of stretched Nescofilm® (Roth) and the overlaying muscle and skin were sutured in layers.

2.3.4 Testing of catheter functionality over time (*in vivo*)

In regard to the very narrow subdural and subarachnoid space in rodents (Haines et al., 1993; Reina et al., 2002), compared with the diameter of intrathecal tubing, negative side effects like spinal cord compression or extensive scarring induced by the tubing material can occur (Jones and Tuszynski, 2001; Zhang et al., 2010). To enable clear interpretation of the experimental approach, the above described intrathecal application method was tested for sufficient catheter fixation, catheter induced compression and catheter occlusion over time.

2.3.4.1 Catheter fixation

Intrathecal infusion is an effective way to distribute drugs locally and continuously over time into the subarachnoid space. Therefore, it is essential to have a strong catheter fixation over the time of drug infusion. To check for a stable catheter fixation, the lesion area was intrathecally infused with 3 % Evans Blue dye (Sigma) and the animals were reopened under isoflurane anaesthesia one day later and shortly before perfusion seven days after injury. To make reopening easier the lesion infusion site was covered with stretched Nescofilm® (Roth) avoiding intense catheter adhesion to the surrounding tissue.

2.3.4.2 Analysis of catheter-induced compression

To examine if the above described intrathecal application method induces spinal cord compression, the animals receiving 3 % Evans Blue dye by intrathecal infusion (see catheter fixation) were perfused after seven days and the spinal cords were dissected. Then, the spinal cords were prepared for the freezing-microtome (see 2.4.1) and sections of 50 µm thickness were cut and stained for Masson's trichrome (see 2.5.1).

2.3.4.3 Testing of catheter patency

In all studies substances were infused over 7 or 14 days. To analyse if the catheter will be occluded over this time period, animals received first an osmotic minipump filled with sterile PBS and after 5 or 12 days, respectively, the minipumps were replaced by minipumps filled with 6 % Evans Blue dye. Since the perfusion procedure can wash the dye out, the animals were first reopened under anaesthesia to document the infusion area after 7 or 14 days post intrathecal tubing and were then perfused. The perfusion time was additionally reduced by half.

2.3.5 Anterograde labelling of corticospinal tract axons

Three weeks prior to sacrifice, the corticospinal tract (CST) was anterogradely labelled by injections of biotinylated dextran amine (BDA; 10 %, Molecular Probes) into the sensorimotor cortex layer V. As soon as the animal was in deep anaesthesia, the skull was shaved and the head fixed in the stereotactic device (Small Animal Adaptor, David Kopf Instruments) at both external acoustic meati and the front teeth. To expose the brain, the skin was cut and retracted and two small windows as shown in red in Fig. 2.2A were cut with a drill (Fine Science Tools, Ø 1.4 mm) into the *cranium*.

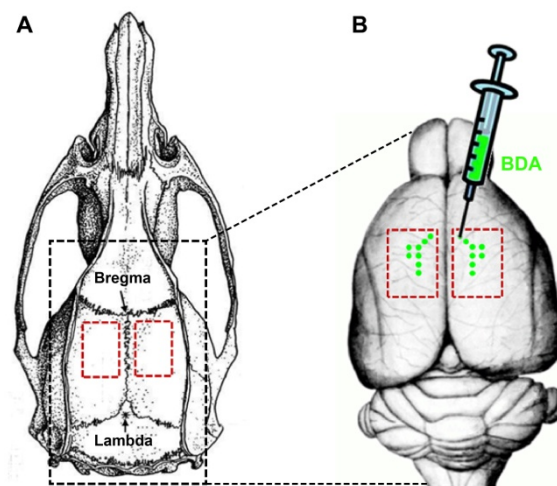


Fig. 2.2: BDA labelling of the corticospinal tract (CST). (A) Rat skull with the stereotaxic reference points bregma and lambda (Paxinos and Watson, 2005). BDA injection points were calculated by identifying the coordinates of bregma through aligning the injection syringe to the point of bregma. Red rectangles represent the area of craniotomy. (B) Schematic illustration of BDA injections into the sensorimotor cortex of the rat (rat brain modified from <http://instruct.uwo.ca/anatomy/530/ratdorsl.gif>) to label CST neurons.

After determination of the coordinates of bregma (Fig. 2.2A), defined as the point of intersection of the sagittal suture with the curve of best fit along the coronal suture (Paxinos and Watson, 2005), the BDA injection coordinates were calculated as shown in table 2.6. These coordinates of the sensorimotor cortex layer V have been previously established (Hermanns, 2001) with the aid of Paxinos and Watson's Stereotaxic Atlas of the Rat Brain (1982). At each injection coordinate (Fig. 2.2B) 0.2 µl BDA was injected at a depth of 1.2 mm using a Hamilton microlitre-syringe (10 µl, Model 701 RN) modified with an attached glass capillary (Ø 40-60 µm) (Klapka et al., 2005). To avoid leakage of BDA at the injection points, the syringe was removed with a 2-minute delay. After all coordinates have been labelled, the skin was closed by using metal clips (Michel).

Table 2.6: Coordinates for BDA labelling of corticospinal neurons in layer V of the sensorimotor cortex

Anterior/posterior: Bregma	Lateral:			
	left		right	
-0.08	+0.2		-0.2	
-0.13	+0.22		-0.22	
-0.18	+0.24	+0.29	-0.24	-0.29
-0.23	+0.24	+0.29	-0.24	-0.29
-0.28	+0.24		-0.24	
-0.33	+0.24		-0.24	

2.3.6 Anterograde labelling of sciatic afferents

Four days prior to sacrifice, the sensory sciatic afferents were anterogradely labelled with 1 % cholera toxin B (CTB, List). Five animals of each group were re-anaesthetized and the skin of both thighs was shaved. Using a scalpel blade an incision was made at the dorsal surface along the femur area. The muscles biceps femoris and gluteus superficialis were separated and then forced apart by a muscle retractor to expose the sciatic nerve (Fig. 2.3A). A loose suture was tied around the nerve after it was raised and stabilized by a fine spatula. To reduce leakage of CTB, only a small incision was made in the epineurium and a glass capillary, attached to a Hamilton microlitre-syringe and aligned to the angle of the nerve, was gently inserted up to 2 mm deep inside (Fig. 2.3B). 2 μ l of 1 % CTB was slowly injected over 3 min and after additional 4 min the capillary was withdrawn. Afterwards, the suture was immediately tightened and the sciatic nerve was crushed proximal to the injection site for 10 sec with a fine forceps for better CTB uptake. Finally, the upper hindlimb muscles and skin were sutured.

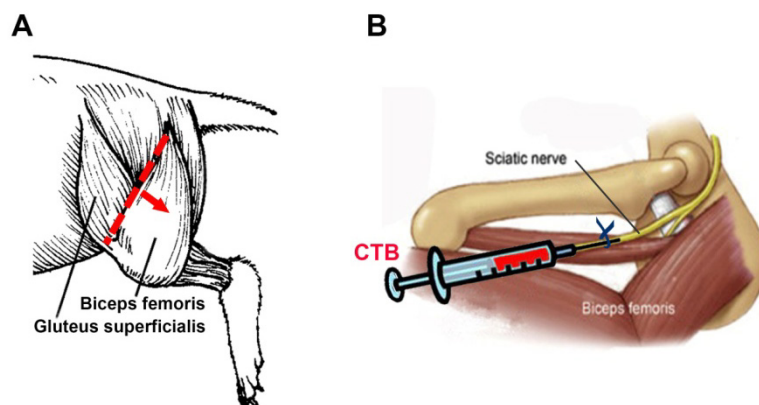


Fig. 2.3: CTB labelling of sciatic afferents. (A) Separation of the muscles biceps femoris and gluteus superficialis (red dashed line) and retraction of biceps femoris (red arrow) to expose the sciatic nerve (rat muscles modified from <http://www2.sluh.org/bioweb/fieldbio/labsheets/ratmuscles2.png>). (B) Schematic illustration of CTB injection into the sciatic nerve. Aligned to the angle of the nerve, the glass capillary of the Hamilton syringe was inserted up to 2 mm (modified from <http://origin-ars.els-cdn.com/content/image/1-s2.0-S0165027013000071-gr1.jpg>).

2.3.7 Post-operative care

Post-operative care included pain relief by s.c. injection of Rimadyl (5 mg/kg, Pfizer) for 2 days post-lesion and prophylactic daily oral administration of the antibiotic Baytril® (0.1 ml, Bayer HealthCare) over one week. Urinary bladders were manually expressed until the normal function returned. If there was blood in the urine or the animal lost more than 20 g of body weight, 5 ml physiological saline was additionally administered s.c.. Veterinary assistance was consulted when animals had signs of infection or autotomy. In case of autotomy the affected area was covered daily with an aluminium spray (Selectavet).

2.3.8 Animal sacrifice

Deeply anaesthetized rats were transcardially perfused with ice-cold phosphate-buffered saline (PBS) for 2 min followed by 4 % paraformaldehyde (PFA, Merck) for 12 min using a perfusion pump (505S Watson-Marlowe) with a pump rate of 25 ml/min. The complete spinal cord was dissected out and post-fixed in 4 % PFA for 24 h at 4°C. Till further processing the spinal cords were stored in PBS at 4°C.

2.4 Tissue preparation

2.4.1 Freezing-Microtome sections

For cutting spinal cord samples with a freezing-microtome (HM 430, Microm) the segments containing the lesion area were cryoprotected in 30 % sucrose at 4°C for 3-4 days. Segments, parasagittally aligned, were freeze-mounted with Tissue-Tek® compound (Sakura) onto the microtome cutting area. Serial sections of 50 µm thickness were cut (cutting temperature: -28 to -24°C) and collected in 24well plates (Costar) prefilled with PBS.

2.4.2 Paraffin sections

To perform immune histology of the fibrous scar after seven days post-lesion, the lesion-containing part of the spinal cord was embedded in paraffin. The paraffin embedding procedure was started by dehydration with ethanol (EtOH). First, the spinal cord segments were incubated in 70 % EtOH for 30 min followed by 90 % EtOH for 60 min and 3 x 60 min in 100 % EtOH. After this EtOH series the spinal cords were incubated in methyl benzoate over night and transferred to benzene on the next day. After 15 min it was filled up with paraffin to a 10 % benzene/paraffin mix and after an incubation time of 30 min at 59°C the benzene/paraffin mix was replaced by pure paraffin for 1 h at 59°C. Two additional paraffin changes (incubation time 1 h at 59°C each) were made before the spinal cords were finally

incubated in pure paraffin over night at 59°C. On the next day the spinal cord segments were parasagittally aligned and embedded in moulds.

The hardened paraffin blocks were cut parasagittally into 10 µm thick sections on a paraffin-microtome (RM 2035, Jung). For mounting them on HistoBond® slides (Marienfeld), sections were transferred into a ~ 40°C warm water bath and dried on a heating plate. Finally, the sections were baked in an oven at 56°C for 10 h.

2.4.3 Gelatine sections

Spinal cord segments were transferred from PBS into 10 % gelatine (BD) in PB with 0.1 % sodium azide (Merck) and kept overnight inside an incubator at 37°C. A thin layer of gelatine was poured in plastic embedding moulds (Peel-A-Way® Embedding Molds, Polysciences Inc.) and after the gelatine had gelled the spinal cord segment was parasagittally placed on top of the gelatine layer. Gradually, the mold was carefully filled up with 'cooled' gelatine (less than 37°C) until the tissue was completely covered. After 30 min at room temperature the molds were stored for complete gelation for at least 12 h at 4°C. One day prior to sectioning, gelatine blocks were incubated overnight in 4 % PFA at 4°C. Glued with superglue (Pattex Sekundenkleber, Henkel) onto the vibratome cutting stage (Thermo Scientific Microm HM650V) and fixed into the PBS filled buffer tray, the spinal cord tissue was cut parasagittally into 50 µm thick serial sections which were collected in 24well plates prefilled with PBS.

2.5 Histological staining protocols

2.5.1 Masson trichrome staining (without nucleus labelling)

To check for catheter induced spinal cord compression, Masson`s trichrome staining, an easy and fast staining method for connective tissue in histological samples, was chosen. The staining procedure for this issue consisted as in the protocol described by Bancroft et al. (1996) of three different solutions (shown in table 2.7), but the cell nuclei staining was omitted (Bancroft et al., 1996). The dyes in solution A stain muscles, fibrin, cytoplasm and erythrocytes red, whereas fibres like collagen are coloured green by solution C. Solution B is essential for the differentiation of the staining.

Table 2.7: Compounds of Masson`s trichrome solutions

Solution A	Solution B	Solution C
0.5 g Acid Fuchsin	1 g Phosphomolybdic acid	2 g Light Green SF yellowish
0.5 g Xylidine Ponceau	200 ml <i>aqua bidest.</i>	200 ml <i>aqua bidest.</i>
198 ml <i>aqua bidest.</i>		4 ml acetic acid
2 ml acetic acid		

The trichrome staining procedure was started by washing the slices in *aqua bidest.* For 10 min the slices were immersed in solution A and subsequently rinsed with *aqua bidest.* Then, the slices were immersed in solution B for 5 min, subsequently rinsed in *aqua bidest.* and incubated for 10 min in solution C. After a last rinsing step in *aqua bidest.*, the tissue slices were mounted on microscope slides and dehydrated with an ascending ethanol sequence (50 %, 70 %, 90 %, 2 x 100 %, each 1 min). Afterwards, the slides were transferred to RotiHistol® (2 x 3 min) and embedded in DPX (Fluka).

2.5.2 Immunohistochemical staining of Coll IV / vWF

The dimension of scarring after treatment was examined by immunofluorescent staining with antibodies against collagen type IV (Coll IV; 1:500, mouse, monoclonal, DSHB) and von Willebrand factor (vWF; 1:500, rabbit, polyclonal, Dako). The staining procedure of 10 µm thick parasagittal paraffin sections was started by deparaffinization with RotiHistol® (3 x 10 min) followed by EtOH 100 % (3 x 5 min), EtOH 90 %, 70 % and 50 % (each 5 min) and 3 washing steps with PBS. To retrieve the Coll IV epitope, the tissue slices were incubated with protease XXIV (0.05 % in 20 mM Tris buffer) for 8 min at 37°C. The epitope retrieval reaction was stopped by washing with PBS (3 x 5 min). After blocking with 5 % donkey serum for 1 h at room temperature (RT) the slices were incubated overnight at 4°C with primary antibodies directed to Coll IV and vWF, then washed again and incubated with secondary antibodies (donkey anti-mouse Alexa488 and donkey anti-rabbit Alexa594, Molecular Probes, 1:500 dilution, respectively) for 1 h at room temperature. To reduce background staining, the slides were additionally stained with 0.3 % Sudan Black dye (Fluka) and after further washing steps with PBS embedded in Fluoromount G (Southern Biotech).

2.5.3 Immunohistochemical staining of axons

For visualization of axons in 50 µm thick parasagittal spinal cord sections, embedded in gelatine, the tissue sections were stained free-floating on a shaker. After washing with PBS (3 x 10 min), sections were blocked with 5 % donkey serum for 1 h at room temperature (RT), followed by dye or antibody incubation. BDA-labelled axons were visualized by Oregon Green® 488 dye incubation (Molecular Probes, 1:1000) overnight at 4°C, CTB-labelled axons by incubation with goat anti-CTB antibody (List Biological Laboratories, 1:80.000) for 72 h at 4°C and the calcitonin gene-related peptide (CGRP) fibre population was stained overnight at 4°C using a goat anti-CGRP antibody (Serotec, 1:1500). All antibodies were diluted in PBS containing 0.3 % Triton X-100 and 5 % donkey serum. Afterwards, the sections were rinsed with PBS (3 x 10 min) and incubated (except Oregon Green stained sections) for 2 h at room temperature with donkey anti goat Alexa 594 (Molecular Probes,

1:500). Every section was additionally stained for glial fibrillary acidic protein (GFAP; Chemicon, 1:500) overnight at 4°C to identify the (GFAP-negative) lesion area, followed by fluorescent visualization by donkey anti-mouse Alexa 647 (Molecular Probes, 1:500, 2 h at RT). Cell nuclei were labelled with 4,6'-diamidino-2-phenylindole (DAPI, Roche). Finally, the sections were rinsed again in PBS (3x), mounted on adhesive microscope slides (HistoBond®, Marienfeld) and coverslipped with Immu-Mount (Thermo Scientific).

2.6 Analysis of tissue sections

2.6.1 Coll IV quantification in the scar

Images of the complete spinal cord scar area of sections stained for Coll IV and vWF were captured at 10x magnification using the mosaic scan function of the BZ-8000 Keyence fluorescent digital microscope. All images of Coll IV (or respectively vWF) were taken with the same exposure times and were merged by the BZ Analyzer software from Keyence.

Coll IV, which is normally present only on CNS meninges and blood vessels (Shellswell et al., 1979; Azzi et al., 1989), becomes a major structural component of basement membrane deposits in the fibrous scar after spinal cord injury (Fig. 2.4A) (Tobin et al., 1979; Risling et al., 1993). To evaluate the lesion-induced Coll IV deposition and its reduction by iron chelators, the Coll IV positive blood vessels in the scar area (Fig. 2.4C) have to be excluded from the Coll IV scar images. The most accurate but time-consuming method is to excise them manually from the images. In this context a faster quantification method was tested by co-staining with the endothelial specific cell marker vWF (Jaffe et al., 1973) and with subsequent subtraction from the Coll IV image.

2.6.1.1 Manual removal of blood vessels from Coll IV images

Using the layer function of Adobe Photoshop, an additional Coll IV image without blood vessels in the scar area was created (Fig. 2.4B). Starting with closing the image background layer, a vector mask was generated and a new layer (filled with black colour) was added and dropped below the image layer. Every single blood vessel was then manually painted black in the vector mask using the brush tool in Adobe Photoshop.

After blood vessel removal the new Coll IV image was further analysed with the NIH open source software ImageJ. Converted to a 16-bit greyscale picture, the scar area was outlined as illustrated in Fig. 2.4 or Fig. 2.5C to measure the area fraction, which is the percentage of pixels in the image that have been highlighted in red by applying a threshold (Fig. 2.5C1). The threshold value was kept constant for every section and was determined by averaging the previously identified threshold values of the control group consisting of animals with only a lesion but no treatment.

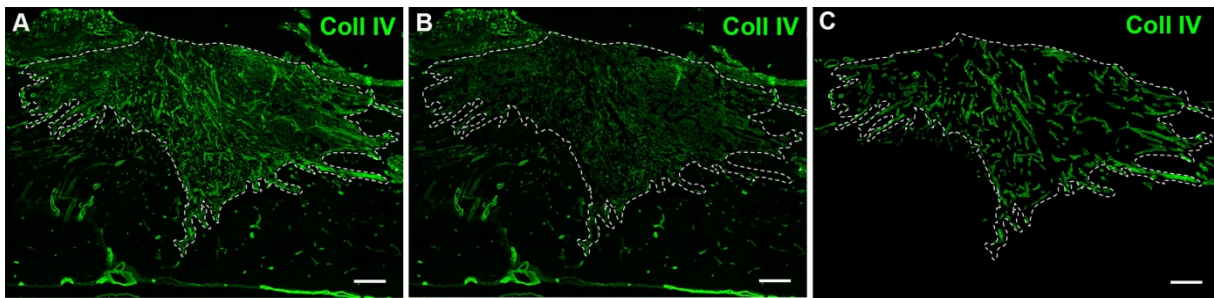


Fig. 2.4: Manual removal of Coll IV positive blood vessels in the scar. (A) Immunohistochemical staining of Coll IV on a parasagittal spinal cord section 7 days after spinal cord injury. (B) Every single blood vessel of the scar was 'painted' black using Adobe Photoshop. (C) Inverted image of (B) showing only labelled blood vessels. Scale bar: 200 μm .

2.6.1.2 vWF pixel subtraction

With ImageJ software Coll IV (Fig. 2.5A) and its corresponding vWF image (Fig. 2.5B) were converted to 16-bit greyscale pictures (Fig. 2.5A1,B1). For the subtraction process a threshold, highlighting the vWF pixels (Fig. 2.5B2), was applied to the image (Fig. 2.5B3) and was then subtracted from the Coll IV image by using the image calculator. In the new image (Fig. 2.5C) the scar area was outlined and the area fraction (Fig. 2.5C1) was measured. All Coll IV area fraction measurements were made at the same threshold level, determined as described before in 2.6.1.1, whereas the vWF threshold was tested for both a constant value and individually varied values. In total, two sections per animal were analysed for evaluation of the quantification methods and were increased to six sections per animal for the analysis of Coll IV reduction through iron chelators.

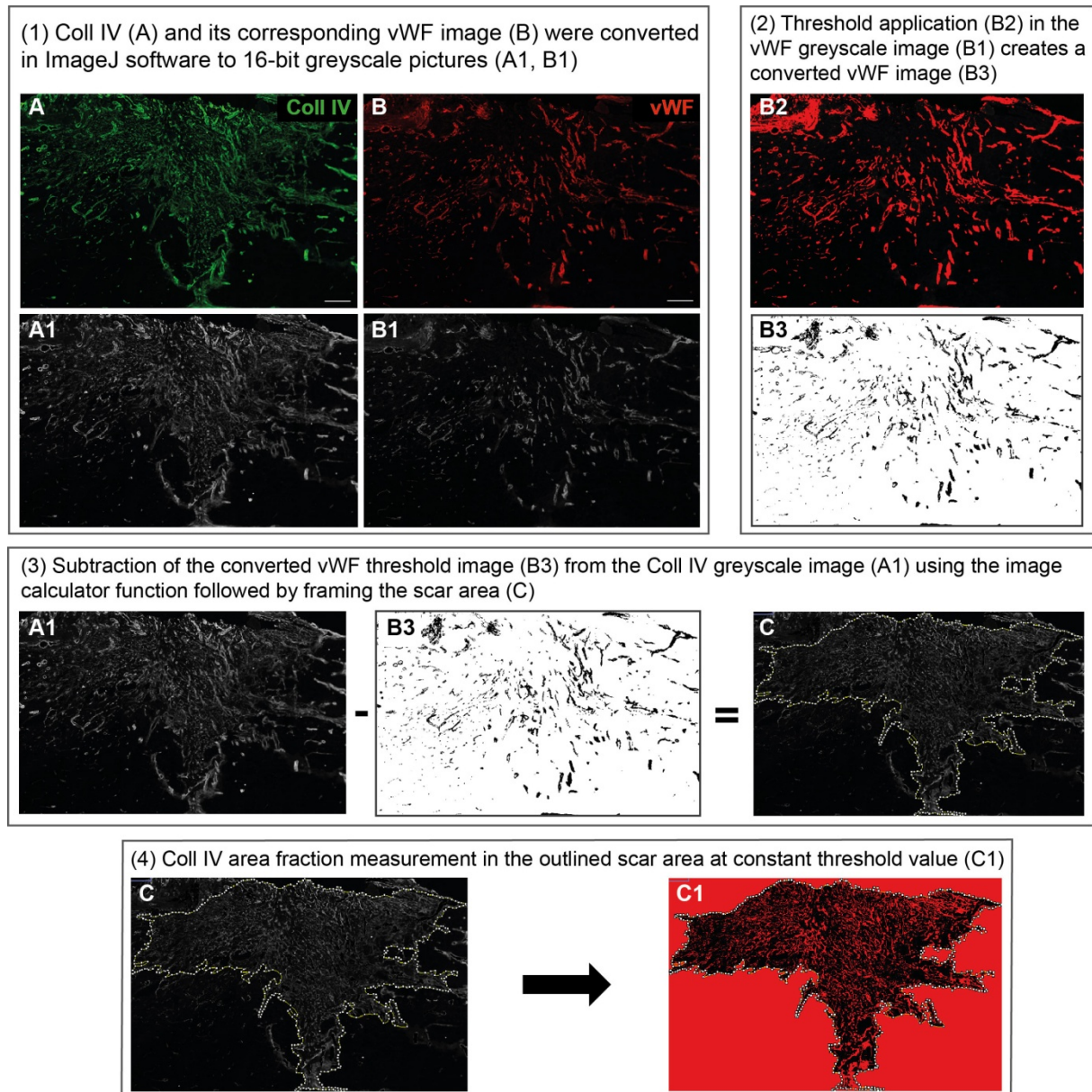


Fig. 2.5: Coll IV quantification by vWF pixel subtraction. 10 μm thick parasagittal spinal cord sections were double-stained for Coll IV (A) and vWF (B) and analysed with ImageJ software. After conversion of both images to 16-bit greyscale pictures (A1,B1) the vWF pixels were highlighted (B2, B3) both with a constant threshold value and individually varied values and were then subtracted from the Coll IV image (A1) using the image calculator function. In the new generated image (C) the Coll IV area fraction was measured in the outlined scar area by applying a constant threshold value (C1). The Coll IV area fraction is defined as the percentage of pixels highlighted in red in the selection (scar). To determine the constant threshold value for Coll IV, the average of individually identified threshold values in sections of control animals (no treatment) was taken.

2.6.2 Analysis of blood vessel density in the Coll IV positive scar area

The analysis of blood vessel density was performed with the vWF images captured for the Coll IV quantification in the scar after iron chelator treatment (see 2.6.1). In total, six spinal cord sections per animal were analysed. For the evaluation of lesion-induced Coll IV deposition after spinal cord injury, as previously described, the Coll IV positive scar was outlined using ImageJ software to measure the Coll IV area fraction. After transferring this scar outline to the corresponding vWF image, the number of vWF stained blood vessels inside the outline was manually counted using the cell counter tool of ImageJ. The blood vessel density was then calculated as the number of vWF positive blood vessels per mm² spinal cord area. Since clear demarcation of neighbouring blood vessels was not always possible, the blood vessel density represents a relative rather than an absolute value.

2.6.3 Evaluation of lesion depth, lesion area and tissue sparing

For standardization of lesion size in the study analysis addressing functional recovery, injury of the central canal was included. Every animal was blindly verified on the basis of GFAP-stained parasagittal spinal cord sections where the lesion area (GFAP negative) can be easily identified. In cases of an intact central canal, the animal was excluded from the study. Additionally, the lesion and spared tissue areas were determined as described by Iannotti et al. (2011) and Schira et al. (2012) with slight modifications. Briefly, the lesion area (GFAP negative) and spinal cord area were outlined in GFAP-stained parasagittal sections using ImageJ software. The section containing the transected central canal and two additional sections in 0.2 mm distance left and right to the central canal were taken for the quantification. The spinal cord area was rostrally and caudally limited to a total length of 2.5 mm with the lesion centrally located. To determine the percent lesion area, the lesion area was divided by the outlined spinal cord area from the same section. The spared tissue area (mm²) was calculated by subtracting the lesion area from the spinal cord area.

2.6.4 Axon quantification

Every 6th parasagittal spinal cord section (4-6 sections per animal) was stained either for BDA, CTB or CGRP to quantify axon regeneration after spinal cord injury. To identify regenerated axons clearly from spared axons, characteristics of regenerating axons described by Steward et al. (2003) were considered during quantification. Due to the lesion model, however, it was not possible to differentiate between regenerated or sprouted axons. With a BZ-8000 Keyence fluorescent digital microscope, axon profiles of all 3 fibre populations were manually counted within the GFAP-negative lesion area (red coloured in Fig. 2.6) and normalized to the lesion area (axons/mm²) using ImageJ software. Additional to

the lesion area, BDA-positive axon profiles were also quantified in the complete dorsal white matter segment caudal to lesion (Fig. 2.6) and CTB-positive axons were counted in the entire rostral spinal cord segment.

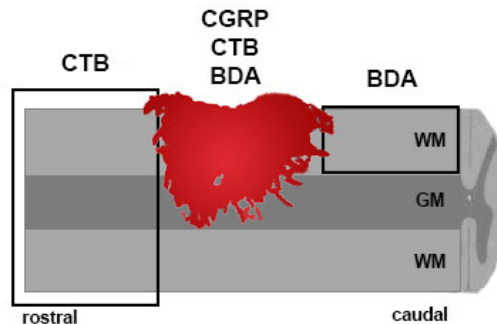


Fig. 2.6: Schematic illustration of the axon quantification areas in parasagittal spinal cord sections. Axon profiles of CGRP-, CTB- and BDA-labelled fibres were manually counted within the GFAP-negative lesion area (red coloured). To investigate axon regeneration beyond the lesion area, BDA-positive axon profiles were additionally quantified in the complete dorsal white matter (WM, boxed area) caudal to the lesion and CTB-labelled axon profiles were counted in the entire rostral spinal cord segment. GM: grey matter; WM: white matter.

2.7 Behavioural testing

2.7.1 Open field Basso, Beattie and Bresnahan (BBB) locomotor test

Locomotor hindlimb function was assessed using the Basso, Beattie and Bresnahan (BBB) rating scale (Basso et al., 1995) and the derived BBB subscore (Lankhorst et al., 1999). The BBB scale consists of an ordinal scale from 0 (no hindlimb movement) to 21 points (consistent, coordinated gait with parallel paw placement and consistent trunk stability). As fine motor control aspects (i.e. toe clearance, predominant paw position, trunk stability and tail position) are only scored in the BBB after consistent coordination of the animal, they were analysed separately in the BBB subscore (regardless of the other BBB parameters).

For measuring locomotor function, rats were placed in a square-cut Plexiglas® open field (1 x 1 m) and while they were freely exploring the surrounding their hindlimb movements were observed by two examiners blinded to the treatment. To make evaluation of toe clearance easier, the open field's floor was covered with a grey rubber mat. The BBB locomotor score was assessed 1 day post-lesion and 1, 2, 12 and 16 weeks post-lesion.

Due to the difficulty of the correct assessment of coordination during BBB observation, forelimb-hindlimb coordination was determined using the regularity index (RI) (see 2.7.3), obtained from the CatWalk gait analysis system (Hamers et al., 2001; Koopmans et al., 2005). The RI-based coordination was defined accordingly to Jeong et al. (2011): As 4 runs were recorded with the CatWalk system, an animal was designated as occasional coordinated, if the animal had performed at least one CatWalk run with 100 % RI; frequent

coordination was assigned to an average of 95 % RI or above, and more than one run (in this case two runs) of 100 % RI. To be considered as consistent coordinated, the animal had to have an average RI of 95 % or more, and with at least half of the runs (in this case at least 3 runs) being at 100 % RI.

2.7.2 Horizontal ladder walking test (Gridwalk)

Deficits in descending fine motor control (i.e. limb placing, stepping and coordination) were examined by assessing the ability to cross a 1 m long horizontal ladder of metal grid bars (\varnothing 3 mm) arranged at random distances, ranging from 1 to 5 cm (Metz et al., 2000; Metz and Whishaw, 2002; Metz and Whishaw, 2009). The distance between the bars was altered in every testing week to prevent animals from learning a movement pattern (Metz and Whishaw, 2002). Starting four weeks prior to the spinal cord lesioning, the rats were handled and familiarized to the horizontal ladder task. Baseline data were collected in the last week prior to surgery and the postoperative testing was started two weeks post-lesion with a two-week testing-rhythm. The performance of each animal was video-recorded and analysed frame by frame counting the number of missteps (slips and falls) in relation to the total number of steps. If an animal was not able to cross the ladder, a maximum error rate of 100 % was given. A total of four uninterrupted crossings per animal and per time point were evaluated for the analysis of locomotor recovery.

2.7.3 CatWalk gait analysis

Differences in gait and footfall patterns were studied using the CatWalk setup and software from Noldus Information Technology. The animals had to cross without interruption a horizontal glass walkway, which is equipped with the Illuminated Footprints™ technology, i.e. whenever the rat makes contact with the glass plate, green illuminated paw prints are visible and captured by the high speed colour camera underneath the walkway. Recordings of the animals' gait were taken in the last week prior to surgery (baseline) and every second week post-lesion as described for the horizontal ladder test. Handling and pre-training for the CatWalk device was done in parallel to the horizontal ladder training. A total of four uninterrupted runs per animal and time point were analysed with the CatWalk XT software. As problems in hindpaw detection turned up after the rats were injured, some CatWalk parameters, which are known to be impaired after spinal cord injury [e.g. base of support – distance between both hindpaws (Hamers et al., 2001)] had to be excluded from the analysis. Though the problem could be solved in close cooperation with Noldus by hardware modifications, we had to stick to the settings created at the beginning of the study. The following parameters could be analysed:

- (1) *Frequencies of regular stepping patterns* (table 2.8) [%]: Six different orders of normal step sequence patterns can be distinguished with prevalence on the Ab pattern. In more than 90 % of all step patterns, Ab pattern is used and a transection injury leads to a pronounced shift in the frequency distribution of the step patterns (Hamers et al., 2001).
- (2) *Regularity index (RI)* [%]: expresses the number of normal step sequence patterns relative to the total number of paw placements. Hence, it is a measure of interlimb coordination. If only normal step sequences (table 2.8), regardless of its sequence, are used during uninterrupted locomotion, the animal has full coordination and a RI of 100 %.
- (3) *Stride length* [cm]: distance between successive placements of the same paw. In uninjured animals the forelimb (FL) and hindlimb (HL) stride lengths are nearly identical, and hence subtracting the HL stride length from FL stride length yields a value near zero (Jeong et al., 2011). After thoracic spinal cord injury rats make smaller FL strides compared to their HL strides, which is reflected in large negative difference values.
- (4) *Swing duration* [s]: duration of no contact of a paw with the glass plate. Similar to stride length, the swing duration of forelimbs and hindlimbs of uninjured animals during coordinated walking are nearly identical. Hence, subtracting the HL swing duration from the FL swing duration reveals a slightly positive value close to zero (Jeong et al., 2011). After injury, HL swing duration rises compared to the fore limbs, resulting in a negative value.

Table 2.8: Normal Step Sequence Patterns

<i>Category</i>	<i>Abbreviation</i>	<i>Sequence</i>
Cruciate	Ca	RF-LF-RH-LH
	Cb	LF-RF-LH-RH
Alternate	Aa	RF-RH-LF-LH
	Ab	LF-RH-RF-LH
Rotate	Ra	RF-LF-LH-RH
	Rb	LF-RF-RH-LH

RF: right forelimb; RH: right hindlimb; LF: left forelimb; LH: left hindlimb. Adapted from Cheng et al. (1997)

2.8 Statistics

For all data (except Coll IV reduction after DFO treatment and analysis of spared tissue) the non-parametric Wilcoxon's Sum of Rank Test for paired comparison and Holm-Bonferroni correction for multiple testing with the type I error rate $\alpha = 0.05$ were applied using Statistix 8.1 software (Analytical Software). As the data of Coll IV reduction (DFO) and spared tissue were normally distributed, the parametric Student's t-test was used for statistical analysis followed by Holm-Bonferroni correction for multiple testing. The experimental groups were considered significantly different at $p < 0.05$. All data are presented as mean \pm SEM.

3 Results

3.1 Intrathecal catheter infusion

Previous results of the iron chelator BPY-DCA have shown the potential of iron chelators to reduce scar formation effectively and to contribute in axonal and functional recovery (Klapka et al., 2005). The application method used consisted of several local injections into the lesion centre and into the adjacent intact spinal cord tissue, which is necessary to reduce scarring also at the rim of the lesion zone. However, this application method is not suitable for clinical use. Intrathecal infusion, on the contrary, is a widely accepted application method for local delivery of pharmacological drugs in patients and in preclinical animal models. Currently intrathecal infusion is clinically used to deliver analgesics or antispasticity drugs (Burchiel and Hsu, 2001; Kumar et al., 2001; Zuniga et al., 2002; Saval and Chiodo, 2010). In order to investigate scar reduction via intrathecally infused iron chelators and its impact on functional recovery, catheter functionality (fixation stability, adverse effects, catheter patency over time) was tested at first.

3.1.1 Catheter fixation and compression

Due to the very narrow subdural and subarachnoid space in rodents in regard to the size of the infusion catheter, several intrathecal catheter application modalities, considering earlier reports of catheter-induced adverse effects in rats, were tested for fixation stability and spinal cord compression. The catheter application described in Materials and Methods in detail (see 2.3.3) and schematically illustrated in Fig. 2.1B turned out to be the most promising approach. Guiding the catheter as far as possible on top of the dura and finally inserting it into the subarachnoid space near-by the dura suture (Fig. 3.1A) is one of the key points of this application.

Furthermore, it was essential to fix the catheter on an autologous fat cushion covering the exposed spinal cord area of Th11 to avoid retraction. To visualize catheter location and distribution of infusion liquid in the injured spinal cord, catheter and osmotic minipump were filled with 3 % Evans Blue dye. After one and seven days post-lesion, just before perfusion, the animals were re-opened to evaluate the catheter position. In seven of eight animals no retraction was visible as blue staining was located only to the lesion area (Fig. 3.1B,D) and one animal showed a slight retraction. In animals which had no additional fixation at Th11, the catheter was drawn back in nearly every case. Here, Evans Blue staining was exclusively found caudal to the lesion site (Fig. 3.1C,E) or in some cases retraction was already obvious after reopening the skin, because the catheter reducing adaptor placed between Th10 and

Th12, which should be normally covered by sutured overlaying muscles, was already visible on top of the muscles (data not shown).

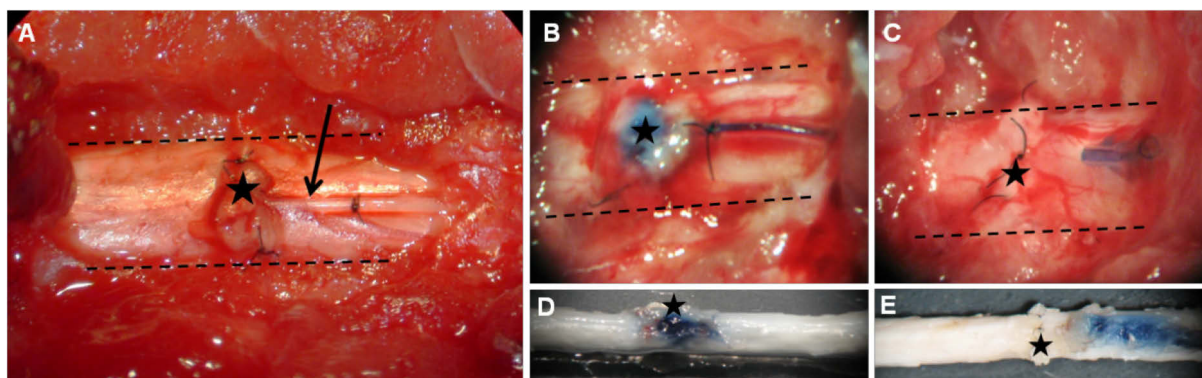


Fig. 3.1: Intrathecal catheter fixation. (A) Guided below Th10 but on top of the dura to the lesion site (asterisk), the catheter was finally inserted into the subarachnoid space (arrow) close to the dura suture. To visualize the distribution of infused liquids in the injured spinal cord and hence the catheter position, catheter and osmotic minipump were filled with 3 % Evans Blue dye. After one day post-lesion animals were reopened (B,C) and after seven days post-lesion the spinal cords were dissected (D,E) to examine the stability of catheter fixation. (B) and (D), representing animals with the additional catheter fixation on the autologous fat cushion, show a blue stained lesion area, indicating no catheter retraction. In contrast, (C) and (E), animals with no additional fixation, show a blue staining only caudal to the lesion site resulting from catheter retraction. Dashed lines outline the spinal cord. Asterisks indicate the lesion area. Orientation in A-E, caudal = right, with view on the dorsal side.

Additional to the fixation between Th10 and Th12 it was necessary to perform a total laminectomy of Th11, so that the catheter could be placed without sharp bending to create a smooth angle between the catheter and the spinal cord at Th10. In doing so, spinal cord compression could be entirely avoided in this area (Fig. 3.2A), but if the angle was too steep, intense compressions like the one shown in Fig. 3.2B were visible.

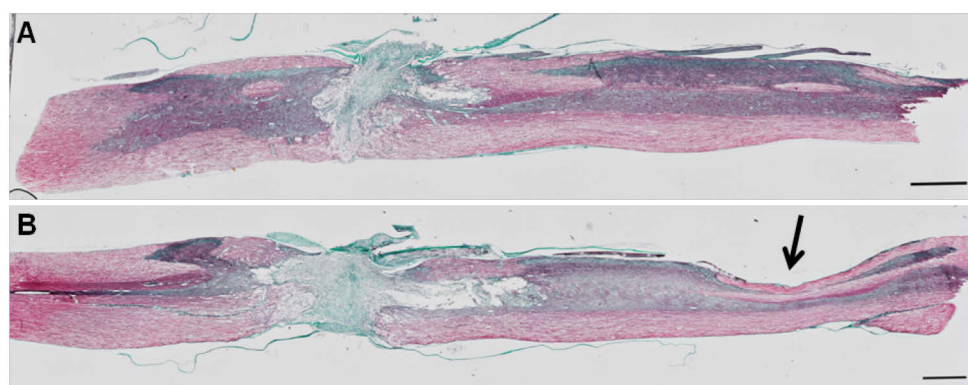


Fig. 3.2: Catheter induced compression. Trichrom staining (Weigert) was used to visualize catheter-induced compressions of the spinal cord at seven days post-lesion. (A) Animals which received a total laminectomy of Th11, allowing a smooth angle between catheter and the spinal cord at Th10, showed no compression of the caudal spinal cord. (B) In contrast, intense compression was visible (arrow) in animals with a small laminectomy of Th11 exercising pressure on the spinal cord through the sharp bending of the catheter. Orientation in A and B, caudal = right, dorsal = up. Scale bar: 1 mm.

3.1.2 Catheter patency

To ensure unrestricted drug infusion over 7 and 14 days, catheter patency was tested by replacing PBS filled osmotic minipumps after 5 or 12 days post-lesion with 6 % Evans Blue dye primed minipumps. Already at reopening before perfusion (7 or 14 days post-lesion) blue stained tissue was visible in both infusion paradigms. While the surrounding tissue in animals with 7 day infusion was clearly stained blue, the staining after 14 days appeared to be mainly localised to the spinal cord (not shown). In these animals, uncovering of the lesion area was tougher than after 7 days indicating a stronger formation of connective tissue around the lesion area. The dissection of the complete spinal cord after perfusion revealed in both infusion paradigms deeply stained lesion areas (Fig. 3.3A,C) and confirmed continuous drug infusion over 7 and 14 days. Beyond the lesion area, blue staining was visible in a weakening gradient in the rostral-caudal direction following the natural flow of cerebrospinal fluid. Especially, the central canal (arrow in Fig. 3.3B,D) was still stained deep blue at the caudal end of the spinal cord segment in comparison to the surrounding spinal cord tissue.

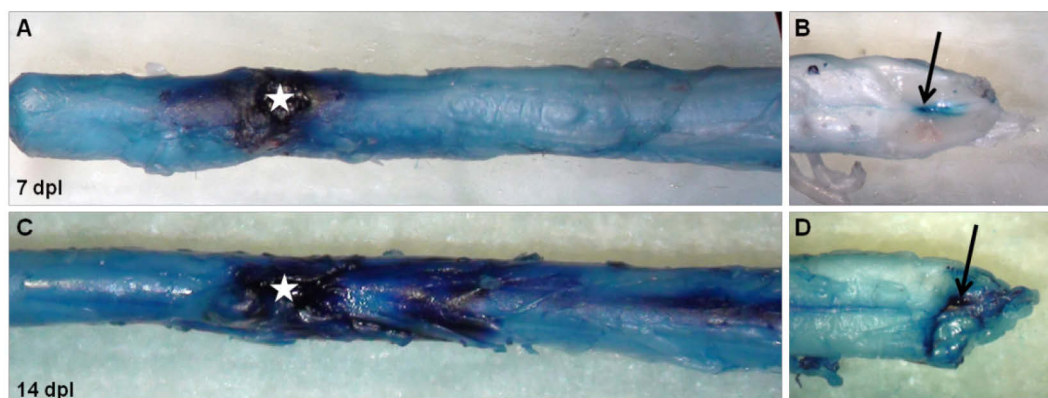


Fig. 3.3: Continuous liquid infusion over 7 and 14 days. In order to evaluate catheter patency for an intrathecal infusion period of 7 (A,B) and 14 days (C,D), PBS filled osmotic minipumps were replaced 5 or 12 days after injury by minipumps primed with 6 % Evans Blue dye. In both cases, extensive blue staining of the lesion area (white asterisk in A and C) and beyond was visible. Dye intensity decreased in rostral and caudal direction, whereas the end of the caudal spinal cord segment showed an intensely stained central canal (arrow in B and D). Orientation in A and C, caudal = right with dorsal view; B and D shows the ventral side of the slanted end segment of the caudal spinal cord. dpl: days post-lesion.

3.2 Coll IV reduction in the scar using iron chelators

Previous work by Stichel et al. (1999a), Hermanns et al. (2001b) and Klapka et al. (2005) has shown that the anti-scarring treatment (AST), consisting of the iron-chelator BPY-DCA and 8-Br-cAMP, which were locally injected, reduces effectively the collagen scar formation and promotes functional recovery after spinal cord injury in rats. As injections into the adjacent intact spinal cord tissue were necessary to reduce scarring also at the rim of the lesion zone, which is clinically not applicable, intrathecally infused BPY-DCA was tested in regard to its

potency to reduce Coll IV scarring after dorsal hemisection. One disadvantage of BPY-DCA is that it has to be solved in Tris buffer, which can penetrate biological membranes in its un-ionized form and cause cytotoxicity (ANGUS chemical company technology review). Hence, it is hardly imaginable that BPY-DCA would be used for clinical applications. For this reason, the efficacy of two PBS-/water-soluble iron chelators, 2,2'-bipyridine (BPY) and deferoxamine mesylate (DFO; Desferal[®]), on Coll IV reduction was also examined and compared with BPY-DCA. For quantitative evaluation of the forming Coll IV network in the lesion area, a suitable analysis method with consideration of Coll IV positive blood vessels was developed at first.

3.2.1 Coll IV quantification method

To measure the lesion-induced Coll IV expression in histological sections, double-stained for Coll IV and vWF, the percentage of Coll IV positive pixels in the scar area (area fraction) was determined using ImageJ software. As Coll IV is also present on blood vessels (Shellswell et al., 1979; Azzi et al., 1989) and iron chelators are able to promote angiogenesis (Beerepoot et al., 1996; Ikeda et al., 2011), Coll IV positive pixels of blood vessels have to be excluded from Coll IV images before quantification. The most accurate way for blood vessel removal on histological stainings is to excise them manually in the Coll IV images. Due to the very time-consuming aspect, a faster but slightly imprecise method via subtraction of the co-stained vWF was compared with the manual removal technique. Two sections of each animal were analysed for both conditions using a constant Coll IV threshold. Since blood vessel stainings with Coll IV and vWF are not congruent, the vWF subtraction method was performed with both a constant and individually varied vWF thresholds. The comparison of vWF subtraction using an individually varied vWF threshold with the manual removal method revealed no significant difference between them (Fig. 3.4). In contrast, vWF subtraction using a constant vWF threshold for every section showed in all groups the highest percentage of Coll IV pixels and in two of them (20 mM Tris and 1.1 µg/d BPY-DCA), the difference to the manual removal method was even statistical significant (* $p < 0.05$). Concluding, vWF subtraction via an individually adjusted vWF threshold can be used as an equivalent method to analyse lesion-induced Coll IV expression in the scar. Following evaluations of Coll IV expression after iron chelator treatment were done accordingly to this method.

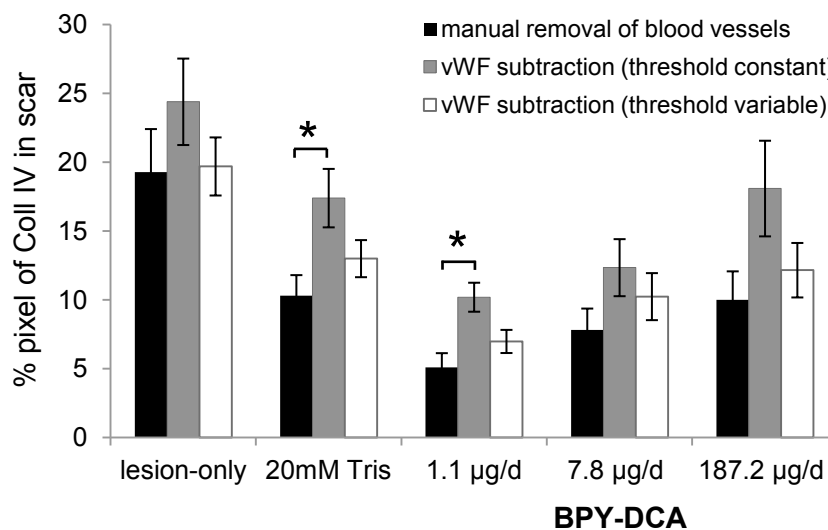


Fig. 3.4: Comparison of the Coll IV quantification methods. The most accurate method to exclude Coll IV positive blood vessels from lesion-induced Coll IV expression is to excise them manually (black bars). The quantification of the two alternatives revealed that vWF subtraction using individually varied vWF thresholds (white bars) showed no statistical difference to the manual removal method, whereas a constant vWF threshold (grey bars) led in every group to the highest Coll IV pixels percentage and in two of them a statistical significance could be found. Results are shown as mean \pm SEM; * $p < 0.05$ (Wilcoxon's Sum of Rank Test).

3.2.2 Coll IV reduction via BPY-DCA infusion

Three different BPY-DCA concentrations (1.1 $\mu\text{g/d}$; 7.8 $\mu\text{g/d}$; 187.2 $\mu\text{g/d}$ solved in 20 mM Tris-buffer), adapted from the single injection concentration of 40 mM (7.8 μg) (Schiwy et al., 2009), were tested for their potential to reduce Coll IV scarring after seven days of infusion. As controls, a group receiving 20 mM Tris-buffer and a group with only a lesion but no treatment were included. In six sections per animal, stained for Coll IV (Fig. 3.5 A-C) and vWF, the area pixel percentage of Coll IV in the scar was measured. The highest Coll IV reduction with 57 % in relation to the lesion-only group and 36 % to the Tris group was achieved by the lowest BPY-DCA concentration (1.1 $\mu\text{g/d}$). As shown in Fig. 3.5D the infusion of 1.1 $\mu\text{g/d}$ BPY-DCA reduced highly significantly the Coll IV pixel percentage in comparison to both control groups. Additionally, the infusion of 7.8 $\mu\text{g/d}$ BPY-DCA significantly reduced Coll IV in the scar but only in comparison with the lesion-only group (reduction of 49 %), whereas 187.2 $\mu\text{g/d}$ BPY-DCA had no statistical effect. Two of six animals of this group had to be excluded due to strong haemorrhage. Interestingly, even the Tris infused animals showed a highly significant reducing effect (33 %) on Coll IV scarring compared to the lesioned-only animals.

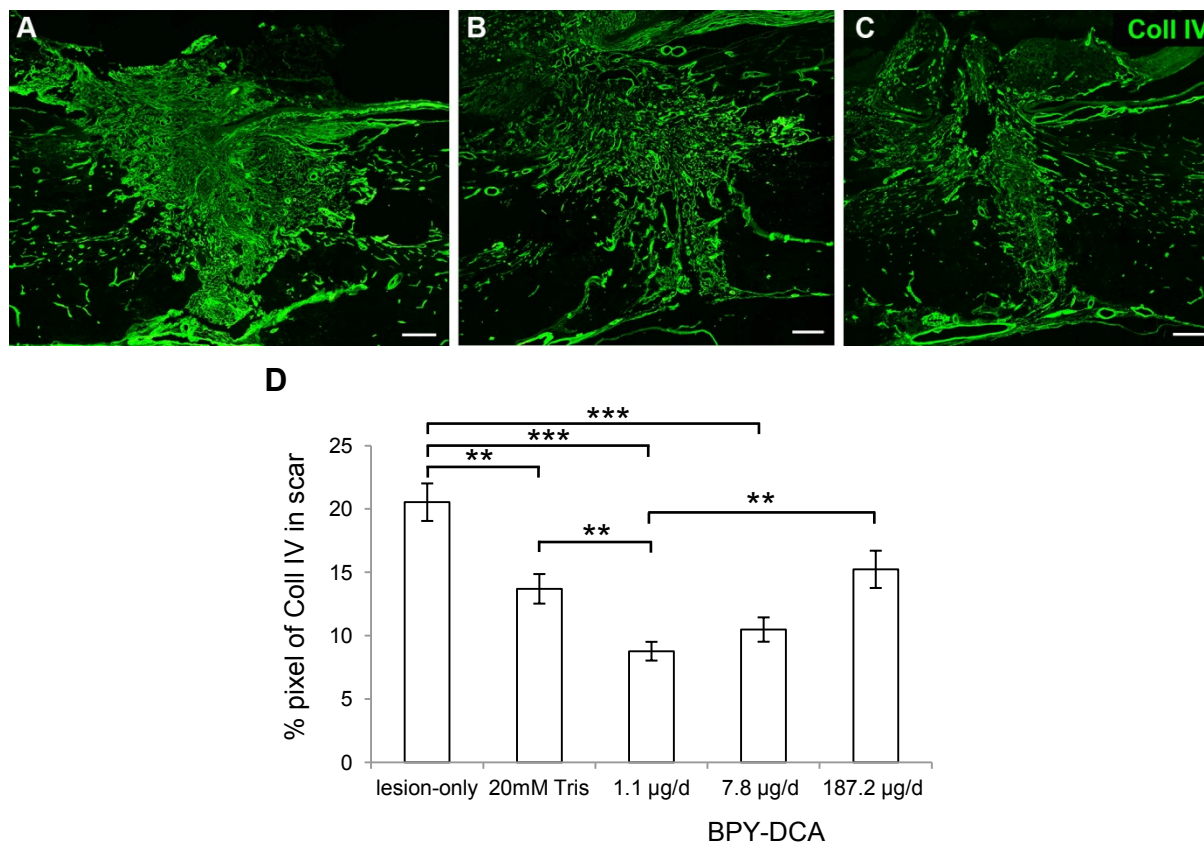


Fig. 3.5: BPY-DCA, intrathecally infused over 7 days, significantly reduces Coll IV in the scar. (A-C) Immunohistochemical staining of Coll IV on parasagittal spinal cord sections representing the treatment groups lesion-only (A), 20 mM Tris (B) and 1.1 µg/d BPY-DCA (C). (D) Quantification of the Coll IV pixel percentage in the scar area revealed that 1.1 µg/d BPY-DCA infused for 7 days has the highest Coll IV reducing effect and was highly significant in comparison to the lesion-only group as well to the vehicle group (20 mM Tris). Note, Tris-buffer alone has also a significant reducing effect on Coll IV scarring compared to the lesion-only group. Orientation in A-C, caudal = right, dorsal = up. Scale bars: 200 µm. Results are shown as mean ± SEM. * $p < 0.05$, ** $p < 0.01$, *** $p < 0.001$ (Wilcoxon's Sum of Rank Test with Holm-Bonferroni correction).

3.2.3 Coll IV reduction via BPY infusion

In order to compare the Coll IV reducing effect of BPY with BPY-DCA, the experiment was equivalent designed. As BPY-DCA is the more potent iron chelator of both, higher concentrations (based on the best BPY-DCA concentration: 1.1 µg/d) were chosen for BPY. 0.71 µg/d, 7.12 µg/d and 71.2 µg/d BPY for 7 days were tested for their potential to reduce Coll IV in the scar area in comparison to the vehicle-group PBS and the lesion-only group. The histological Coll IV quantification (Fig. 3.6A-C) revealed that only the BPY infusion of 7.12 µg/d significantly reduced Coll IV in the scar (Fig. 3.6D) and had a reducing effect of 35 % in relation to the lesion-only group and 30 % in relation to PBS. The other two concentrations had no statistical effect on Coll IV reduction.

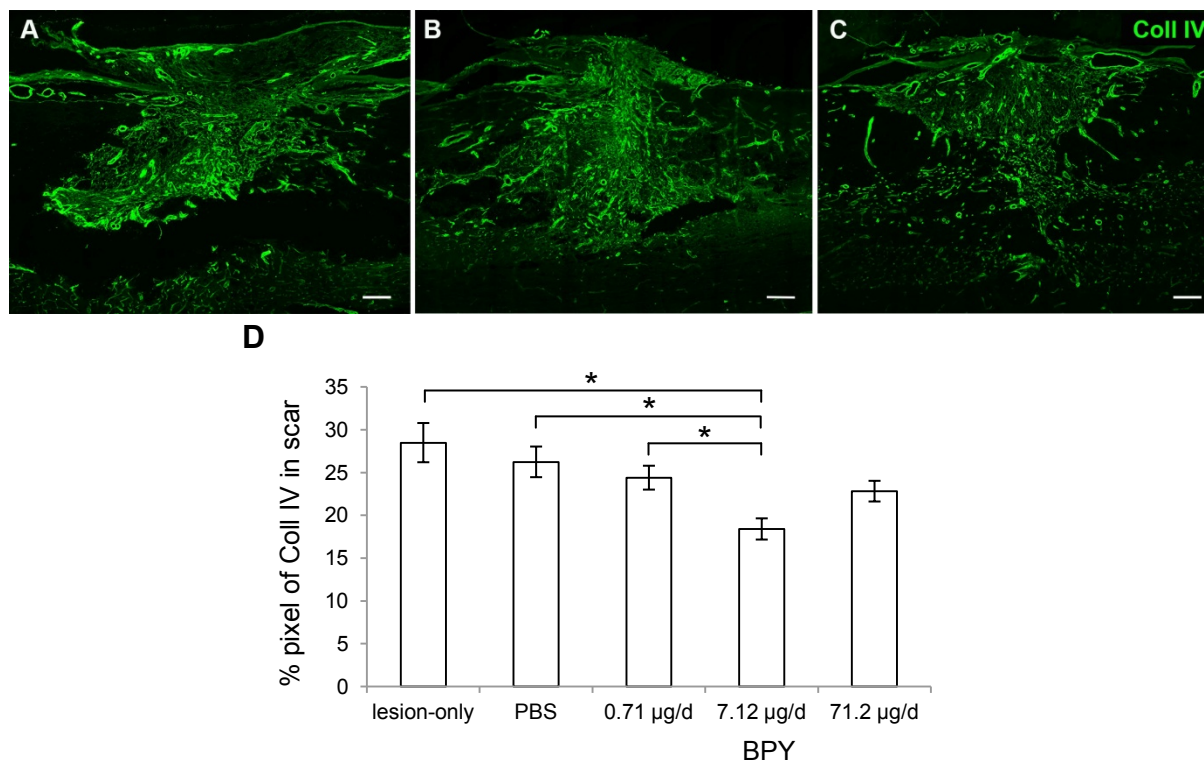


Fig. 3.6: Intrathecal infusion of BPY over 7 days significantly reduces Coll IV in the scar. (A-C) Immunohistochemical staining of Coll IV on parasagittal spinal cord sections representing the treatment groups lesion-only (A), PBS (B) and 7.12 µg/d BPY (C). (D) Quantification of the Coll IV pixel percentage in the scar area showed that only the BPY infusion of 7.12 µg/d significantly reduced Coll IV in the scar. Orientation in A-C, caudal = right, dorsal = up. Scale bars: 200 µm. Results are shown as mean ± SEM. * $p < 0.05$, ** $p < 0.01$, *** $p < 0.001$ (Wilcoxon's Sum of Rank Test with Holm-Bonferroni correction).

3.2.4 Coll IV reduction via DFO infusion or systemic application

Having the advantage of being an approved drug, DFO (Desferal®) was also tested for its potency to reduce Coll IV in the scar. Three different DFO concentrations (10 µg/d, 50 µg/d, 100 µg/d solved in PBS) were intrathecally infused over seven days and were compared to the vehicle group PBS and lesion-only group. All three concentrations showed highly significant reduced Coll IV pixel percentages (Fig. 3.7B,D) in comparison to the lesion-only (Fig. 3.7A) as well to the PBS group. The highest Coll IV reduction effect of 37 % in relation to the lesion-only group (30 % in relation to PBS) was achieved by the DFO infusion of 100 µg/d, but there was no statistical difference between the three DFO concentrations detectable.

Due to this encouraging result, an additional experiment over 14 days was designed to evaluate DFO's systemic potency versus local intrathecal infusion. In order to ensure comparability to the data obtained before, a group with 7-day intrathecal DFO infusion was included. Biochemically assessed by Spinal Cord Therapeutics to be the best concentration for Coll IV reduction in the scar, 10 µg/d was intrathecally applied. For systemic i.p.

administration, 350 mg/kg/d was used. Due to the short terminal elimination half life (~ 6 h) of DFO (Allain et al., 1987; Howland, 2006) the dosage was split into 175 mg/kg every 12 hours. In contrast to the previous experiment, DFO was diluted in pure water according to clinical use. The analysis of Coll IV pixel percentages revealed highly significant Coll IV reduction after systemic (14 days) (Fig. 3.7C,E) and intrathecal (7 days) administration (Fig. 3.7B,E). Intrathecal DFO infusion over 14 days was worse than 7 days, but nevertheless Coll IV was significantly reduced in the scar in comparison to the pure water group (Fig. 3.7E). Among the three DFO groups, no statistical difference could be found. Hence, systemic DFO administration with a reducing effect of 27 % is also effective as intrathecal infusion (32 % after 7 days and 20 % after 14 days).

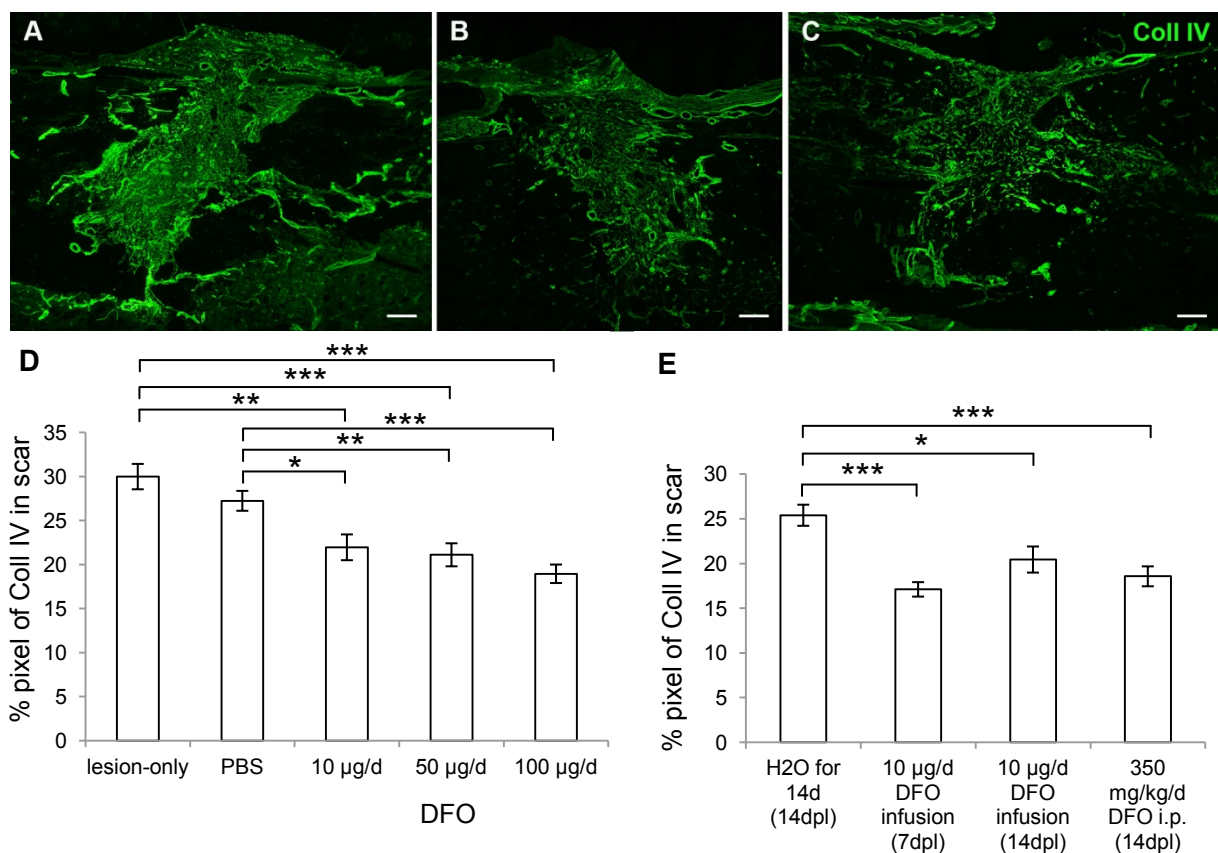


Fig. 3.7: DFO, intrathecally infused or systemically (i.p.) applied, significantly reduces Coll IV in the scar. (A-C) Representative Coll IV stainings of parasagittal spinal cord sections from animals receiving lesion-only (A), 10 µg/d DFO intrathecal infusion for 7 days (B) or systemic i.p. DFO application for 14 days (C). (D) Initially three different DFO concentrations were intrathecally infused and all three concentrations significantly reduced Coll IV in the scar in comparison to the lesion-only as well to the PBS group. The three DFO groups itself were not statistical different from each other. (E) Systemic (i.p.) administration of DFO significantly reduced Coll IV deposition in comparison to the water control group and has an equivalent effect to intrathecal infusion. Among the different DFO groups, no statistical difference could be found. Orientation in A-C, caudal = right, dorsal = up. Scale bars: 200 µm. Results are shown as mean ± SEM. * $p < 0.05$, ** $p < 0.01$, *** $p < 0.001$ (Student's t-test with Holm-Bonferroni correction).

3.3 Effect of DFO on blood vessel density

Several iron chelators including DFO have been shown to induce angiogenesis through upregulation of the vascular endothelial growth factor (VEGF) (Gleadle et al., 1995; Beerepoot et al., 1996; Linden et al., 2003; Ikeda et al., 2011; Hertzberg et al., 2012). Revascularisation of damaged central nervous tissue is an important aspect to support reparative events (Fassbender et al., 2011; Oudega, 2012) and several studies have shown that the promotion of blood vessel formation is involved in the restoration of impaired functions (Lu et al., 2004; Wang et al., 2004; Xiong et al., 2008; Xiong et al., 2010).

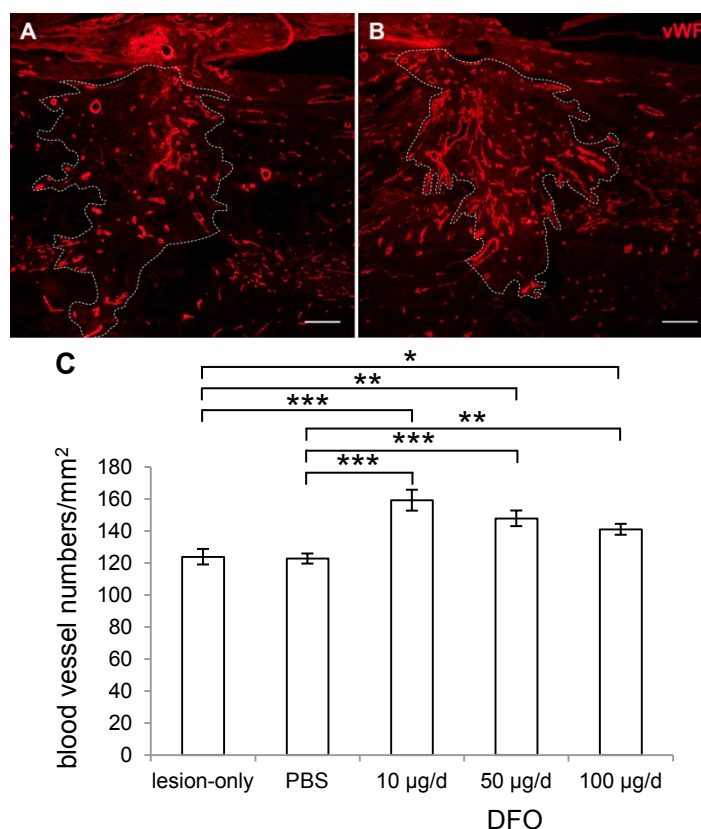


Fig. 3.8: Intrathecally infused DFO enhances the blood vessel density in the Coll IV positive scar area at 7 dpl. Representative vWF images of parasagittal spinal cord sections showing the lesion-only condition (A) and 50 µg/d DFO intrathecally infused (B). VWF stained blood vessels were manually counted inside the Coll IV positive scar area outlined by the dashed line. Scale bar: 200 µm. (C) Quantification of blood vessel density inside the outlined scar area revealed that DFO-treated animals had significantly more blood vessels per mm² than the vehicle-group PBS or the lesion-only group. Results are shown as mean ± SEM. *p < 0.05, **p < 0.01, ***p < 0.001 (Student's t-test with Holm-Bonferroni correction).

To evaluate whether DFO's potential to induce angiogenesis is expressed in increased blood vessel densities in the scar area, the number of vWF stained blood vessels were counted and related to the scar size. The analysis was performed using the Coll IV/vWF double-stained spinal cord sections from animals which received DFO for 7 days intrathecally (the same animals as in 3.2.4). During the evaluation of Coll IV positive area fraction (3.2.4) an

impression was created that some scar areas had more blood vessels than the others (Fig. 3.8). The quantitative analysis confirmed that the blood vessel densities were significantly increased in animals treated with DFO in comparison to the vehicle group PBS and the lesion-only group (Fig. 3.8). All three tested DFO concentrations significantly induced more vWF positive blood vessels per mm² spinal cord area. An equivalent result was also seen after intrathecal infusion of BPY-DCA for 7 days (data not shown).

3.4 Analysis of functional recovery after DFO intrathecal infusion

Being effective in reducing Coll IV and enhancing revascularization in the scar as shown above, DFO's potential on functional recovery after spinal cord injury was tested next. DFO (10 µg/d) was intrathecally infused for 14 days via a subcutaneously implanted osmotic minipump (Alzet pump model 1007D: 0.5 µl/h for 7days), which was replaced after 7 days by a new fresh filled one, as the Coll IV reduction data after continuous infusion for 14 days indicate decreasing efficacy of DFO (see Fig. 3.7E). Due to the very limited axon regeneration in the adult CNS, DFO was combined in an additional group with the chemokine stromal cell-derived factor 1α (SDF-1α). SDF-1α is able to promote neurite outgrowth in the inhibitory environment of CNS myelin and it enhances axonal sprouting (Opatz et al., 2009; Jaerve et al., 2011). So far, less information about the effect of DFO on axonal and functional regeneration after spinal cord injury is available. Nowicki et al. (2009) reported that DFO mediates neurite outgrowth *in vitro* and Sinis et al. (2009) found an increase in the density of regenerating axons in transected peripheral nerves. Significant improvement of functional deficits after intraperitoneally DFO administration in spinal cord injured mice was described by Paterniti et al. (2010), however, based only on a single functional test (modified murine BBB), which was assessed for 10 days. To evaluate long-term locomotor recovery in more detail, three different locomotor tests were performed over 16 weeks. Additionally to the most widely used open field locomotor score (BBB) to assess the overall locomotor behaviour, deficits in descending fine motor control were studied with the horizontal ladder walking test and differences in gait and footfall patterns with the CatWalk system. The latter two tests were performed every second week, starting two weeks post-lesion, whereas the BBB was assessed at 1 day post-lesion, and 1, 2, 12 and 16 weeks post-lesion. Due to the lesion asymmetry both hindlimbs were analysed separately. In total, five groups were tested: DFO (10 µg/d), DFO-vehicle PBS, SDF-1α (10 µM), SDF-1α-vehicle BSA and DFO+SDF-1α (see table 2.5.). The combinatorial treatment DFO+SDF-1α was applied by separate osmotic minipumps connected to a self-made Y catheter.

3.4.1 Autotomy

11 of 60 animals developed severe autotomy during the functional testing time and had to be killed prematurely. In most cases first signs of autotomy were seen at approximately four weeks post-lesion and only on the right hindlimb side, which is less injured due to the lesion asymmetry. Despite treatment with aluminium spray, the autotomy progress could not be stopped, leading to prematurely killing of the animal and exclusion from the study. Decoding the treatment identity at the end of the study revealed that all groups were affected by autotomy but with a higher incidence in the BSA group. In total, four animals of the BSA group (40 %), two animals of DFO (20 %), SDF-1 α (18 %) and DFO+SDF-1 α (20 %) respectively and one animal in the PBS group (11 %) showed severe autotomy. These animals are not listed in the overview table 2.5.

3.4.2 Horizontal ladder walking test (Gridwalk)

Crossing a horizontal ladder requires that the animal places accurately its limbs on the randomly spaced bars. By counting the number of missteps (slips and falls), deficits in descending fine motor control can be examined. In four uninterrupted crossings per animal and per time point, the percentage of missteps in relation to the total number of steps was assessed. The statistical analysis revealed that treating spinal cord injured rats with DFO did not result in an overall significant improvement of locomotor performance. Only in one time point for the left HL (wpl 6) and two for the right HL (wpl 2 and 6), a significant improvement to the PBS group was detected (see table 3.1 and 3.2). The most surprising result in this analysis showed the BSA group. Included in this study as vehicle for SDF-1 α , BSA treatment induced highly significant functional improvement compared to the PBS group (Fig. 3.9A,B) and it was the group with the fewest missteps in all time points. It was conspicuous that the massive injury-induced increase in missteps was less pronounced in the BSA group than in the other groups, especially for the right HL, which is less affected due to the lesion asymmetry. Quite similar results were also obtained by the DFO+SDF-1 α group, as for the left HL no statistical difference to the BSA group could be found and for the right HL only at 12 weeks post-lesion, where the BSA group made significantly less missteps than the DFO+SDF-1 α group (Fig. 3.9A,B). In comparison to the PBS group, DFO+SDF-1 α treatment significantly induced functional improvement at several time points (see Fig. 3.9A,B). Interestingly, there was no statistical difference detectable between the DFO and DFO+SDF-1 α group at any time point (not shown). Although BSA-treated animals showed impressive improvements of locomotor performance, the SDF-1 α group, which contained the same amount of BSA, was less effective. At several time points, as illustrated in Fig. 3.9C,D, SDF-1 α -treated animals performed significantly worse than the BSA-treated animals and in

comparison to the PBS group significant improvement could be only found for the right HL, where, except of two time points (2 and 8 wpl), the SDF-1 α -treated animals made significantly less missteps than the PBS-treated animals.

Table 3.1: Summary of missteps [%] of the left hindlimb

<i>wpl</i>	<i>PBS</i>	<i>BSA</i>	<i>DFO</i>	<i>DFO+SDF-1</i>	<i>SDF-1</i>
2	47.48 \pm 3.37	37.76 \pm 3.22	44.70 \pm 3.11	50.64 \pm 4.58	58.86 \pm 3.43 ^{###}
4	60.49 \pm 5.56	33.52 \pm 4.05*	49.63 \pm 5.06	33.91 \pm 3.27**	48.03 \pm 2.93
6	54.89 \pm 4.22	36.06 \pm 4.00*	39.97 \pm 2.81*	38.42 \pm 3.06*	49.15 \pm 2.98
8	46.58 \pm 3.72	29.68 \pm 3.89	38.83 \pm 4.21	34.66 \pm 2.87	50.39 \pm 3.65 ^{###}
10	50.28 \pm 3.33	30.31 \pm 3.83**	49.42 \pm 4.70	32.26 \pm 3.28**	41.50 \pm 2.99
12	50.76 \pm 3.85	34.11 \pm 3.85	51.28 \pm 5.65	34.86 \pm 3.63	49.40 \pm 3.56
14	56.87 \pm 3.29	30.37 \pm 3.70***	49.42 \pm 4.83 [#]	40.04 \pm 3.04**	47.52 \pm 3.11 ^{###}
16	53.95 \pm 4.00	31.97 \pm 2.88**	50.36 \pm 4.79	37.40 \pm 2.28*	41.27 \pm 3.19

Results are shown as mean \pm SEM. Statistical differences were determined with Kruskal-Wallis followed by Wilcoxon's Sum of Rank Test and Holm-Bonferroni correction. *p < 0.05, **p < 0.01, ***p < 0.001 vs. PBS group; #p < 0.05, ##p < 0.01, ###p < 0.001 vs. BSA group.

Table 3.2: Summary of missteps [%] of the right hindlimb

<i>wpl</i>	<i>PBS</i>	<i>BSA</i>	<i>DFO</i>	<i>DFO+SDF-1</i>	<i>SDF-1</i>
2	46.54 \pm 2.94	14.52 \pm 3.33***	28.58 \pm 3.62**	21.24 \pm 3.82***	39.60 \pm 3.93 ^{###}
4	50.94 \pm 6.44	12.48 \pm 2.50***	34.84 \pm 6.44	24.47 \pm 3.40*	24.32 \pm 2.71* [#]
6	41.99 \pm 5.27	10.35 \pm 2.48***	20.42 \pm 2.83**	25.27 \pm 3.76	24.22 \pm 3.05* [#]
8	33.45 \pm 3.68	10.40 \pm 2.53***	22.00 \pm 2.85 [#]	17.13 \pm 3.61*	31.75 \pm 4.71 ^{###}
10	42.29 \pm 2.68	16.23 \pm 3.51***	35.41 \pm 5.92	18.50 \pm 2.85***	25.92 \pm 3.23**
12	38.00 \pm 3.96	13.42 \pm 3.33***	40.14 \pm 6.69 [#]	25.30 \pm 3.22 [#]	20.53 \pm 2.52**
14	40.68 \pm 3.62	15.26 \pm 2.70***	32.88 \pm 5.51	23.81 \pm 2.82*	24.69 \pm 3.61*
16	43.96 \pm 4.66	18.02 \pm 2.83**	32.61 \pm 5.59	29.91 \pm 3.89	22.99 \pm 3.73**

Results are shown as mean \pm SEM. Statistical differences were determined with Kruskal-Wallis followed by Wilcoxon's Sum of Rank Test and Holm-Bonferroni correction. *p < 0.05, **p < 0.01, ***p < 0.001 vs. PBS group; #p < 0.05, ##p < 0.01, ###p < 0.001 vs. BSA group.

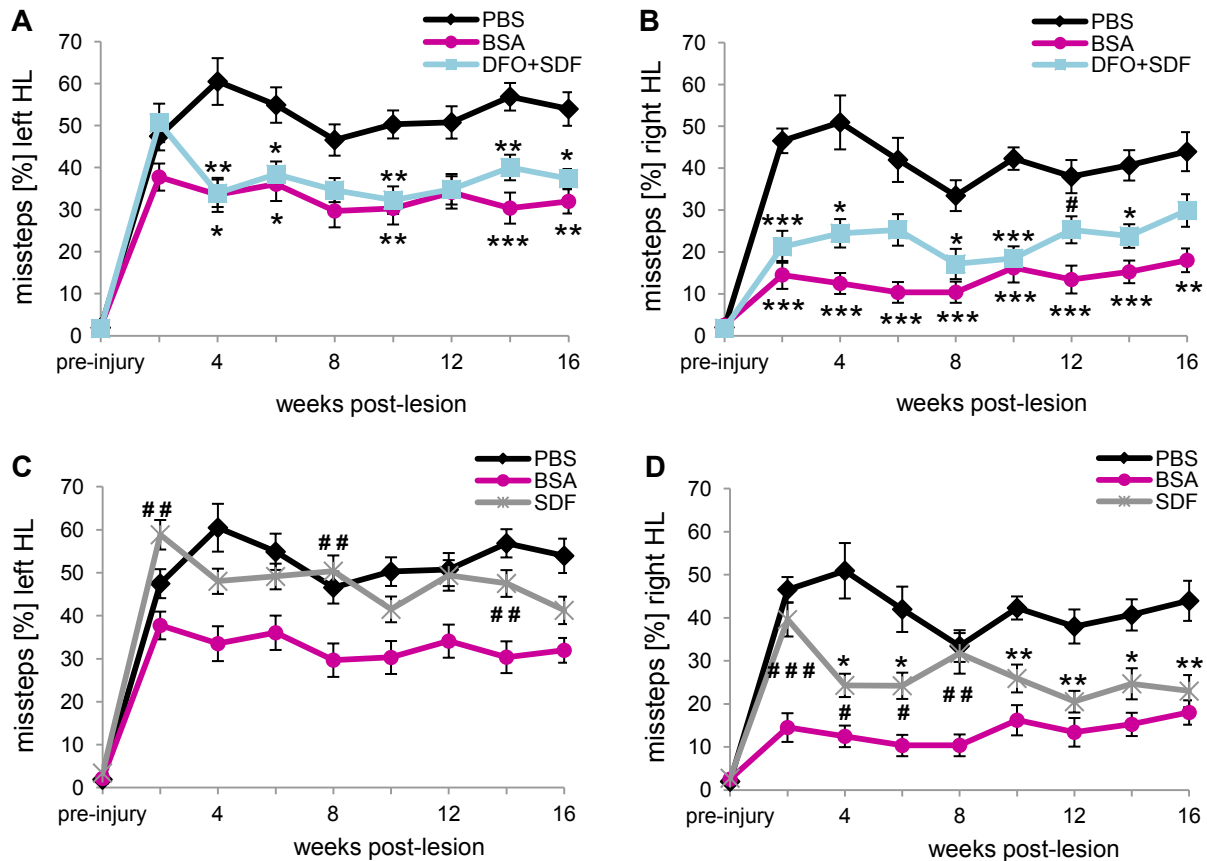


Fig. 3.9: Horizontal ladder walking test. Treating spinal cord injured rats with BSA or DFO+SDF-1 α induced significant functional recovery in both left (A) and right (B) hindlimb compared to the PBS control group. In contrast to the expected injury-induced massive increase in missteps directly after injury, BSA and DFO+SDF-1 α -treated animals showed significantly less impairment. Infusing only DFO (not shown) or SDF-1 α (C,D) failed to induce functional improvement in general. Only the right hindlimb of SDF-1 α -treated animals (D) showed in almost every time point (except wpl 2 and 8) significantly less missteps than PBS animals. However, at several time points SDF-1 α was significantly less effective than its vehicle BSA. In order to simplify the diagrams of (C) and (D), significances of BSA vs. PBS are not presented. Results are shown as mean \pm SEM. * p < 0.05, ** p < 0.01, *** p < 0.001 vs. PBS group; # p < 0.05, ### p < 0.01, #### p < 0.001 vs. BSA group.

3.4.3 CatWalk gait analysis

CatWalk gait analysis provides a large set of quantitative parameters targeting interlimb coordination and dynamic and static gait functions. Due to problems in hindpaw detection after lesioning, only the parameters regularity index (RI), frequencies of footfall patterns, stride length and swing were taken for evaluation.

Interlimb coordination was assessed by the regularity index (RI), which is one of the most-frequently used coordination parameter in the CatWalk and describes the percentage of normal step sequence patterns (table 2.8) used by the animal. A RI of 100 % represents perfect coordination (Hamers et al., 2001). However, an averaged RI of 100 % is rarely reached in all pre-injury tested animals as visible in Fig. 3.10A. This is consistent with previous research using the CatWalk system (Hamers et al., 2001; Van Meeteren et al., 2003; Jeong et al., 2011). A transection injury leads to a decrease of up to 20 %, which is

more or less observable in all tested groups except of BSA (Fig. 3.10A). BSA treatment led only to a drop of approximately 3 % and was significantly different to the PBS and SDF-1 α group. According to the horizontal ladder walking test, BSA shows the highest RI in every time point, but only at 2, 10 and 14 weeks post-lesion it was significantly increased compared to the PBS and SDF-1 α groups. Due to the statistical multiple comparisons correction, BSA was at no time point significantly different to the DFO+SDF-1 α group. While DFO, DFO+SDF-1 α and SDF-1 α showed in almost every time point (except wpl 14 and 16) higher RI values than the PBS group, they never reached significance level. As healthy animals predominantly use the normal step sequence pattern Ab (table 2.8), the further question was, whether the RI recovery is accompanied by renormalisation (frequency increase of Ab pattern) of the lesion-induced shift in the frequency distribution of the step patterns. The BSA group was the only one where the Ab pattern frequency returned to nearly pre-injury level (pre-injury: 96 %, wpl 16: 94 %; Fig. 3.10B). The DFO+SDF-1 α group achieved at least a frequency of 80 % (Fig. 3.10F). In all other groups, the Ab frequency remained steadily at markedly (about 30 – 40 %) decreased levels (Fig. 3.10C-E).

Stride length, which defines the distance between successive placements of the same paw, is a further gait parameter affected after spinal cord injury. In healthy animals the forelimb (FL) and hindlimb (HL) strides are nearly identical and the difference between them is close to zero. After injury, the difference increases due to smaller FL strides compared to their HL strides and results in large negative values (Fig. 3.11A,B). BSA treatment, however, seems to minimize this difference increase already from the first post-injury testing (wpl 2) onwards and was in every tested time point the group with the smallest stride length difference, regardless of which limb side was tested (Fig. 3.11A,B). Due to multiple statistical comparisons, the BSA group reached the significance level in comparison to PBS not until eight weeks post-lesion. In comparison to the SDF-1 α group, the BSA-treated animals had significant smaller stride length differences at every time point except at wpl 10. Within the other groups, no statistical significance could be found.

A similar effect was observed for the difference between FL and HL swing duration (Fig. 3.11C,D). In uninjured animals FL and HL have nearly the same swing duration. However after injury, HL swing duration rises compared to the FL, resulting in negative difference values. As already seen in the stride length parameter, BSA-treated animals showed the smallest difference between the FL and HL swing duration and differed clearly from the other groups from the beginning of the test period onwards (Fig. 3.11C,D). Although the diagram graphs of BSA and PBS appear to be in clear contrast to each other, statistical differences could only be found for the left side at wpl 8 and 12 (Fig. 3.11C) and for the right side at wpl 4, 10, 12 and 14 (Fig. 3.11D). The statistical comparison between BSA and SDF-1 α , however, revealed that BSA-treated animals had significantly smaller swing duration

differences than SDF-1 α -treated animals in all tested time points of the left side (Fig. 3.11C) and only wpl 2 and 8 were missing on the right side (Fig. 3.11D). There was no statistical difference among the other groups.

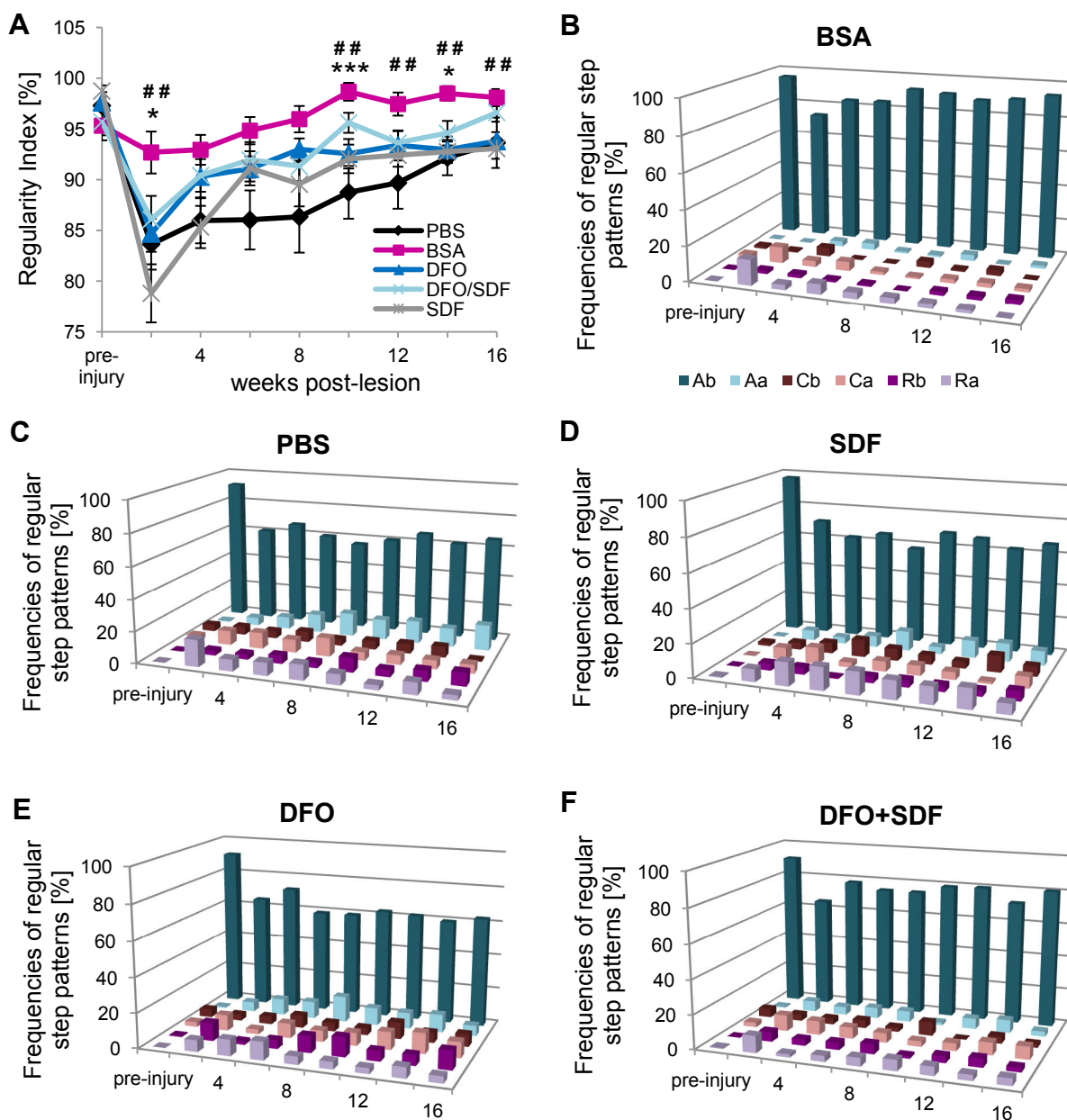


Fig. 3.10: CatWalk: Regularity Index (RI) and frequencies of regular step patterns. (A) After transection injury, RI drops by approximately 15-20 % as visible for all tested groups except BSA (~3 %). From the first testing time point on, BSA-treated animals showed less impairment in their coordination and had a significantly higher RI score at 2, 10 and 14 weeks post-lesion (wpl) compared to the PBS group and at 2, 10, 12, 14 and 16 wpl compared to the SDF-1 α group. DFO, SDF-1 α or the combination DFO+SDF-1 α never reached significance level in comparison to PBS. Results are shown as mean \pm SEM. * p < 0.05, ** p < 0.01, *** p < 0.001 vs. PBS group; # p < 0.05, ### p < 0.01, #### p < 0.001 vs. SDF group (Wilcoxon's Sum of Rank Test with Holm-Bonferroni correction). (B-F) The analysis of regular step pattern frequencies revealed that the BSA group was the only group with an Ab pattern, which is predominantly used in healthy state, returning to nearly pre-injury level (B). The DFO+SDF-1 α group achieved at least a frequency of 80 % (F), whereas the Ab frequency of all other groups remained steadily at decreased level (C-E).

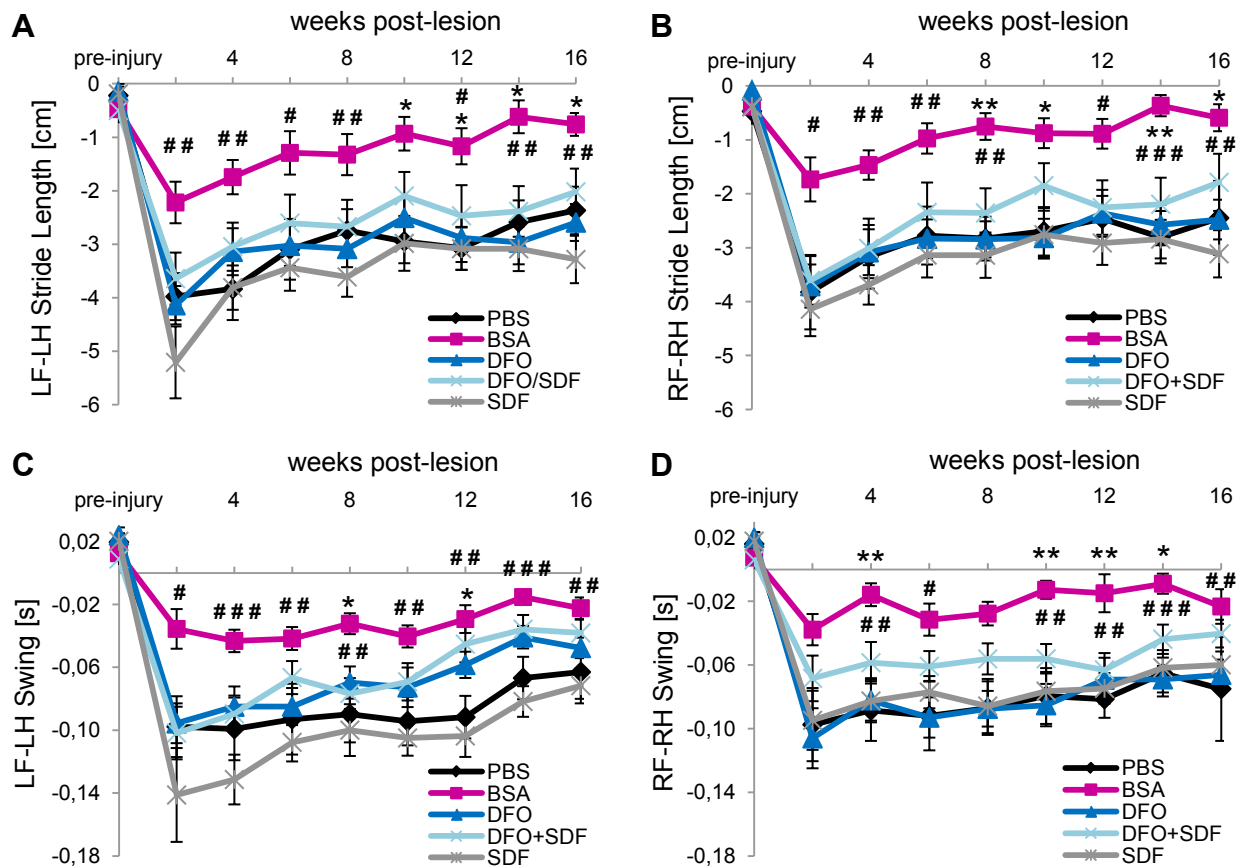


Fig. 3.11: CatWalk: Stride length and swing duration. The difference between forelimb (FL) and hindlimb (HL) stride length (A,B) as well as swing duration (C,D) was clearly improved by BSA treatment. (A,B) The difference between FL and HL stride length prior to injury is near 0. After injury, the animals make smaller FL strides compared to their HL strides, resulting in large negative values. From week 10 on for the left limb side and week 8 on for the right limb side, BSA treatment resulted in a significant smaller difference between FL and HL stride length compared to the PBS group. In comparison to SDF-1 α , BSA had in almost every time point (except wpl 10) significant better recovery. (C,D) Having nearly the same swing duration in healthy state, HL swing duration rises compared to the FL after injury. BSA-treated animals showed at 8 and 12 wpl for the left side and at 4, 10, 12 and 14 wpl for the right side significant smaller swing duration differences compared to the PBS group. In comparison to SDF-1 α , swing duration differences of BSA-treated animals were improved in all tested time points of the left side and only wpl 2 and 8 of the right side did not reach significance level. Results are shown as mean \pm SEM. * $p < 0.05$, ** $p < 0.01$, *** $p < 0.001$ vs. PBS group; # $p < 0.05$, ## $p < 0.01$, ### $p < 0.001$ vs. SDF-1 α group (Wilcoxon's Sum of Rank Test with Holm-Bonferroni correction).

3.4.4 Open field BBB locomotor scoring

Consistent forelimb-hindlimb coordination is necessary that fine motor control aspects (i.e. toe clearance, predominant paw position, trunk stability and tail position) are considered in the BBB scoring. Due to the difficulty of assessing coordination in the open field, the regularity index (RI) of the CatWalk gait analysis was used to determine forelimb-hindlimb coordination. According to Jeong et al. (2011), an animal was assigned occasionally coordinated, if at least one of four CatWalk runs showed 100 % RI; frequently coordinated to an average of 95 % RI or above and two runs with 100 % RI; and consistently coordinated to

an average RI of 95 % and at least three runs with 100 % RI. Considering at first only which stage of coordination each animal achieved, it became apparent that BSA-treated animals showed a faster and better recovery of their coordination than the other animal groups. Already at 4 weeks post-lesion, all BSA-treated animals regained at least occasional coordination or more (Fig. 3.12A), and at 12 weeks post-lesion approximately 80 % were consistently coordinated (Fig. 3.12B). In contrast, the percentage of consistent coordinated animals in the other groups never exceeded more than 50 %. Between 30 and 40 % of the animals even had no coordination at the end of the testing phase (Fig. 3.12A).

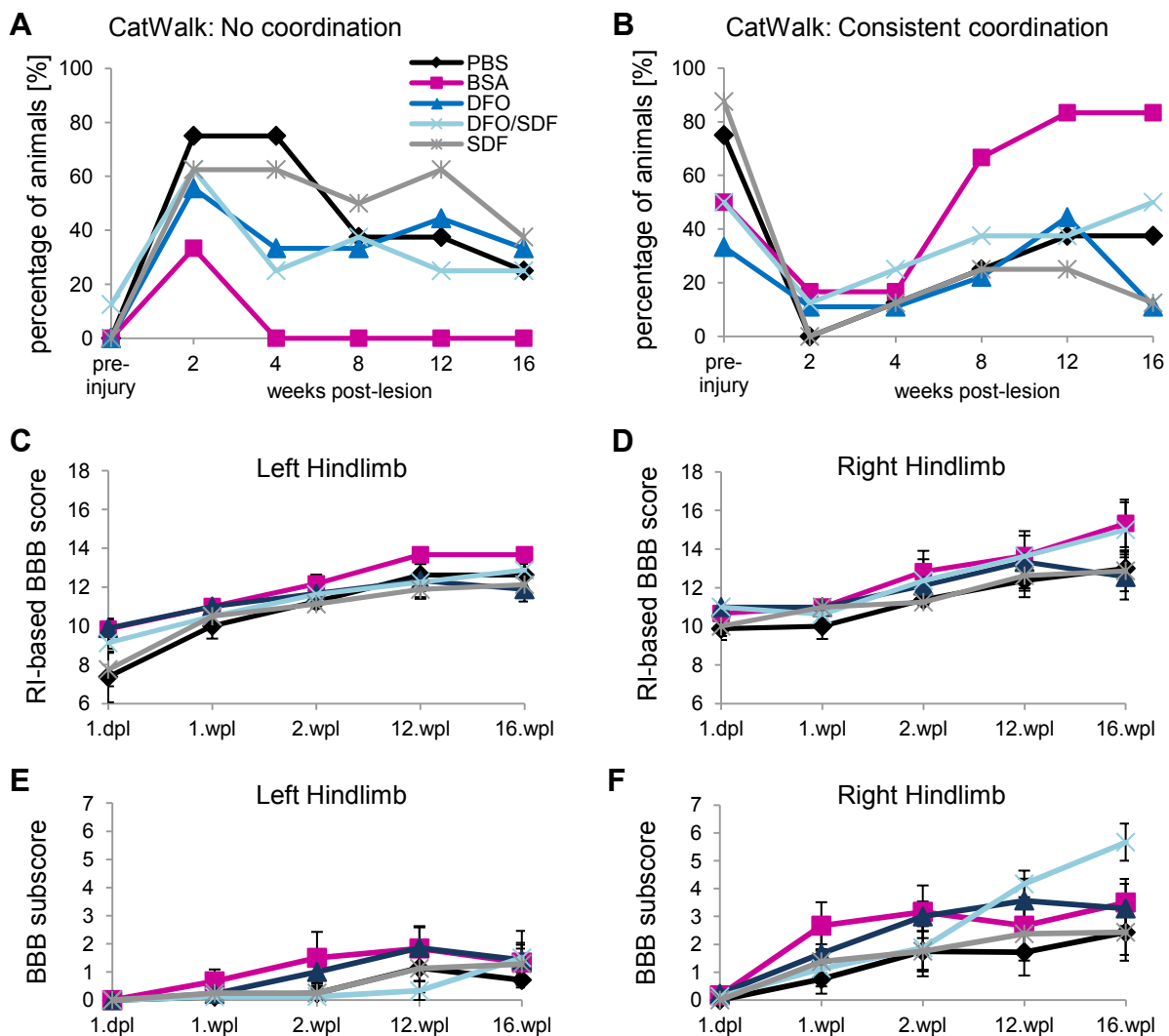


Fig. 3.12: Open field BBB locomotor scoring. For evaluation of forelimb-hindlimb coordination the CatWalk regularity index (RI) was used. Looking at first only at the degree of coordination, it is remarkable that only BSA-treated animals regained already occasional or better coordination at 4 wpl (A). After 12 wpl, approximately 80 % were consistently coordinated, whereas the other animals never exceed more than 50 % (B). The analysis of the RI-based BBB locomotor score (C,D) and BBB subscore (E,F), however, revealed no significant differences between all tested groups neither for the left nor for the right hindlimb, an indication of remaining deficits in fine motor control aspects like, e.g., toe clearance. Results are shown as mean \pm SEM (Wilcoxon's Sum of Rank Test with Holm-Bonferroni correction).

Though the BSA-treated animals showed better recovery of coordination, the evaluation of the RI-based BBB score revealed no significant difference between all groups, neither for the left nor for the right hindlimb (Fig. 3.12C,D), suggesting that fine motor control aspects like toe clearance or paw position are not effectively recovered through BSA treatment. Only when an animal recovers some or even all fine motor control aspects, which would be reflected in the BBB subscore, it can achieve a higher BBB score than 14. The analysis of the BBB subscore confirmed that none of the tested treatments resulted in significant improvement of fine motor control aspects (Fig. 3.12E,F).

3.5 Tissue sparing

The primary mechanical injury of the spinal cord results in physical disruption of neuro-glial tissue and vasculature, which induces a complex set of pathophysiological processes (Kwon et al., 2004). These 'secondary' processes lead to expansion of the initial lesion area, affecting neighbouring intact tissue. Both albumin (Belayev et al., 2001; Cain et al., 2007; Prajapati et al., 2011) and DFO (Nowicki et al., 2009; Dexter et al., 2011; Liu et al., 2011) have been shown to exert neuroprotective effects. Due to this background, the percent lesion area, which is the lesion area (blue framing in Fig. 3.13A,B) in relation to the predefined spinal cord area (white framing in Fig. 3.13A,B), and the area of spared tissue were assessed in all functionally tested animals to examine whether the treatments reduce tissue loss. Visualized by GFAP-staining of parasagittal spinal cord sections, the GFAP-negative lesion area and the corresponding spinal cord area were quantified using ImageJ software. During the quantification it was conspicuous that some spinal cords looked atrophied in the lesion area. Measuring the smallest spinal cord height in the area of the lesion scar showed that the spinal cords of PBS-treated animals in comparison to the other groups were approximately 0.2 mm thinner (Fig. 3.13A) at the smallest point (except SDF-1 α : ~ 0.1 mm), but a significant difference to the other groups could not be determined. The quantification of the percent lesion area revealed that BSA-treated animals developed a significantly smaller relative lesion area (Fig. 3.13C) in comparison to PBS and SDF-1 α , but the significance in the analysis of spared tissue (Fig. 3.13D) was lost after Holm-Bonferroni correction due to multiple comparisons. DFO treatment seemed to have a similar effect as BSA, but after Holm-Bonferroni correction only the significance between DFO and SDF-1 α remained for the relative lesion area (Fig. 3.13C) and no significance for the spared tissue (Fig. 3.13D). Although BSA and DFO show a tendency towards better tissue preservation, the degree is less effective than expected from the observed reduction in lesion area.

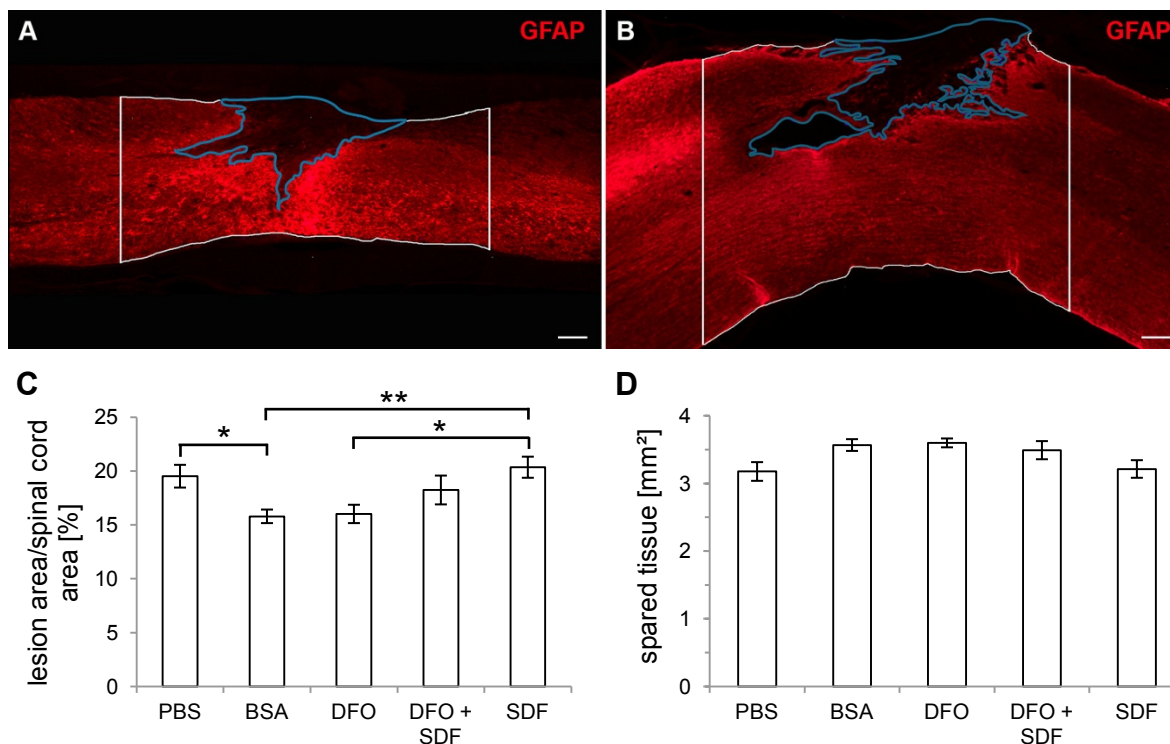


Fig. 3.13: Analysis of relative lesion area and spared tissue. (A,B) Exemplary GFAP-stained parasagittal spinal cord sections illustrating the GFAP-negative lesion area (blue framing) and the predefined spinal cord area (white framing). Several PBS-treated animals (A) had on average 0.2 mm thinner spinal cords than the other animals (B: DFO-treated spinal cord is shown). (C) Quantifying the lesion area in relation to the spinal cord area revealed significant smaller percent lesion areas of BSA-treated animals in comparison to the PBS or SDF-1 α group. DFO-treated animals looked similar to BSA, but lost their significance to the PBS group after Holm-Bonferroni correction. (D) However, the analysis of spared tissue in each animal showed no difference between the groups. Orientation in A and B, caudal = right, dorsal = up. Scale bars: 200 μ m. Results are shown as mean \pm SEM. * $p < 0.05$, ** $p < 0.01$ (Student's t-test with Holm-Bonferroni correction).

3.6 Axonal regeneration into the lesion area and beyond

In 1981, the former “dogma” by Ramón y Cajal (1928) that CNS axons are incapable of regeneration was refuted (David and Aguayo, 1981). Their laboratory was the first who provided the proof that CNS axons have the intrinsic capacity to regenerate. Since then much effort has been spent to improve axonal and functional regeneration after spinal cord injury. To investigate whether the above described functional recovery through BSA or DFO+SDF-1 α treatment is a consequence of axonal regeneration, different fibre populations were immunohistochemically stained and manually counted. Automated quantification was not possible due to high background signals in the lesion area induced by macrophages and cellular debris.

3.6.1 Quantitative analysis of CGRP-positive axons

Regeneration of CGRP-positive axons was blindly quantified by determining the axon density (axons/mm²) in the GFAP-negative lesion area of immunohistochemically stained parasagittal spinal cord sections (Fig. 3.14A). Due to the disturbing high background signals, only CGRP-labelled structures which could be clearly identified as longitudinal axonal profiles were manually counted. The analysis revealed that DFO+SDF-1 α treatment significantly enhanced axon ingrowth in the GFAP-negative lesion area by 2.2-fold (**p < 0.01) as compared to the PBS control group (Fig. 3.14B). The infusion of either DFO or SDF-1 α showed a non-significant trend to enhanced CGRP-axon ingrowth into the lesion area. Interestingly, BSA treatment had no significant effect on regeneration of CGRP-axons when compared to PBS control (Fig. 3.14B).

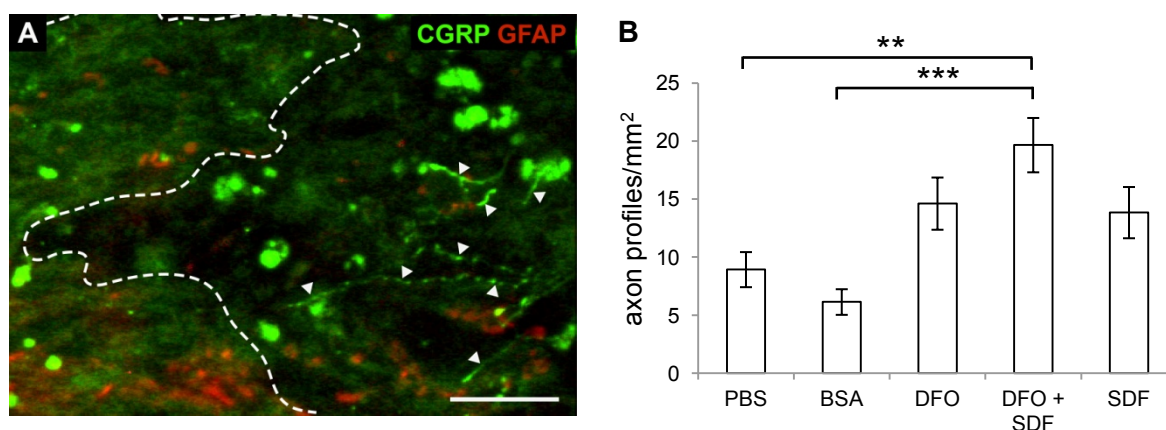


Fig. 3.14: CGRP axon regeneration into the GFAP-negative lesion area. (A) Immunohistochemical staining of a parasagittal section 19 weeks post-lesion showing CGRP axon growth (white arrow heads) into the GFAP-negative lesion area. The rostral lesion border is indicated by a dashed line. Scale bar: 50 μ m. (B) DFO+SDF-1 α infused spinal cords showed significant increased axon ingrowth into the GFAP-negative lesion area compared to PBS. Results are shown as mean \pm SEM. **p < 0.01, ***p < 0.001 (Wilcoxon's Sum of Rank Test with Holm-Bonferroni correction).

3.6.2 Quantitative analysis of CTB-traced axons

Sensory sciatic afferents were anterogradely traced with cholera toxin B (CTB) four days prior to sacrifice and, after immunohistochemical visualization (Fig. 3.15A,B), were manually counted in the GFAP-negative lesion area as well in the entire rostral spinal cord segment (Fig. 2.6). Anterogradely labelling enables the detection of regenerated axons. Initially, it seemed that the combination of DFO and SDF-1 α , in contrast to the single delivery, has also regenerative potential on CTB-labelled axons, but after the Holm-Bonferroni correction due to multiple comparisons the statistical significance to PBS was lost (Fig. 3.15C). However, the infusion of BSA significantly increased the presence of CTB-labelled axons within the lesion area (Fig. 3.15C). Although the axon ingrowth into the GFAP-negative lesion area was

increased, the axon growth beyond the lesion into the rostral spinal cord was not significantly improved in any of the tested groups (Fig. 3.15D).

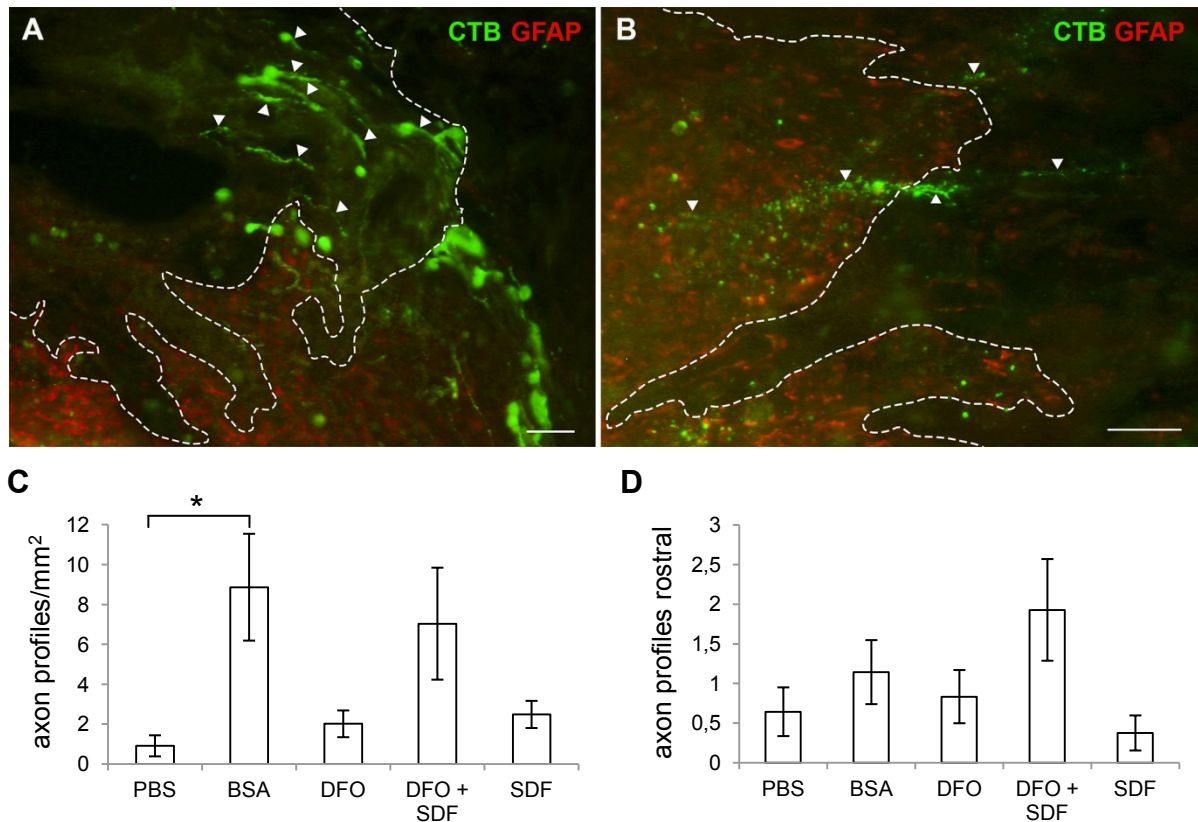


Fig. 3.15: CTB axon regeneration in the GFAP-negative lesion area and in the entire rostral spinal cord. Immunohistochemical staining of a CTB-traced parasagittal spinal cord section from a BSA-treated animal 19 weeks post-lesion showing axon ingrowth into the lesion area (white arrow heads) at the caudal scar border (A) and axon outgrowth from the lesion area into the rostral spinal cord at the rostral scar border (B). The lesion borders are indicated by a dashed line, respectively. Scale bar: 50 µm. The quantitative analysis of axon density in the lesion area (C) revealed significantly enhanced axon ingrowth after BSA treatment in comparison to PBS, but rostral to the lesion area differences in the axon profiles of the tested groups did not reach significance (D). Results are shown as mean ± SEM. * $p < 0.05$ (Wilcoxon's Sum of Rank Test with Holm-Bonferroni correction).

3.6.3 Quantitative analysis of BDA-traced CST axons

Descending corticospinal tract (CST) axons were anterogradely labelled by injecting BDA into the sensorimotor cortex layer V three weeks prior to sacrifice to identify regenerated CST axons in the lesion area and in the complete dorsal white matter distal to the lesion. As only healthy axons are able to transport BDA, axon debris won't be stained. Manual counting of axon profiles revealed that neither in the scar area (Fig. 3.16A) nor in the distal white matter (Fig. 3.16B) the increase in the number of regenerated axons reached significance.

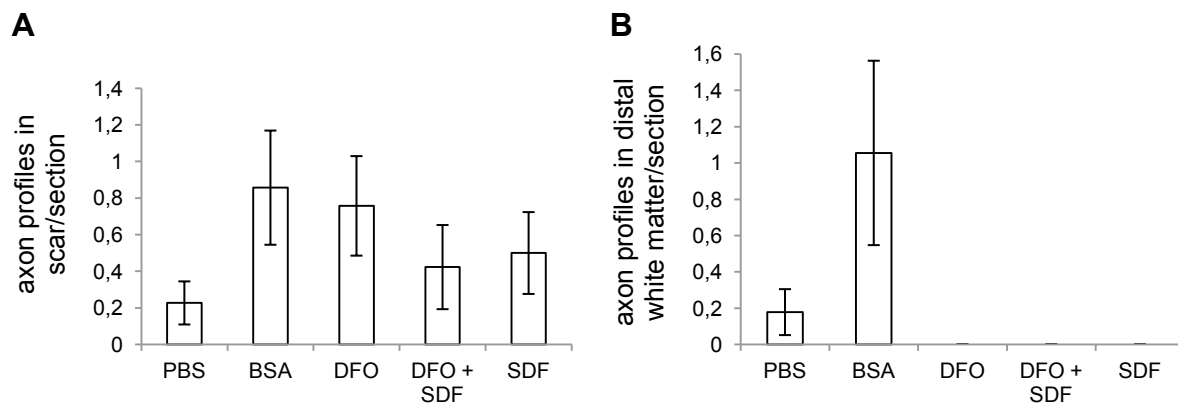


Fig. 3.16: CST axon regeneration in the GFAP-negative lesion area and in the dorsal white matter distal to the lesion. None of the treatments resulted in significantly enhanced CST axon regeneration neither in the lesion area (A) nor in the distal white matter (B). Results are shown as mean \pm SEM (Wilcoxon's Sum of Rank Test).

4 Discussion

4.1 Intrathecal infusion in a rat spinal cord injury model

Intrathecal infusion is a commonly used method for local delivery of a number of substances to the spinal cord both in clinical use [particularly for analgesics or antispasticity drugs (Burchiel and Hsu, 2001; Kumar et al., 2001; Zuniga et al., 2002; Saval and Chiodo, 2010)] or in experimental approaches using laboratory animals (Kojima and Tator, 2002; Iannotti et al., 2004; Weinmann et al., 2006; Fouad et al., 2009). For a clear interpretation of experimental approaches, it is important that the infusion device does not induce further damage to the spinal cord of laboratory animals. However, in regard to the very narrow subdural and subarachnoid space in rodents (Haines et al., 1993; Reina et al., 2002), compared with the smallest possible diameter of intrathecal tubes, extensive scarring can occur (Jones and Tuszynski, 2001; Zhang et al., 2010) presumably induced by the pressure of intrathecally placed catheters onto the spinal cord and/or immune reactions directed against the tubing material. To avoid this additional damage by the application device, several intrathecal catheter application modalities were tested at first.

Catheter diameter, catheter material, length of catheter tubing inside the subarachnoid space and catheter bending at the area of initial contact with the spinal cord (Th11) have been found as the most critical points in provoking additional damage and scarring in the spinal cord. Jones and Tuszynski (2001) applied a polyethylene (PE-10) tube with 0.61 mm outer diameter (OD) and 0.28 mm inner diameter (ID), stretched to a point of maximum elasticity in order to obtain the smallest dimensions possible. After 14 days of catheter implantation they observed scarring and compression of the spinal cord, presumably due to catheter size and material. Sakura et al. (1996) tested different catheter diameters and materials and found that animals, in which comparable PE-10 catheters stretched to double its original length (0.0174''OD x 0.0076''ID) were implanted, showed moderate spinal nerve injury, whereas animals with 32G (0.0107''OD x 0.005''ID) polyurethane (PU) catheters showed no evidence of spinal tissue damage. Only a minimal fibrotic reaction was found delineating the catheter tract. The implantation of a 32G polyimide catheter, however, induced intense fibrotic reaction around the catheter, indicating the different impact of the catheter material on scarring. In the present work, Alzet rat intrathecal 28G (0.36 mm OD x 0.18 mm ID) PU catheters were used for the evaluation of catheter functionality, which are comparable in size to the 28G (0.014''OD x 0.007''ID) PU catheters used by Sakura et al. (1996). While the Sakura group reported that 28G PU catheters (in contrast to 32G PU) caused a moderate spinal nerve injury, no spinal tissue compression was induced by the catheter implantation

method described in this work (Fig. 3.2A). The main difference between both implantation methods is the different length of catheter tubing within the subarachnoid space. Whereas in this work the length of catheter tubing within the subarachnoid space was kept as short as possible, the catheter was mainly guided on top of the dura, the catheters in Sakura's work were advanced 11 cm within the subarachnoid space from the atlanto-occipital membrane up to a position caudal to the conus medullaris. Hence, the strategy to guide the catheter as far as possible on top of the dura and finally to insert it into the subarachnoid space near by the dura suture is sufficient to avoid additional damage and scarring in the spinal cord. However, this kind of catheter implantation requires an appropriate catheter fixation to avoid retraction and spinal cord compression at the area where the catheter contacts the spinal cord for the first time (Th11). Fixation of the catheter adaptor to a cushion of fat tissue, which was placed over the exposed spinal cord at Th11 and glued to the surrounding tissue and bones (see Fig. 2.1), solved this problem. In this context, it is important to perform a total laminectomy of Th11, so that the catheter bending can be reduced to a minimum.

Additionally to extensive scarring and augmented spinal cord tissue damage, Jones and Tuszynski (2001) and Zhang et al. (2010) reported that intrathecal infusion was efficient for 7 days but was markedly reduced after 14 days post-lesion, due to time-dependent occlusion. According to Jones and Tuszynski, catheter patency of the established implantation method was examined by replacing PBS filled osmotic minipumps after 5 or 12 days post-lesion with 6 % Evans Blue dye primed minipumps. After 7 and as well after 14 days post-lesion, the spinal cords of both infusion paradigms were deeply stained blue (Fig. 3.3) and confirmed continuous drug infusion for at least 14 days, probably due to the non-existent scarring around the catheter tract. Hence, the improved application method described in 2.3.3 enables continuous intrathecal drug infusion over a period of at least two weeks without provoking further damage to the spinal cord.

4.2 Intrathecally infused iron chelators reduce collagenous lesion scarring

4.2.1 BPY-DCA (2,2'-bipyridine-5,5'-dicarboxylic acid)

Previous work by Hermanns et al. (2001b) and Klapka et al. (2005) has shown that local injections of the AST, consisting of BPY-DCA and 8-Br-cAMP, suppress transiently the collagen scar formation in the lesioned rat spinal cord. Interestingly, injections of BPY-DCA into the spinal lesion alone were not sufficient to suppress fibrous scarring. It seemed that the combination with 8-Br-cAMP is indispensable for effective collagen reduction. However, the question arises whether a complete suppression of the lesion-induced collagen

production is necessary and useful. The collagenous scar serves as an adhesive scaffold not only for growth-inhibitory molecules but also for ECM components which are growth-promoting such as laminin (Condic and Lemons, 2002). The suppression of the collagenous scar formation in the spinal cord might also result in a massive reduction of growth-promoting molecules as it has been reported for laminin in the fornix transection model after BPY treatment (Stichel et al., 1999a; Brazda and Müller, 2009). Due to the larger extension of the basement membrane in the spinal cord (Hermanns et al., 2001b), a growth-promoting environment becomes more important. Thus, an incomplete suppression of the Coll IV expression, which would allow a higher accumulation ratio of growth-promoting molecules as after a complete Coll IV suppression, could be beneficial for axon regeneration.

If the collagen expression is only reduced, i.e. it is not completely suppressed, by the treatment, a purely qualitative evaluation by microscopic comparison as performed by Hermanns et al. (2001b) and Klapka et al. (2005) is too imprecise. For this purpose, a semi-quantification method was developed in this work to measure Coll IV expression in the scar area of histological spinal cord sections (see chapter 2.6.1). The reason to use Coll IV stained histological sections for analysis instead of a biochemical quantification is based on the fact that blood vessels also express Coll IV. As iron chelators have been shown to promote angiogenesis (Beerepoot et al., 1996; Ikeda et al., 2011), it is necessary to differentiate between lesion-induced Coll IV deposition and Coll IV from blood vessel basement membranes. In a biochemical analysis, however, such a distinction would not be possible. Furthermore, the use of histological sections for the Coll IV quantification allows the simultaneous investigation of additional aspects in the same laboratory animal.

Investigation of Coll IV expression in the scar by using the described quantification method revealed that BPY-DCA, when intrathecally infused over 7 days, has the potential to reduce scarring significantly (Fig. 3.5D). An infusion of BPY-DCA at 1.1 µg/d resulted in the highest Coll IV reduction (57 %) in relation to the lesion-only group. But surprisingly, the infusion of the vehicle control Tris (20 mM) already induced a Coll IV reducing effect of 33 %, indicating that part of the BPY-DCA effect is presumably Tris based. Since Tris can penetrate biological membranes in its un-ionized form and cause cytotoxicity, reduced Coll IV expression after Tris infusion could be the result of increased cell death of collagen producing cells. Accordingly, the application of BPY-DCA, which reduces the collagen biosynthesis by inhibiting prolyl-4-hydroxylase (Hales and Beattie, 1993), would lead to an additional reduction of Coll IV in relation to Tris as seen in the animal group receiving 1.1 µg/d BPY-DCA (see Fig. 3.5D). While a non-significant trend is still visible in the group of 7.8 µg/d BPY-DCA, the group with the highest concentration (187.2 µg/d) showed no additional reduction in relation to Tris and a significantly lower Coll IV reduction than the animals receiving 1.1 µg/d BPY-DCA. The cause for this ineffectiveness of the high BPY-DCA concentration is elusive.

Due to its lipophilicity, BPY-DCA can penetrate cells with relative ease and, therefore, one would expect that a higher BPY-DCA concentration would cause a greater Coll IV reduction until complete reduction of collagenous scarring is achieved. However, lipophilicity also carries the risk of increased toxicity (Hershko et al., 1993). The mechanisms of chelator-induced toxicity are related to either the inhibition of iron containing enzymes and/or the promotion of iron-mediated free radical damage (Chaston and Richardson, 2003). While inhibition of the iron-containing prolyl-4-hydroxylase is the aim of the BPY-DCA treatment, a potentiation of iron-mediated free radical generation by BPY-DCA would enhance the intensity of secondary damage occurring after spinal cord injury. Compared to low BPY-DCA concentrations, excessive BPY-DCA levels would lead to increased invasion of collagen producing cells, as for e.g. fibroblasts, into the lesion area and, thus, to increased collagen expression. Furthermore, it is quite possible that BPY-DCA also chelates other bivalent cations, such as calcium (Ca^{2+}), which plays an essential role in blood coagulation. Since two out of six animals of the 187.2 $\mu\text{g}/\text{d}$ BPY-DCA group had to be removed from the analysis due to severe haemorrhage, BPY-DCA could have been washed out due to poor blood coagulation. Based on the small number of animals, however, it cannot be excluded that the observed haemorrhage was accidentally caused by the surgical procedure. A replication of the experiment with higher numbers of animals and additional BPY-DCA concentrations is necessary to verify the reliability of the results obtained in this study.

4.2.2 BPY (2,2'-bipyridine)

The idea to suppress the collagen biosynthesis in a CNS lesion area by using an iron chelator was first tested in a postcommissural fornix transection model (Stichel et al., 1999a). Local injection of the iron chelator BPY resulted in a remarkable reduction of lesion-induced basement membrane deposition, which was already detectable during microscope viewing. However, single application of BPY into a spinal cord lesion failed to reduce the basement membrane deposition significantly, probably due to the larger amounts of basement membrane deposits in the spinal cord than in the postcommissural fornix (Hermanns et al., 2001b). By adapting the method and duration of administration (e.g. via intrathecal infusion) BPY could though be effective in reducing fibrous scarring. To investigate this aspect, Hermanns et al. (2001b) have also studied the continuous application of BPY via osmotic minipumps. But again, they did not observe any obvious reduction of the lesion-induced basement membrane during microscopic analysis. On the contrary, it seemed that the polyethylene (PE) catheter had induced a more extensive basement membrane expression. Due to the improved intrathecal application method and the histological Coll IV quantification developed in this work, as well as the advantage of BPY to be soluble in PBS, the efficacy of

intrathecally infused BPY to reduce basement membrane deposition (Coll IV expression) was re-investigated. For this purpose three different BPY concentrations were intrathecally tested and analysed according to the Coll IV quantification method described in Fig. 2.5. Although a reduced collagen expression was not obvious during microscopic observation, the histological Coll IV quantification revealed that the BPY infusion of 7.12 µg/d significantly reduced Coll IV reduction in the scar by 30 % to 35 % in comparison to PBS or lesion-only controls, respectively (Fig. 3.6D). If one considers only the best reduction effects of BPY (30 %) and BPY-DCA (36 %) in relation to their vehicle controls, then BPY-DCA, which is known to be the more potent inhibitor of prolyl-4-hydroxylase (Hales and Beattie, 1993), has only a slightly higher efficacy than BPY. Consequently, BPY would be an alternative to BPY-DCA. However, it must be noted that the BPY-DCA solvent Tris already causes significant collagen reduction in the scar in contrast to PBS and the combination of Tris and BPY-DCA probably has an additive effect. As Tris is not the solvent of choice for clinical use and BPY-DCA is neither soluble in PBS nor saline, a direct comparison of the reduction effect of both iron chelators and identical conditions is not possible. And the question whether BPY-DCA in combination with PBS would be just as effective in Coll IV reduction as with Tris remains open.

Based on the results of the three BPY concentrations tested (Fig. 3.6D), the most effective concentration of BPY in relation to Coll IV reduction seems to be between 0.71 and 71.2 µg/d. While both of these concentrations showed only a non-significant tendency, the infusion of 7.12 µg/d, instead, resulted in a significant Coll IV reduction in relation to the control groups (Fig. 3.6D). However, the comparison of the three BPY concentrations with each other revealed that 7.1 µg/d BPY significantly reduced Coll IV in comparison to 0.71 µg/d. As a lipophilic iron chelator BPY can penetrate cell membranes easily and has direct access to intracellular iron (Kicic et al., 2001). Hence, a lack of accessibility to intracellular iron can be excluded as the reason for low Coll IV reduction. This implies that the BPY concentration of 0.71 µg/d is too low to deprive the prolyl-4-hydroxylase of ferrous iron (Fe^{2+}) effectively, and consequently, an increase in the BPY concentration would result in a significant Coll IV reduction as it is seen with 7.12 µg/d BPY. As already observed with BPY-DCA, the highest BPY concentration (71.2 µg/d) also shows a decrease in the reduction efficacy (Fig. 3.6D), but without significant difference in comparison to 7.12 µg/d. A possible reason for this decrease could be the potentiation of secondary damage leading to increased invasion of collagen producing cells as discussed before in 4.2.1. Since none of the BPY-treated animals showed severe haemorrhage, blood coagulation seems not to be impaired. However, on the basis of the current data, it cannot be excluded that a further increase in the BPY concentration would lead to persistent bleeding, as signs of severe haemorrhage in BPY-DCA-treated animals occurred with a concentration twice as high.

4.2.3 DFO (deferroxamine mesylate)

DFO is, due to its proven antioxidant and neuroprotective character (Gutteridge et al., 1979; Almlı et al., 2001; Nowicki et al., 2009; Yu et al., 2009; Paterniti et al., 2010; Liu et al., 2011) and its status as a clinically approved drug for iron intoxication, an attractive alternative to BPY-DCA. It has been demonstrated that DFO can attenuate secondary tissue damage occurring after spinal cord injury by inhibiting iron-mediated glutamate excitotoxicity, lipid peroxidation and free radical formation (Nowicki et al., 2009; Yu et al., 2009; Paterniti et al., 2010; Liu et al., 2011). Since DFO has low lipid solubility, it cannot cross cell membranes easily (Lloyd et al., 1991; Kicic et al., 2001), which might be considered as a disadvantage in terms of intracellular iron deprivation to inhibit collagen synthesis. However, it has been shown that DFO can enter cells slowly via pinocytosis (Lloyd et al., 1991; Palmer et al., 1994; Samuni et al., 1999; Simonart et al., 2000) and thus has access to intracellular iron. Compared to lipophilic iron chelators, DFO seems less effective at short incubation periods, but it has been reported to be very effective in chelating intracellular iron when incubated over long periods (≥ 24 h) (Simonart et al., 2000; Kicic et al., 2001). Based on the results of the lipophilic iron chelators BPY-DCA and BPY [ineffective when administered only once (Hermanns et al., 2001b), but effective when infused continuously over 7 days (see Fig. 3.5 and Fig. 3.6)], a continuous infusion over several days seems to be generally necessary for significant reduction of collagenous scarring after spinal cord injury. This favours the use of DFO as a substitute for BPY-DCA. Results presented in this work demonstrate for the first time that DFO significantly reduces collagenous scarring after spinal cord injury (see Fig. 3.7). Additionally, it supports the finding that DFO depletes intracellular iron. The target enzyme for iron deprivation is the intracellular prolyl-4-hydroxylase, which catalyses the hydroxylation of procollagen chains (Klapka et al., 2002) and requires ferrous iron (Fe^{2+}) as co-substrate (Kivirikko et al., 1989). As DFO chelates, in contrast to BPY and BPY-DCA, predominantly ferric iron (Fe^{3+}) (Keberle, 1964), the inhibition of prolyl-4-hydroxylase by DFO is effected indirectly by preventing the reduction of ferric to ferrous iron. Consequently, ferrous iron will no longer be available for harmless (e.g. collagen synthesis) and harmful (e.g. hydroxyl radical formation via Haber-Weiss reaction) chemical effects (Hershko et al., 1998).

In contrast to BPY-DCA and BPY, all three DFO concentrations significantly reduced Coll IV in the scar (Fig. 3.7D). The strongest Coll IV reduction in relation to the lesion-only group was 37 % (30 % in relation to PBS) and was generated by the infusion of 100 $\mu\text{g}/\text{d}$ DFO. However, there was no statistical difference between the three DFO concentrations, suggesting that all three concentrations were equally effective. Due to the hydrophilicity and its delayed onset of intracellular iron deprivation, DFO could have a lower effectiveness in Coll IV reduction than a lipophilic iron chelator. Compared to BPY (7.12 $\mu\text{g}/\text{d}$), DFO

(100 µg/d) showed, however, similar Coll IV reduction values. Both iron chelators reduced the Coll IV expression in the scar in relation to their control group PBS by approximately 30 %. Although DFO has only slow access to intracellular iron, it has instead a much higher iron-binding affinity constant than BPY (10^{31} vs. 10^{18}) and chelates almost exclusively iron in contrast to BPY. It even seems that DFO is slightly more effective than BPY as a 10-fold diluted DFO concentration (10 µg/d) still induced a significant Coll IV reduction (see Fig. 3.7D), whereas a 10-fold decrease (0.71 µg/d) in the BPY concentration had no longer a significant scar reducing effect (see Fig. 3.6D). This wider range of effective concentration favoured the use of DFO instead of BPY for further research regarding the impact on axonal and functional recovery. The question of whether DFO is an equivalent alternative to BPY-DCA to treat spinal cord injury cannot be clearly answered on the basis of the Coll IV evaluation. A direct comparison between DFO and BPY-DCA is, as already discussed earlier with BPY (see 4.2.2), not possible due to the different vehicle conditions (PBS vs. Tris) and the presumably additive effect of BPY-DCA and Tris. Disregarding the different vehicle conditions, both chelators would have similar effects on Coll IV reduction in relation to their vehicle controls (BPY-DCA: 36 % vs. DFO: 30 %). Consequently, DFO would be an alternative to BPY-DCA, but finally the evaluation of axonal and functional regeneration after DFO-treatment will determine whether DFO is as effective as BPY-DCA.

According to the present state of knowledge, it is very likely that a therapy for spinal cord injured patients will consist of various components that combine two or more complementary repair strategies (see chapter 1.4 and Fig. 1.3). Hence, it might be beneficial to have the possibility to choose between different types of application. Since DFO could also be applied systemically, an additional experiment was carried out to assess the efficacy of systemic (i.p.) versus local intrathecally applied DFO on collagenous scarring (see Fig. 3.7E). As biochemical analyses by Spinal Cord Therapeutics revealed that 350 mg/kg/d DFO for 14 days is the most effective concentration to reduce collagenous scarring systemically, the comparison of systemic versus intrathecally applied DFO was limited to this concentration. The histological Coll IV quantification showed that systemic application of 350 mg/kg/d DFO is just as effective as intrathecally infused DFO (10 µg/d) and reduced collagenous scarring significantly in relation to its vehicle control (see Fig. 3.7). Consequently, a comparable quantity of DFO must have been delivered via the systemic route to the lesion area. However, such a high concentration of DFO could be associated with severe adverse effects. In iron-overloaded patients DFO treatment is associated with ocular and auditory abnormalities, sensorimotor neurotoxicity, changes in renal function and pulmonary toxicity (Porter and Huehns, 1989; Olivieri and Brittenham, 1997). Most of these toxic effects have been observed in patients when doses of more than 50 mg/kg/d were administered (Porter and Huehns, 1989). Patients without iron overload, however, are more sensitive to DFO

toxicity. It was detected, that the toxicity of DFO correlates inversely with the concentration of serum ferritin, i.e. patients with low ferritin levels are more affected by adverse effects than patients with high ferritin levels (Porter and Huehns, 1989; Olivieri and Brittenham, 1997). In view of this context, the concentration used in this work might cause severe adverse effects and, therefore, further investigations need to be done to evaluate the risk of DFO toxicity as a treatment for spinal cord repair. During the two-week study, no physical differences were noticed between the systemically and the intrathecally treated groups, but these animals have not been tested for toxicity.

In addition to the efficacy of systemic DFO administration, the efficacy of 7- and 14-days intrathecal DFO (10 µg/d) infusions were also examined. Although both intrathecal infusions significantly reduced Coll IV in relation to their vehicle control, it seems that the efficacy of DFO starts to deteriorate after 7 days of infusion (Fig. 3.7E). While the Coll IV expression after 7 days was reduced by 32 %, the reduction of Coll IV was only 20 % when DFO was infused for 14 days. Statistically, the Coll IV levels do not differ from each other, but may reflect the reported stability of reconstituted DFO. Reconstituted DFO is chemically and physically stable for one week at room temperature (Eghianruwa, 2014), and for clinical use, the manufacturer Novartis even recommends to use the reconstituted DFO solution immediately or within 3 hrs for microbiological safety (Novartis, 2012). Therefore, the use of 14-days pumping osmotic minipumps is rather inappropriate for DFO administration and a better alternative would be to use 7-day minipumps, which will be replaced after 7 days by a new one containing freshly prepared DFO.

4.3 DFO enhances blood vessel density in the scar area

Blood vessels supply cells with oxygen and nutrients and, therefore, they play a crucial role in the maintenance and functioning of cells and tissues. Injury-induced loss of blood vessels and the breakdown of the blood-spinal cord barrier contribute to the pathophysiologic processes of secondary damage and significantly determine the severity of spinal cord injury (Fassbender et al., 2011; Oudega, 2012). During the first week after SCI, the damaged spinal cord attempts to restore proper vascularisation by inducing the formation of new blood vessels in the injury site (Casella et al., 2002; Loy et al., 2002). This angiogenic response, however, fails to establish properly functioning blood vessels, thereby limiting regenerative events (Oudega, 2010; Oudega, 2012). Hence, interventions that promote revascularisation of damaged spinal cord tissue are considered beneficial for tissue repair and functional recovery after SCI, as shown in a number of SCI animal models (Zhang and Guth, 1997; Widenfalk et al., 2003; Glaser et al., 2004; Kaneko et al., 2006). A key regulator of blood vessel formation is the vascular endothelial growth factor (VEGF) (Leung et al., 1989; Breier

and Risau, 1996). Gleadle et al. (1995) and Beerepoot et al. (1996) have demonstrated independently that DFO (and other iron chelators) upregulate the production of VEGF *in vitro*, indicating that iron chelators might affect angiogenesis *in vivo*. Since then several studies, mainly focussing on ischemia, have confirmed that DFO promotes angiogenesis (Chekanov et al., 2003a; Chekanov et al., 2003b; Ikeda et al., 2011). Consequently, DFO could also enhance angiogenesis in a spinal cord lesion, which would result in an increased blood vessel density in the lesion area. The quantitative analysis of vWF stained spinal cord sections (see Fig. 3.8) confirmed that DFO significantly increases the density of blood vessels in the lesion zone. Since vWF is an endothelial specific cell marker, this finding suggests that DFO could promote repair of damaged spinal cord tissue and, consequently, functional recovery by increasing revascularisation. An equivalent result was also seen after BPY-DCA administration (data not shown), leading to the assumption that the iron availability plays an essential role in inducing and inhibiting angiogenesis. Most likely, DFO (and other iron chelators) activate the hypoxia inducible factor (HIF) pathway by inhibiting prolyl-4-hydroxylase (Asikainen et al., 2005), an important enzyme not only for the synthesis of collagen (Kivirikko et al., 1989; Pihlajaniemi et al., 1991), but also for the proteasomal degradation of HIF-1 α (Jaakkola et al., 2001). The inhibition of the HIF-prolyl-4-hydroxylase leads to the stabilisation and activation of the HIF complex and finally to the upregulation of VEGF (Karuppagounder and Ratan, 2012).

4.4 Effect of DFO on functional recovery and its synergy with SDF-1 α

Due to the scientifically proven characteristics of DFO – cell and tissue protection through its antioxidant activity (Gutteridge et al., 1979; Almlı et al., 2001; Paterniti et al., 2010; Liu et al., 2011), stimulation of neurite outgrowth *in vitro* (Nowicki et al., 2009), promotion of revascularisation (see Fig. 3.8) (Gleadle et al., 1995; Beerepoot et al., 1996; Ikeda et al., 2011; Hertzberg et al., 2012) and reduction of collagenous scarring (see Fig. 3.7) – it is imaginable that DFO could also improve motor performance. Currently, there are only two publications reporting functional recovery after DFO treatment in spinal cord injured animals (Paterniti et al., 2010; Liu et al., 2011). In both, locomotor tests were performed only over a short period of time. Paterniti et al. (2010) assessed motor functions (modified murine BBB) of DFO-treated mice once a day for 10 days after spinal cord compression. The animals received 30 mg/kg DFO i.p. each at 30 min before and at 1 h and 6 h after SCI. Liu et al. (2011) injected i.p. a bolus of 100 mg/kg DFO in spinal cord contused rats and assessed functional recovery using the Modified Tarlov's scale (less sensitive than BBB) and inclined plane test at 7, 14, and 21 days after SCI. In the present thesis, the potential of DFO to

improve functional regeneration was studied for the first time over a period of 16 weeks. In contrast to Paterniti et al. (2010) and Liu et al. (2011), DFO (10 µg/d) was intrathecally infused into a dorsal hemisection lesion model for 2 weeks. To evaluate long-term locomotor recovery in more detail, three different functional tests (horizontal ladder walking test, CatWalk gait analysis and BBB open field test) were performed. The BBB open field test was primarily included in this study to uncover lesion-induced differences among all animals. Within the first week post-lesion, the BBB can be used as a measure for lesion severity, as strong variations in lesion size will be reflected in widely varying BBB values. Although the BBB is now also regarded as sensitive in hemisection injuries (Metz et al., 2000), the evaluation of functional recovery in this study focuses mainly on the horizontal ladder walking test and the CatWalk gait analysis. Due to the fact that the used lesion type affects only the dorsal part of the spinal cord, it is very likely that normal overground locomotion, which is mainly controlled by the CPG network and its reticulospinal input (Jordan, 1998), will be only slightly impaired. Deficits are primarily expected in the BBB subscore, representing fine motor control aspects, and interlimb coordination. Additionally, the BBB open field test is a subjective method, leading finally to the decision to assess the BBB score and subscore only at 1 day post-lesion and 1, 2, 12 and 16 weeks post-lesion. Within one week post-lesion, all animals of this study showed equivalent deficits. As expected, they were able to make occasional (BBB score: 10) to consistent (BBB score: 11) weight supported plantar steps, but they had no interlimb coordination and a subscore of 0 (see Fig. 3.12). In the further course of investigation, however, none of the treatments improved the BBB or BBB subscore significantly compared to the PBS control group. The more sensitive test for dorsal spinal motor tracts (CST and RST) is the horizontal ladder test, as sensory-motor coordination of the forelimbs and hindlimbs is required to cross the ladder without missteps (Metz et al., 2000).

4.4.1 A 2-week intrathecal DFO infusion temporarily and marginally improves functional outcome

In all three tests, an overall long-term improvement of motor performance following DFO treatment was absent or modest compared to the PBS control group. However, in the early weeks of the study (up to week 8 post-lesion), it seems that DFO-treated animals are performing obviously but not always significantly better on the horizontal ladder than the control animals (see table 3.1 and 3.2). Significant differences between DFO and PBS were found for the right hindlimb at wpl 2 and wpl 6 and for the left hindlimb at wpl 6. From week 10 on, however, the error rate of DFO-treated animals deteriorated abruptly towards the PBS group, indicating that a 2-week intrathecal infusion of DFO probably causes only a temporary

moderate functional recovery. Since the processes of the secondary injury phase take place over several weeks (Tator, 1995; Bareyre and Schwab, 2003), a 2-week DFO infusion is probably too short to induce a long-lasting attenuation of secondary damage by its antioxidative and angiogenic effect. Consequently, a DFO-infusion for more than 2 weeks would lead to long-lasting functional improvements. This is supported by the findings of Rathore et al. (2008). They described that after spinal cord injury macrophages store large quantities of iron incorporated by phagocytosis of red blood cells and tissue debris (e.g. iron-rich myelin). Due to ongoing pathophysiological processes including cell membrane damage by lipid peroxidation, reactive iron is released from these macrophages between 3 and 6 weeks after injury, thus assisting secondary damage by free radical formation. By treating spinal cord contused mice systemically with the iron chelator salicylaldehyde isonicotinoyl hydrazone (SIH) for 42 days, they demonstrated that with the onset of iron release from macrophages (after 21 days) the iron chelator treatment induced persistent locomotor recovery, which was assessed with the Basso Mouse Scale (BMS). Based on these findings, a well-founded evaluation of DFO's potential on functional recovery is only possible if infusion periods of at least 6 weeks are investigated. As DFO-treated animals did not show any significant improvements in the CatWalk or the BBB open field test compared to the PBS control group [only a non-significant trend in the regularity index was detectable (see Fig. 3.10A)], a 2-week DFO infusion is probably not sufficient to promote long-term functional recovery in general. Further testings on different infusion periods and varying concentrations should clarify this issue.

4.4.2 Synergistic effect of DFO+SDF-1 α enables long-term regeneration of precise limb control (horizontal ladder)

Simultaneous treatment with SDF-1 α , however, seems to have a synergistic effect on locomotor recovery. Similar to DFO the administration of SDF-1 α alone also causes only minor improvements in locomotor functions (see Fig. 3.9C,D). Therefore, it can be excluded that the effect observed for the double treatment DFO+SDF-1 α is based solely on SDF-1 α . DFO+SDF-1 α -treated animals made significantly less missteps with both hindlimbs on the horizontal ladder than PBS control animals (see table 3.1 and 3.2, Fig. 3.9A,B). Moreover, the evaluation of the CatWalk parameters regularity index (Fig. 3.10A), stride length and swing duration (Fig. 3.11) revealed that the DFO+SDF-1 α group recovered always better than the PBS control group and usually better than DFO, but they never reached significance level. Only the frequency of the regular step pattern Ab, which is predominantly used by uninjured animals, seems clearly to recover towards pre-injury level (Fig. 3.10F), indicating renormalisation of the lesion-induced shift in the frequency distribution of normal step

sequence patterns. DFO+SDF-1 α -treated animals used in 80 % of cases the step pattern Ab, whereas the Ab frequency of PBS-, SDF-1 α - or DFO-treated animals remained steadily at decreased level (~ 60 %).

The behavioural findings are demonstrating that only the combined treatment with DFO and SDF-1 α enables long-term improvement of precise limb control, which is necessary to walk on the grid of the horizontal ladder, but they fail to improve CatWalk gait parameters significantly. Although there are indications that the CatWalk gait parameters are positively influenced by DFO+SDF-1 α , it seems that the synergistic effect of DFO+SDF-1 α is not sufficient to trigger functional regeneration in general. Perhaps an overall long-term recovery could be achieved by varying the concentrations of both components or the duration of their treatment.

4.4.3 A 2-week intrathecal infusion of SDF-1 α induces moderate unilateral improvements in precise limb control

Interestingly, in almost every time point SDF-1 α -treated animals showed significantly less missteps with the right hindlimb than PBS animals, whereas the left hindlimb was at no time point significantly different to PBS (see table 3.1 and 3.2, Fig. 3.9C,D). Due to the Scouten wire knife (SWK)-induced lesion asymmetry, the right spinal cord side is less affected than the left side, indicating that SDF-1 α could stimulate the spared fibres via adaptive reorganization to compensate the lost neural pathways. In contrast to the left RST, the right RST is probably only partially damaged in this lesion model. Since it is assumed that an intact RST may compensate for the loss of the CST (Kennedy, 1990), it is quite possible that SDF-1 α could promote the compensatory ability of spared RST fibres by lateral axonal sprouting. However, this unilateral promotion of motor performance by SDF-1 α could not be observed in any other behaviour analysis. In the CatWalk analysis, it seems that SDF-1 α is rather detrimental than supportive to functional regeneration (see Fig. 3.11). Statistically, the difference between the SDF-1 α and the PBS group was not significant, but SDF-1 α -treated animals mostly performed worse on the CatWalk than PBS-treated animals. Zendedel et al. (2012) observed in spinal cord contused rats that a high concentration of SDF-1 α (1000 ng/ml) induced less distinct functional improvements in the BBB open field test than an intermediate dose (500 ng/ml). Since the SDF-1 α high dose was also associated with a significantly more intense astrocytosis compared to the SDF-1 α intermediate dose, the authors hypothesized that high SDF-1 α concentrations may impair functional recovery by enhancing anti-regenerative effects of astrocytes. Another explanation, which was mentioned by them, might be the desensitization of the CXCR4 receptor. Compared to the study by Zendedel et al. (2012), which is so far the only one investigating functional recovery after

SDF-1 α infusion in spinal cord injured rats, an 80 times higher SDF-1 α concentration was used in the present work. Hence, the missing improvement in locomotor performance observed in the CatWalk analysis could be the result of an excessive SDF-1 α concentration. However, the question why SDF-1 α has a promoting effect on functional recovery in the horizontal ladder task but seems to act detrimental in the CatWalk analysis remains open. Further investigations are necessary to evaluate the overall potential of SDF-1 α on functional recovery and the mechanisms behind it.

4.4.4 BSA treatment promotes long-lasting functional recovery

The most surprising finding of this study was, however, that an intrathecal infusion of BSA induced significant functional recovery in both the horizontal ladder walking test (see table 3.1 and 3.2, Fig. 3.9A,B) and the CatWalk gait analysis (see Fig. 3.10 and Fig. 3.11) compared to the PBS group. Due to its function as a carrier protein for SDF-1 α , BSA was included in this study as an individual group. Although both groups received exactly the same amount of BSA, SDF-1 α -treated animals performed generally worse than BSA-treated animals, and many times they differed even significantly. The SDF-1 α concentration used in this work seems to counteract the effect of BSA, thus supporting the hypothesis by Zendedel et al. (2012) that excessive concentrations of SDF-1 α are rather impairing than promoting functional recovery. On the other hand, it raises the question of whether the observed functional improvement by Zendedel et al. (2012) is partially based on a BSA effect. As a pure PBS control is missing in their study and, additionally, an underdosed concentration of BSA (1 % BSA in PBS) is used as vehicle control, it cannot be ruled out that some of their observed functional recovery is based on BSA. Lyophilized SDF-1 α contains 50 μ g BSA per 1 μ g SDF-1 α , which must be considered in the calculation of the vehicle control in addition to the reconstitution solution of SDF-1 α (1 % BSA in PBS), unless carrier-free SDF-1 α is used. This, however, was not stated by Zendedel et al. (2012) and due to their infusion period of 28 days and the short half-life of SDF-1 α [less than half an hour in the blood (Misra et al., 2008)], it is very unlikely that they have used carrier-free SDF-1 α . Therefore, the use of the reconstitution solution alone is not sufficient as control. Consequently, the functional improvement of SDF-1 α -treated animals may have been positively influenced by their higher BSA content as indicated by the results of the present thesis. Treating spinal cord injured rats with BSA induced a long-lasting functional benefit in general. The only behavioural test that did not show any significant improvement in locomotor performance was the BBB open field test (Fig. 3.12). However, a tendency towards higher BBB values is visible at least for the right hindlimb. Due to the higher incidence of autotomy in BSA-treated animals (BSA: 40 % vs. PBS: 11 %), only 6 animals are left in the BSA group, thus leading to a higher

statistical spreading. Therefore, a clear statement about the efficacy of BSA to promote regeneration of overground locomotion in the open field is nearly impossible and requires replication of the experiment with a higher number of animals. One aspect of the BBB evaluation, however, was striking: the interlimb coordination of BSA-treated animals recovered faster and better than in all other groups (Fig. 3.12A,B).

In addition to the long-lasting functional improvement, it was eye-catching that from the very first moment of post-injury testing (wpl 2) BSA-treated animals performed better in the behavioural tasks than the other groups, suggesting that BSA could be neuroprotective. For quite some time, albumin is attributed with neuroprotective properties, mainly based on research focussing on stroke and brain traumas (Belayev et al., 1997; Belayev et al., 1999a; Belayev et al., 1999b; Belayev et al., 2001; Liu et al., 2001). These pre-clinical studies were so promising that albumin was tested in clinical trials for acute stroke (ALIAS – Albumin in Acute Stroke). After a successful phase II pilot trial (Ginsberg et al., 2006; Palesch et al., 2006), the subsequent phase III trial was, however, stopped after 3.5 years because of futility (Ginsberg et al., 2013). Inexplicably, patients enrolled during the first half of the trial showed signs of albumin's therapeutic efficacy, but by the end of the study the beneficial improvement compared to the placebo control group had disappeared because the placebo group had later improved to the same level as the albumin group. In contrast, very little is known about the therapeutic effect of albumin in spinal cord injury. A beneficial neuroprotective effect of albumin in a spinal cord injury animal model was first described by Cain et al. (2007). They observed that, regardless of whether bovine serum albumin, rat albumin or human recombinant albumin was used, cultured spinal cord cells were protected against the toxicity of glutamate. The administration of albumin intravenously or directly into the epicentre of spinal cord contused rats induced significant improvements in BBB scores and increased the distance travelled in the Photobeam Activity System (PAS). Locomotor improvements were already apparent after 7 days post-lesion confirming that albumin is able to promote early recovery of locomotor functions as observed in this work. Multiple mechanisms are thought to be responsible for albumin's neuroprotective properties (Belayev et al., 2001; Cain et al., 2007; Prajapati et al., 2011): In addition to its hemodynamic function, albumin is an excellent carrier of many substances including fatty acids, hormones, enzymes, metals, anions, cations, drugs and metabolites (Emerson, 1989). Substances which are toxic in the unbound state are harmless when bound to albumin. Albumin also has antioxidant properties due to its ability to bind copper ion and thereby inhibiting copper ion-dependent lipid peroxidation and formation of the highly reactive hydroxyl radical species (Halliwell, 1988). Furthermore, albumin has been shown to play an important role in astrocyte functions. It affects the energy metabolism of cultured astrocytes by activating the pyruvate dehydrogenase reaction (Taberner et al., 1999). Transcytosis of albumin in astrocytes

stimulates the synthesis and release of oleic acid which induces neuronal differentiation by promoting axonal growth, neuronal clustering and expression of GAP-43 (Taberner et al., 2001; Medina and Taberner, 2002; Taberner et al., 2002). It is believed that albumin sequesters oleic acid during the passage through the endoplasmic reticulum (ER) and is released as an albumin-oleic acid complex. Avila-Martin et al. (2011) demonstrated that this albumin-oleic acid complex intrathecally applied in spinal cord contused rats synergistically induces early (4-14 day) recovery of motor functions measured with the rotarod setup, whereas albumin alone promoted functional recovery specifically in the subacute phase (21-28 day). The results of Cain et al. (2007) and Avila-Martin et al. (2011) provide the first evidence for a therapeutic benefit of albumin in spinal cord injury. The present work is the first detailed analysis of functional recovery after albumin treatment over a long-term period of 16 weeks. A 2-week intrathecal infusion seems sufficient to induce long-lasting improvements in locomotor performance, probably due to albumin's prolonged circulating half-life (\approx 20 days) (Peters Jr, 1975).

4.5 Tissue preservation as a possible reason for functional recovery

The neurological deficits occurring after spinal cord injury are the consequence of not only the primary mechanical injury, but also a complex set of secondary pathophysiological processes. By attenuating or eliminating the effects of secondary injury processes, further destruction of neighbouring healthy spinal cord tissue can be avoided and results in increased spared tissue. An increase in spared fibres is found to be highly correlated with functional improvement (Schucht et al., 2002; Ballermann and Fouad, 2006). As described in the previous chapters, DFO and BSA possess antioxidant character and consequently the ability to attenuate secondary tissue damage. If functional recovery was induced by tissue- or rather neuroprotection, this should be indicated in the lesion size and extent of spared tissue. Therefore, the GFAP-negative lesion area and the area of spared tissue were measured in all functionally tested animals according to Iannotti et al. (2011) and Schira et al. (2012) with slight modifications as described in Materials and Methods. During the blinded quantification it was already striking that some spinal cords looked atrophied in the area of the lesion scar, indicating the absence of tissue protection as it would be expected in the PBS group. In order to substantiate this suspicion, the smallest spinal cord height was measured in parasagittal spinal cord sections containing the central canal. Since only spinal cord heights measured in the same section plane can be compared with each other due to the spinal cord shape, the evaluation was limited to one section from the area of the central canal. Indeed, the spinal cord height of PBS-treated animals was on average 0.2 mm thinner than in the other groups

(except SDF-1 α : ~ 0.1 mm). Although no significant differences could be found between the groups, probably due to the small number of analysed spinal cord sections and animals (1 section per animal, n = 8), this implies a reduction in the spinal cord height of approximately 8 % when an average spinal cord height of 2.5 mm is assumed. It would, therefore, be interesting to investigate how much the spinal cord volume is affected.

The analysis of tissue sparing revealed that both BSA and DFO show a tendency towards improved tissue preservation, but the degree is less effective than expected. Due to statistical correction for multiple comparisons, the significance between BSA vs. PBS and DFO vs. PBS was lost in the analysis of spared tissue (Fig. 3.13D). Solely BSA-treated animals had significantly smaller lesion areas than PBS-treated animals (Fig. 3.13C) leading to the assumption that tissue protection could, at least in part, explain the better functional outcome after BSA treatment. However, a neuroprotective effect of DFO cannot be entirely excluded. DFO-treated animals tended to have a smaller lesion size than PBS-treated animals, but due to the short half-life of DFO (Howland, 2006) and the finding of Rathore et al. (2008) that macrophages release large quantities of iron between 3 and 6 weeks after injury, it is very likely that a 2-week infusion is not sufficient for long-lasting tissue preservation. This is particularly supported by the results of the horizontal ladder walking test where functional improvements were observed only in the early phase of behavioural testing. Furthermore, it must be noted that the analysis of tissue preservation is based on three spinal cord sections per animal. A more precise evaluation would be an unbiased estimation of the lesion volume by a stereological analysis using the Cavalieri method (Gundersen and Jensen, 1987; Ditor et al., 2008) and should be addressed in future investigations.

SDF-1 α is also considered to be neuroprotective as it protects neurons from apoptotic cell death after spinal cord injury, which was correlated with their observed functional improvement (Zendedel et al., 2012). Tissue preservation should, therefore, be detectable in the SDF-treated animal group of this work. The evaluation of the lesion area and spared tissue, however, revealed no signs of tissue sparing (Fig. 3.13C,D). As already discussed in the previous chapter (see 4.4), the observed lack of tissue protection is probably a result of an excessive SDF-1 α concentration. Zendedel et al. (2012) observed that animals treated with high doses of SDF-1 α show a significantly more intense astrocytosis than animals treated with an intermediate dose. They speculated that the SDF-1 α -induced astrocytosis possibly promotes anti-regenerative effects compromising functional recovery. Significant higher numbers of neuronal cell bodies were still present in the spinal cords of SDF-1 α high dose treated animals compared to the controls, but a slight decrease was observable in comparison to the intermediate dose. Since an 80-fold higher SDF-1 α concentration is used in this work, it is quite conceivable that an intense astrocytosis outweighs the neuroprotective

effect of SDF-1 α and probably also of DFO+SDF-1 α . To verify this assumption, further investigations are necessary.

4.6 Observed functional recovery is associated with modest axon regeneration

The analysis of tissue preservation showed that the observed functional recovery cannot be based solely on neuroprotection. Especially, functional improvements induced by DFO+SDF-1 α appear to be based on other repair mechanisms than tissue preservation, as neither lesion size (see Fig. 3.13C) nor spared tissue (see Fig. 3.13D) have been found to be significantly influenced by DFO+SDF-1 α compared to the PBS group. Due to the ability of DFO (Nowicki et al., 2009), BSA via the synthesis of oleic acid (Tabernero et al., 2001; Tabernero et al., 2002) and SDF-1 α (Opatz et al., 2009) to stimulate axon growth, axonal regeneration could also be considered as a possible reason for functional recovery. To investigate whether axonal regeneration is involved in the observed functional recovery, three different fibre populations (CGRP, CTB-labelled sciatic afferents, CST) were analysed within and beyond the lesion area. It seems that DFO+SDF-1 α treatment supports regenerative growth of ascending sensory fibres. Significantly enhanced axon densities of sensory CGRP fibres have been found in the GFAP-negative fibrous scar area (see Fig. 3.14). Furthermore, sensory sciatic afferents, anterogradely traced with CTB, showed a clear trend towards enhanced ingrowth into the scar area as well as enhanced axon outgrowth into the rostral spinal cord under DFO+SDF-1 α treatment (see Fig. 3.15C,D). As DFO+SDF-1 α treatment improved predominantly skilled walking over the horizontal ladder, which requires sensory-motor coordination of the forelimbs and hindlimbs, the regenerated sensory fibres could be involved in the observed locomotor recovery. However, skilled walking depends also on the input of the CST, but enhanced CST axon profiles could neither be found in the lesion area nor in the distal white matter (see Fig. 3.16). In comparison to other fibre populations, such as sensory or serotonergic axons, the CST has the lowest inherent regenerative growth capacity (Schiwy et al., 2009; Jaerve et al., 2011), which is corroborated in this study by an extremely small number of CST fragments in and beyond the scar area in PBS control animals. Several pharmacological interventions, including the original AST (BPY-DCA plus 8-Br-cAMP) (Klapka et al., 2005; Schiwy et al., 2009), were able to enhance this low regenerative growth capacity to a limited extent. Only a small percentage (< 10 %) of the original CST has been reported to regenerate (Bradbury and McMahon, 2006). Hence, DFO+SDF-1 α treatment is incapable to promote regeneration of CST-axons through the lesion site. Even treatment with BSA, which led to long-lasting functional recovery in general, induced also no regenerative growth of CST-axons (see Fig. 3.16). Consequently, axon

regeneration of lesioned CST fibres can be excluded in both groups as a possible reason for the observed functional recovery.

However, spontaneous functional recovery of CST-controlled fine motor skills has been reported after complete dorsal CST lesions and without experimental interventions (Weidner et al., 2001; Bareyre et al., 2004). This spontaneous functional recovery was correlated with extensive reorganization of the CST pathway through collateral axon sprouting. Weidner and colleagues (2001) demonstrated that complete transection of the dorsal CST led to compensatory sprouting of the uninjured ventral CST. Subsequent lesioning of the ventral CST abolished the previously observed recovery of skilled forelimb use and confirmed the existence of inherent CST plasticity. Furthermore, Bareyre et al. (2004) showed that, after mid-thoracic (Th8) dorsal hemisection, lesioned hindlimb CST axons sprouted into the cervical gray matter where they innervated descending propriospinal neurons. As long propriospinal axons are ventrally running in the spinal cord, they are spared by a midthoracic dorsal hemisection and mediate an indirect connection to the lumbar spinal cord. They further showed that these long propriospinal axons increased their terminal arborisation onto lumbar motor neurons, leading to reconnection of the deafferented lower spinal cord, accompanied by spontaneous functional recovery. Apart from the capability of the CST to reorganize, anatomical plasticity has also been observed in other fibre tracts. For example, enhanced sprouting of spared ReST fibres caudal to the lesion has been reported by Ballermann and Fouad (2006) after a thoracic spinal lesion, and has been suggested to be involved in their observed functional recovery. Hence, an injured spinal cord has the capability to reorganize in different ways, which could be complemented by therapeutic interventions. The functional recovery observed in this study after BSA or DFO+SDF-1 α treatment could be based on such an anatomical reorganization. Particularly, SDF-1 α has already been reported to promote rostral sprouting of dorsal CST axons as well as 5-HT and TH-positive fibres (Opatz et al., 2009; Jaerve et al., 2011), thus supporting this hypothesis at least for DFO+SDF-1 α treatment. Since axonal sprouting has not been studied in this work, the involvement of anatomical reorganization in the observed functional recovery remains speculative. In future studies, a detailed analysis of intraspinal remodelling (collateral sprouting of lesioned axons, compensatory sprouting of spared axons) should be considered.

4.7 Concluding remarks and further considerations

Data presented in this thesis demonstrate that intrathecal infusion of DFO over 2 weeks significantly reduces Coll IV and promotes angiogenesis in the fibrous scar of spinal cord injured animals, but it is ineffective to promote long-lasting functional recovery. However, as moderate functional improvements were seen in the early phase of behavioural testing, it

seems that DFO has regenerative potential, and probably longer treatment periods are necessary to enable long-lasting recovery. Nevertheless, it seems unlikely that this would cause a higher degree of functional regeneration, making combinations with appropriate components necessary. Indeed, a synergistic effect was obtained through simultaneous application of SDF-1 α together with DFO, which was reflected in long-term regeneration of skilled walking over the horizontal ladder. The mechanism of this functional recovery, which was restricted to skilled walking, remains unclear, as histological analyses revealed limited axonal regeneration through the lesion site and no evidence of treatment-induced tissue preservation. Given the fact that SDF-1 α has the capability to stimulate axonal sprouting, anatomical reorganization could be a possible mechanism of the observed functional recovery and should be taken into consideration for future studies. Furthermore, for a final statement on treatment efficacy of DFO+SDF-1 α a detailed investigation of the best treatment condition (treatment duration, dosage) is necessary, as the present results indicate that the infusion time of DFO is probably too short and the dose of SDF-1 α too high. This will show whether DFO+SDF-1 α is able to promote long-lasting functional recovery in general and whether it can be regarded as an equivalent alternative to the clinically inapplicable AST (BPY-DCA plus 8-Br-cAMP).

Surprisingly, the present data also show that BSA, which was initially planned as the SDF-1 α control group, has a more potent effect on functional recovery of spinal cord injured animals than DFO and SDF-1 α together. In functional analyses such as horizontal ladder walking and CatWalk gait analysis, BSA treatment always resulted in the largest functional recovery from the very first post-injury testing session (wpl 2). Significantly smaller lesion areas and a tendency towards better tissue preservation suggest that tissue protection is one of the repair mechanisms induced by BSA. However, the degree of tissue protection appears too small to be solely responsible for the observed functional improvements. For verification, a more precise evaluation by estimating the lesion volume using stereological methods should be used in future investigations. In this context, it will also be of particular interest to examine the effect of BSA on spinal plasticity, as axonal regeneration through the lesion site seems unlikely according to the moderate results. However, the involvement of axonal regeneration in the observed locomotor improvements cannot be totally excluded as not all fibre populations, as e.g. the RST, has been investigated. Additionally, it would be interesting to investigate whether the effect of BSA on functional recovery can be synergistically boosted by combinatorial approaches. As the present results indicate that BSA can probably cause only moderate axonal regeneration, an interesting approach would be, e.g., the combination with cell transplants (OEG, neural precursor or stem cells) into the lesion area to replace the perished cells. Furthermore, investigations addressing neuropathic pain are required to examine whether BSA treatment enhances the development of neuropathic pain after spinal

cord injury, as indicated in this study by the increased incidence of autotomy. Autotomy reflects the presence of abnormal sensations and is particularly a phenomenon in transection injuries. To study the occurrence of neuropathic pain after BSA treatment, the spinal cord contusion model would therefore be better suited.

5 References

- Afshari, F. T., Kappagantula, S., and Fawcett, J. W. (2009). Extrinsic and intrinsic factors controlling axonal regeneration after spinal cord injury. *Expert Rev Mol Med* **11**, e37.
- Allain, P., Mauras, Y., Chaleil, D., Simon, P., Ang, K. S., Cam, G., Le Mignon, L., and Simon, M. (1987). Pharmacokinetics and renal elimination of desferrioxamine and ferrioxamine in healthy subjects and patients with haemochromatosis. *Br J Clin Pharmacol* **24**(2), 207-12.
- Almli, L. M., Hamrick, S. E., Koshy, A. A., Tauber, M. G., and Ferriero, D. M. (2001). Multiple pathways of neuroprotection against oxidative stress and excitotoxic injury in immature primary hippocampal neurons. *Brain Res Dev Brain Res* **132**(2), 121-9.
- Alstermark, B., Isa, T., Kummel, H., and Tantisira, B. (1990). Projection from excitatory C3-C4 propriospinal neurones to lamina VII and VIII neurones in the C6-Th1 segments of the cat. *Neurosci Res* **8**(2), 131-7.
- Alstermark, B., Kummel, H., Pinter, M. J., and Tantisira, B. (1987a). Branching and termination of C3-C4 propriospinal neurones in the cervical spinal cord of the cat. *Neurosci Lett* **74**(3), 291-6.
- Alstermark, B., Lundberg, A., Pinter, M., and Sasaki, S. (1987b). Long C3-C5 propriospinal neurones in the cat. *Brain Res* **404**(1-2), 382-8.
- Alstermark, B., Lundberg, A., Pinter, M., and Sasaki, S. (1987c). Subpopulations and functions of long C3-C5 propriospinal neurones. *Brain Res* **404**(1-2), 395-400.
- Alstermark, B., Ogawa, J., and Isa, T. (2004). Lack of monosynaptic corticomotoneuronal EPSPs in rats: disynaptic EPSPs mediated via reticulospinal neurons and polysynaptic EPSPs via segmental interneurons. *J Neurophysiol* **91**(4), 1832-9.
- Anderberg, L., Aldskogius, H., and Holtz, A. (2007). Spinal cord injury--scientific challenges for the unknown future. *Ups J Med Sci* **112**(3), 259-88.
- Anderson, K. D., Gunawan, A., and Steward, O. (2005). Quantitative assessment of forelimb motor function after cervical spinal cord injury in rats: relationship to the corticospinal tract. *Exp Neurol* **194**(1), 161-74.
- ANGUS Chemical Company Technology Review.
http://msdssearch.dow.com/PublishedLiteratureDOWCOM/dh_0035/0901b8038003559b.pdf?filepath=angus/pdfs/noreg/319-00072.pdf&fromPage=GetDoc
- Antal, M., Sholomenko, G. N., Moschovakis, A. K., Storm-Mathisen, J., Heizmann, C. W., and Hunziker, W. (1992). The termination pattern and postsynaptic targets of rubrospinal fibers in the rat spinal cord: a light and electron microscopic study. *J Comp Neurol* **325**(1), 22-37.
- Asikainen, T. M., Ahmad, A., Schneider, B. K., Ho, W. B., Arend, M., Brenner, M., Gunzler, V., and White, C. W. (2005). Stimulation of HIF-1alpha, HIF-2alpha, and VEGF by prolyl 4-hydroxylase inhibition in human lung endothelial and epithelial cells. *Free Radic Biol Med* **38**(8), 1002-13.

- Avila-Martin, G., Galan-Arriero, I., Gomez-Soriano, J., and Taylor, J. (2011). Treatment of rat spinal cord injury with the neurotrophic factor albumin-oleic acid: translational application for paralysis, spasticity and pain. *PLoS One* **6**(10), e26107.
- Azzi, G., Jouis, V., Godeau, G., Groult, N., and Robert, A. M. (1989). Immunolocalisation of extracellular matrix macromolecules in the rat spinal cord. *Matrix* **9**(6), 479-85.
- Bains, M., and Hall, E. D. (2012). Antioxidant therapies in traumatic brain and spinal cord injury. *Biochim Biophys Acta* **1822**(5), 675-84.
- Balabanian, K., Lagane, B., Infantino, S., Chow, K. Y., Harriague, J., Moepps, B., Arenzana-Seisdedos, F., Thelen, M., and Bachelier, F. (2005). The chemokine SDF-1/CXCL12 binds to and signals through the orphan receptor RDC1 in T lymphocytes. *J Biol Chem* **280**(42), 35760-6.
- Balcerzak, S. P., Jensen, W. N., and Pollack, S. (1966). Mechanism of Action of Deferoxaminum on Iron Absorption. *Scandinavian Journal of Haematology* **3**(3), 205-212.
- Ballermann, M., and Fouad, K. (2006). Spontaneous locomotor recovery in spinal cord injured rats is accompanied by anatomical plasticity of reticulospinal fibers. *Eur J Neurosci* **23**(8), 1988-96.
- Bancroft, J. D., Stevens, A., and Turner, D. R. (1996). "Theory and practice of histological techniques." 4. ed ed. Churchill Livingstone, New York [u.a.].
- Bareyre, F. M., Kerschensteiner, M., Raineteau, O., Mettenleiter, T. C., Weinmann, O., and Schwab, M. E. (2004). The injured spinal cord spontaneously forms a new intraspinal circuit in adult rats. *Nat Neurosci* **7**(3), 269-77.
- Bareyre, F. M., and Schwab, M. E. (2003). Inflammation, degeneration and regeneration in the injured spinal cord: insights from DNA microarrays. *Trends Neurosci* **26**(10), 555-63.
- Barritt, A. W., Davies, M., Marchand, F., Hartley, R., Grist, J., Yip, P., McMahon, S. B., and Bradbury, E. J. (2006). Chondroitinase ABC promotes sprouting of intact and injured spinal systems after spinal cord injury. *J Neurosci* **26**(42), 10856-67.
- Basso, D. M., Beattie, M. S., and Bresnahan, J. C. (1995). A sensitive and reliable locomotor rating scale for open field testing in rats. *J Neurotrauma* **12**(1), 1-21.
- Beattie, M. S., Faroqui, A. A., and Bresnahan, J. C. (2000). Review of current evidence for apoptosis after spinal cord injury. *J Neurotrauma* **17**(10), 915-25.
- Becerra, J. L., Puckett, W. R., Hiester, E. D., Quencer, R. M., Marcillo, A. E., Post, M. J., and Bunge, R. P. (1995). MR-pathologic comparisons of wallerian degeneration in spinal cord injury. *AJNR Am J Neuroradiol* **16**(1), 125-33.
- Beerepoot, L. V., Shima, D. T., Kuroki, M., Yeo, K. T., and Voest, E. E. (1996). Up-regulation of vascular endothelial growth factor production by iron chelators. *Cancer Res* **56**(16), 3747-51.
- Belayev, L., Alonso, O. F., Huh, P. W., Zhao, W., Busto, R., and Ginsberg, M. D. (1999a). Posttreatment with high-dose albumin reduces histopathological damage and improves neurological deficit following fluid percussion brain injury in rats. *J Neurotrauma* **16**(6), 445-53.

- Belayev, L., Busto, R., Zhao, W., Clemens, J. A., and Ginsberg, M. D. (1997). Effect of delayed albumin hemodilution on infarction volume and brain edema after transient middle cerebral artery occlusion in rats. *J Neurosurg* **87**(4), 595-601.
- Belayev, L., Liu, Y., Zhao, W., Busto, R., and Ginsberg, M. D. (2001). Human albumin therapy of acute ischemic stroke: marked neuroprotective efficacy at moderate doses and with a broad therapeutic window. *Stroke* **32**(2), 553-60.
- Belayev, L., Saul, I., Huh, P. W., Finotti, N., Zhao, W., Busto, R., and Ginsberg, M. D. (1999b). Neuroprotective effect of high-dose albumin therapy against global ischemic brain injury in rats. *Brain Res* **845**(1), 107-11.
- Benson, M. D., Romero, M. I., Lush, M. E., Lu, Q. R., Henkemeyer, M., and Parada, L. F. (2005). Ephrin-B3 is a myelin-based inhibitor of neurite outgrowth. *Proc Natl Acad Sci U S A* **102**(30), 10694-9.
- Berry, M., Maxwell, W. L., Logan, A., Mathewson, A., McConnell, P., Ashhurst, D. E., and Thomas, G. H. (1983). Deposition of scar tissue in the central nervous system. *Acta Neurochir Suppl (Wien)* **32**, 31-53.
- Beyer, L., and Cornejo, J. A. (2012). Anwendung. In "Koordinationschemie", pp. 195-351. Vieweg+Teubner Verlag.
- Bomze, H. M., Bulsara, K. R., Iskandar, B. J., Caroni, P., and Skene, J. H. (2001). Spinal axon regeneration evoked by replacing two growth cone proteins in adult neurons. *Nat Neurosci* **4**(1), 38-43.
- Bosse, F. (2012). Extrinsic cellular and molecular mediators of peripheral axonal regeneration. *Cell Tissue Res* **349**(1), 5-14.
- Bradbury, E. J., and McMahon, S. B. (2006). Spinal cord repair strategies: why do they work? *Nat Rev Neurosci* **7**(8), 644-53.
- Bradbury, E. J., Moon, L. D., Popat, R. J., King, V. R., Bennett, G. S., Patel, P. N., Fawcett, J. W., and McMahon, S. B. (2002). Chondroitinase ABC promotes functional recovery after spinal cord injury. *Nature* **416**(6881), 636-40.
- Brazda, N., and Müller, H. W. (2009). Pharmacological modification of the extracellular matrix to promote regeneration of the injured brain and spinal cord. *Prog Brain Res* **175**, 269-81.
- Breier, G., and Risau, W. (1996). The role of vascular endothelial growth factor in blood vessel formation. *Trends Cell Biol* **6**(12), 454-6.
- Brösamle, C., and Schwab, M. E. (1997). Cells of origin, course, and termination patterns of the ventral, uncrossed component of the mature rat corticospinal tract. *J Comp Neurol* **386**(2), 293-303.
- Brown, L. T. (1974). Rubrospinal projections in the rat. *J Comp Neurol* **154**(2), 169-87.
- Brown, L. T., Jr. (1971). Projections and termination of the corticospinal tract in rodents. *Exp Brain Res* **13**(4), 432-50.
- Buchli, A. D., and Schwab, M. E. (2005). Inhibition of Nogo: a key strategy to increase regeneration, plasticity and functional recovery of the lesioned central nervous system. *Ann Med* **37**(8), 556-67.

- Bunge, M. B. (2001). Bridging areas of injury in the spinal cord. *Neuroscientist* **7**(4), 325-39.
- Büngner, O. v. (1891). Über die Degenerations- und Regenerationsvorgänge am Nerven nach Verletzungen. *Beitr. Pathol. Anat.* **10**, 321-387.
- Burchiel, K. J., and Hsu, F. P. (2001). Pain and spasticity after spinal cord injury: mechanisms and treatment. *Spine (Phila Pa 1976)* **26**(24 Suppl), S146-60.
- Busch, S. A., and Silver, J. (2007). The role of extracellular matrix in CNS regeneration. *Curr Opin Neurobiol* **17**(1), 120-7.
- Bush, T. G., Puvanachandra, N., Horner, C. H., Polito, A., Ostenfeld, T., Svendsen, C. N., Mucke, L., Johnson, M. H., and Sofroniew, M. V. (1999). Leukocyte infiltration, neuronal degeneration, and neurite outgrowth after ablation of scar-forming, reactive astrocytes in adult transgenic mice. *Neuron* **23**(2), 297-308.
- Buss, A., Brook, G. A., Kakulas, B., Martin, D., Franzen, R., Schoenen, J., Noth, J., and Schmitt, A. B. (2004). Gradual loss of myelin and formation of an astrocytic scar during Wallerian degeneration in the human spinal cord. *Brain* **127**(Pt 1), 34-44.
- Cai, D., Deng, K., Mellado, W., Lee, J., Ratan, R. R., and Filbin, M. T. (2002). Arginase I and polyamines act downstream from cyclic AMP in overcoming inhibition of axonal growth MAG and myelin in vitro. *Neuron* **35**(4), 711-9.
- Cain, L. D., Nie, L., Hughes, M. G., Johnson, K., Echetebe, C., Xu, G. Y., Hulsebosch, C. E., and McAdoo, D. J. (2007). Serum albumin improves recovery from spinal cord injury. *J Neurosci Res* **85**(7), 1558-67.
- Camand, E., Morel, M. P., Faissner, A., Sotelo, C., and Dusart, I. (2004). Long-term changes in the molecular composition of the glial scar and progressive increase of serotonergic fibre sprouting after hemisection of the mouse spinal cord. *Eur J Neurosci* **20**(5), 1161-76.
- Carbonell, A. L., and Boya, J. (1988). Ultrastructural study on meningeal regeneration and meningo-glial relationships after cerebral stab wound in the adult rat. *Brain Res* **439**(1-2), 337-44.
- Casella, G. T., Marcillo, A., Bunge, M. B., and Wood, P. M. (2002). New vascular tissue rapidly replaces neural parenchyma and vessels destroyed by a contusion injury to the rat spinal cord. *Exp Neurol* **173**(1), 63-76.
- Cazalets, J. R., Borde, M., and Clarac, F. (1995). Localization and organization of the central pattern generator for hindlimb locomotion in newborn rat. *J Neurosci* **15**(7 Pt 1), 4943-51.
- Cazalets, J. R., Sqalli-Houssaini, Y., and Clarac, F. (1992). Activation of the central pattern generators for locomotion by serotonin and excitatory amino acids in neonatal rat. *J Physiol* **455**, 187-204.
- Chalasani, S. H., Sabelko, K. A., Sunshine, M. J., Littman, D. R., and Raper, J. A. (2003). A chemokine, SDF-1, reduces the effectiveness of multiple axonal repellents and is required for normal axon pathfinding. *J Neurosci* **23**(4), 1360-71.
- Chaston, T. B., and Richardson, D. R. (2003). Iron chelators for the treatment of iron overload disease: relationship between structure, redox activity, and toxicity. *Am J Hematol* **73**(3), 200-10.

- Chekanov, V. S., Nikolaychik, V., Maternowski, M. A., Mehran, R., Leon, M. B., Adamian, M., Moses, J., Dangas, G., Kipshidze, N., and Akhtar, M. (2003a). Deferoxamine enhances neovascularization and recovery of ischemic skeletal muscle in an experimental sheep model. *Ann Thorac Surg* **75**(1), 184-9.
- Chekanov, V. S., Zargarian, M., Baibekov, I., Karakozov, P., Tchekanov, G., Hare, J., Nikolaychik, V., Bajwa, T., and Akhtar, M. (2003b). Deferoxamine-fibrin accelerates angiogenesis in a rabbit model of peripheral ischemia. *Vasc Med* **8**(3), 157-62.
- Chen, M. S., Huber, A. B., van der Haar, M. E., Frank, M., Schnell, L., Spillmann, A. A., Christ, F., and Schwab, M. E. (2000). Nogo-A is a myelin-associated neurite outgrowth inhibitor and an antigen for monoclonal antibody IN-1. *Nature* **403**(6768), 434-9.
- Cheng, H., Almstrom, S., Gimenez-Llort, L., Chang, R., Ove Ogren, S., Hoffer, B., and Olson, L. (1997). Gait analysis of adult paraplegic rats after spinal cord repair. *Exp Neurol* **148**(2), 544-57.
- Choi, D. W. (1992). Excitotoxic cell death. *J Neurobiol* **23**(9), 1261-76.
- Condic, M. L., and Lemons, M. L. (2002). Extracellular matrix in spinal cord regeneration: getting beyond attraction and inhibition. *Neuroreport* **13**(3), A37-48.
- Coutts, M., and Keirstead, H. S. (2008). Stem cells for the treatment of spinal cord injury. *Exp Neurol* **209**(2), 368-77.
- Crowe, M. J., Bresnahan, J. C., Shuman, S. L., Masters, J. N., and Beattie, M. S. (1997). Apoptosis and delayed degeneration after spinal cord injury in rats and monkeys. *Nat Med* **3**(1), 73-6.
- David, S., and Aguayo, A. J. (1981). Axonal elongation into peripheral nervous system "bridges" after central nervous system injury in adult rats. *Science* **214**(4523), 931-3.
- Davies, S. J., Goucher, D. R., Doller, C., and Silver, J. (1999). Robust regeneration of adult sensory axons in degenerating white matter of the adult rat spinal cord. *J Neurosci* **19**(14), 5810-22.
- Deumens, R., Koopmans, G. C., and Joosten, E. A. (2005). Regeneration of descending axon tracts after spinal cord injury. *Prog Neurobiol* **77**(1-2), 57-89.
- Dexter, D. T., Statton, S. A., Whitmore, C., Freinbichler, W., Weinberger, P., Tipton, K. F., Della Corte, L., Ward, R. J., and Crichton, R. R. (2011). Clinically available iron chelators induce neuroprotection in the 6-OHDA model of Parkinson's disease after peripheral administration. *J Neural Transm* **118**(2), 223-31.
- Ditor, D. S., John, S., Cakiroglu, J., Kittmer, C., Foster, P. J., and Weaver, L. C. (2008). Magnetic resonance imaging versus histological assessment for estimation of lesion volume after experimental spinal cord injury. Laboratory investigation. *J Neurosurg Spine* **9**(3), 301-6.
- Donnelly, D. J., and Popovich, P. G. (2008). Inflammation and its role in neuroprotection, axonal regeneration and functional recovery after spinal cord injury. *Exp Neurol* **209**(2), 378-88.

- Dumont, R. J., Okonkwo, D. O., Verma, S., Hurlbert, R. J., Boulos, P. T., Ellegala, D. B., and Dumont, A. S. (2001). Acute spinal cord injury, part I: pathophysiologic mechanisms. *Clin Neuropharmacol* **24**(5), 254-64.
- Duncan, M. R., Frazier, K. S., Abramson, S., Williams, S., Klapper, H., Huang, X., and Grotendorst, G. R. (1999). Connective tissue growth factor mediates transforming growth factor beta-induced collagen synthesis: down-regulation by cAMP. *FASEB J* **13**(13), 1774-86.
- Dusart, I., and Sotelo, C. (1994). Lack of Purkinje cell loss in adult rat cerebellum following protracted axotomy: degenerative changes and regenerative attempts of the severed axons. *J Comp Neurol* **347**(2), 211-32.
- Eghianruwa, K. (2014). "Essential Drug Data for Rational Therapy in Veterinary Practice." AuthorHouse, Bloomington.
- Emerit, J., Beaumont, C., and Trivin, F. (2001). Iron metabolism, free radicals, and oxidative injury. *Biomed Pharmacother* **55**(6), 333-9.
- Emerson, T. E., Jr. (1989). Unique features of albumin: a brief review. *Crit Care Med* **17**(7), 690-4.
- Facchinetti, F., Dawson, V. L., and Dawson, T. M. (1998). Free radicals as mediators of neuronal injury. *Cell Mol Neurobiol* **18**(6), 667-82.
- Fassbender, J. M., Whittlemore, S. R., and Hagg, T. (2011). Targeting microvasculature for neuroprotection after SCI. *Neurotherapeutics* **8**(2), 240-51.
- Faulkner, J. R., Herrmann, J. E., Woo, M. J., Tansey, K. E., Doan, N. B., and Sofroniew, M. V. (2004). Reactive astrocytes protect tissue and preserve function after spinal cord injury. *J Neurosci* **24**(9), 2143-55.
- Fawcett, J. W. (1998). Spinal cord repair: from experimental models to human application. *Spinal Cord* **36**(12), 811-7.
- Fawcett, J. W., and Asher, R. A. (1999). The glial scar and central nervous system repair. *Brain Res Bull* **49**(6), 377-91.
- Fawcett, J. W., Schwab, M. E., Montani, L., Brazda, N., and Müller, H. W. (2012). Defeating inhibition of regeneration by scar and myelin components. *Handb Clin Neurol* **109**, 503-22.
- Fehlings, M. G., and Hawryluk, G. W. (2010). Scarring after spinal cord injury. *J Neurosurg Spine* **13**(2), 165-7; discussion 167-8.
- Fenrich, K., and Gordon, T. (2004). Canadian Association of Neuroscience review: axonal regeneration in the peripheral and central nervous systems--current issues and advances. *Can J Neurol Sci* **31**(2), 142-56.
- Feraboli-Lohnherr, D., Barthe, J. Y., and Orsal, D. (1999). Serotonin-induced activation of the network for locomotion in adult spinal rats. *J Neurosci Res* **55**(1), 87-98.
- Feringa, E. R., Kowalski, T. F., Vahlsing, H. L., and Frye, R. A. (1979). Enzyme treatment of spinal cord transected rats. *Ann Neurol* **5**(2), 203-6.

- Fisher, L. J. (1997). Neural precursor cells: applications for the study and repair of the central nervous system. *Neurobiol Dis* **4**(1), 1-22.
- Fitch, M. T., and Silver, J. (2008). CNS injury, glial scars, and inflammation: Inhibitory extracellular matrices and regeneration failure. *Exp Neurol* **209**(2), 294-301.
- Fouad, K., Dietz, V., and Schwab, M. E. (2001). Improving axonal growth and functional recovery after experimental spinal cord injury by neutralizing myelin associated inhibitors. *Brain Res Brain Res Rev* **36**(2-3), 204-12.
- Fouad, K., Ghosh, M., Vavrek, R., Tse, A. D., and Pearse, D. D. (2009). Dose and chemical modification considerations for continuous cyclic AMP analog delivery to the injured CNS. *J Neurotrauma* **26**(5), 733-40.
- Fouad, K., Schnell, L., Bunge, M. B., Schwab, M. E., Liebscher, T., and Pearse, D. D. (2005). Combining Schwann cell bridges and olfactory-ensheathing glia grafts with chondroitinase promotes locomotor recovery after complete transection of the spinal cord. *J Neurosci* **25**(5), 1169-78.
- Fouad, K., and Tse, A. (2008). Adaptive changes in the injured spinal cord and their role in promoting functional recovery. *Neurol Res* **30**(1), 17-27.
- Fournier, A. E., Takizawa, B. T., and Strittmatter, S. M. (2003). Rho kinase inhibition enhances axonal regeneration in the injured CNS. *J Neurosci* **23**(4), 1416-23.
- Freret, T., Valable, S., Chazalviel, L., Saulnier, R., Mackenzie, E. T., Petit, E., Bernaudin, M., Boulouard, M., and Schumann-Bard, P. (2006). Delayed administration of deferoxamine reduces brain damage and promotes functional recovery after transient focal cerebral ischemia in the rat. *Eur J Neurosci* **23**(7), 1757-65.
- Garcia-Alias, G., Lin, R., Akrimi, S. F., Story, D., Bradbury, E. J., and Fawcett, J. W. (2008). Therapeutic time window for the application of chondroitinase ABC after spinal cord injury. *Exp Neurol* **210**(2), 331-8.
- George, R., and Griffin, J. W. (1994). Delayed macrophage responses and myelin clearance during Wallerian degeneration in the central nervous system: the dorsal radiculotomy model. *Exp Neurol* **129**(2), 225-36.
- Ginsberg, M. D., Hill, M. D., Palesch, Y. Y., Ryckborst, K. J., and Tamariz, D. (2006). The ALIAS Pilot Trial: a dose-escalation and safety study of albumin therapy for acute ischemic stroke--I: Physiological responses and safety results. *Stroke* **37**(8), 2100-6.
- Ginsberg, M. D., Palesch, Y. Y., Hill, M. D., Martin, R. H., Moy, C. S., Barsan, W. G., Waldman, B. D., Tamariz, D., and Ryckborst, K. J. (2013). High-dose albumin treatment for acute ischaemic stroke (ALIAS) Part 2: a randomised, double-blind, phase 3, placebo-controlled trial. *Lancet Neurol* **12**(11), 1049-58.
- Giovanelli Barilari, M., and Kuypers, H. G. (1969). Propriospinal fibers interconnecting the spinal enlargements in the cat. *Brain Res* **14**(2), 321-30.
- Glaser, J., Gonzalez, R., Perreau, V. M., Cotman, C. W., and Keirstead, H. S. (2004). Neutralization of the chemokine CXCL10 enhances tissue sparing and angiogenesis following spinal cord injury. *J Neurosci Res* **77**(5), 701-8.

- Gleadle, J. M., Ebert, B. L., Firth, J. D., and Ratcliffe, P. J. (1995). Regulation of angiogenic growth factor expression by hypoxia, transition metals, and chelating agents. *Am J Physiol* **268**(6 Pt 1), C1362-8.
- GrandPre, T., Nakamura, F., Vartanian, T., and Strittmatter, S. M. (2000). Identification of the Nogo inhibitor of axon regeneration as a Reticulon protein. *Nature* **403**(6768), 439-44.
- Graumann, U., Ritz, M. F., Rivero, B. G., and Hausmann, O. (2010). CD133 expressing pericytes and relationship to SDF-1 and CXCR4 in spinal cord injury. *Curr Neurovasc Res* **7**(2), 144-54.
- Grillner, S., Deliagina, T., Ekeberg, O., el Manira, A., Hill, R. H., Lansner, A., Orlovsky, G. N., and Wallen, P. (1995). Neural networks that co-ordinate locomotion and body orientation in lamprey. *Trends Neurosci* **18**(6), 270-9.
- Grimpe, B., and Silver, J. (2002). The extracellular matrix in axon regeneration. *Prog Brain Res* **137**, 333-49.
- Gundersen, H. J., and Jensen, E. B. (1987). The efficiency of systematic sampling in stereology and its prediction. *J Microsc* **147**(Pt 3), 229-63.
- Gurtner, G. C., Werner, S., Barrandon, Y., and Longaker, M. T. (2008). Wound repair and regeneration. *Nature* **453**(7193), 314-21.
- Guth, L., Albuquerque, E. X., Deshpande, S. S., Barrett, C. P., Donati, E. J., and Warnick, J. E. (1980). Ineffectiveness of enzyme therapy on regeneration in the transected spinal cord of the rat. *J Neurosurg* **52**(1), 73-86.
- Gutteridge, J. M., Richmond, R., and Halliwell, B. (1979). Inhibition of the iron-catalysed formation of hydroxyl radicals from superoxide and of lipid peroxidation by desferrioxamine. *Biochem J* **184**(2), 469-72.
- Haines, D. E., Harkey, H. L., and al-Mefty, O. (1993). The "subdural" space: a new look at an outdated concept. *Neurosurgery* **32**(1), 111-20.
- Hales, N. J., and Beattie, J. F. (1993). Novel inhibitors of prolyl 4-hydroxylase. 5. The intriguing structure-activity relationships seen with 2,2'-bipyridine and its 5,5'-dicarboxylic acid derivatives. *J Med Chem* **36**(24), 3853-8.
- Hall, E. D. (1989). Free radicals and CNS injury. *Crit Care Clin* **5**(4), 793-805.
- Hall, E. D. (2011). Antioxidant therapies for acute spinal cord injury. *Neurotherapeutics* **8**(2), 152-67.
- Halliwell, B. (1988). Albumin--an important extracellular antioxidant? *Biochem Pharmacol* **37**(4), 569-71.
- Halliwell, B., and Gutteridge, J. M. C. (2008). "Free radicals in biology and medicine." 4. ed. Oxford Univ. Press, Oxford [u.a.].
- Hamers, F. P., Lankhorst, A. J., van Laar, T. J., Veldhuis, W. B., and Gispen, W. H. (2001). Automated quantitative gait analysis during overground locomotion in the rat: its application to spinal cord contusion and transection injuries. *J Neurotrauma* **18**(2), 187-201.

- Hermanns, S. (2001). "Stimulation axonaler Regeneration im durchtrennten Rückenmark der adulten Ratte." PhD thesis.
- Hermanns, S., Klapka, N., Gasis, M., and Müller, H. (2006). The Collagenous Wound Healing Scar in the Injured Central Nervous System Inhibits Axonal Regeneration. *In* "Brain Repair" (M. Bähr, Ed.), Vol. 557, pp. 177-190. Springer US.
- Hermanns, S., Klapka, N., and Müller, H. W. (2001a). The collagenous lesion scar--an obstacle for axonal regeneration in brain and spinal cord injury. *Restor Neurol Neurosci* **19**(1-2), 139-48.
- Hermanns, S., Reiprich, P., and Müller, H. W. (2001b). A reliable method to reduce collagen scar formation in the lesioned rat spinal cord. *J Neurosci Methods* **110**(1-2), 141-6.
- Hershko, C., Link, G., and Cabantchik, I. (1998). Pathophysiology of iron overload. *Ann N Y Acad Sci* **850**, 191-201.
- Hershko, C., Link, G., Tzahor, M., and Pinson, A. (1993). Potential clinical applications of iron chelating therapy. *In* "The Development of Iron Chelators for Clinical Use" (R. J. Bergeron, and G. M. Brittenham, Eds.), pp. 75-96. CRC Press.
- Hertzberg, B. P., Holt, J. B., Graff, R. D., Gilbert, S. R., and Dahners, L. E. (2012). An evaluation of carrier agents for desferoxamine, an up-regulator of vascular endothelial growth factor. *J Biomater Appl*.
- Hill, W. D., Hess, D. C., Martin-Studdard, A., Carothers, J. J., Zheng, J., Hale, D., Maeda, M., Fagan, S. C., Carroll, J. E., and Conway, S. J. (2004). SDF-1 (CXCL12) is upregulated in the ischemic penumbra following stroke: association with bone marrow cell homing to injury. *J Neuropathol Exp Neurol* **63**(1), 84-96.
- Houle, J. D., and Ziegler, M. K. (1994). Bridging a complete transection lesion of adult rat spinal cord with growth factor-treated nitrocellulose implants. *J Neural Transplant Plast* **5**(2), 115-24.
- Howland, M. A. (2006). ANTIDOTES IN DEPTH: Deferoxamine. 8th ed. *In* "Goldfrank's toxicologic emergencies", pp. 638-641. McGraw-Hill Medical Pub. Division, New York.
- Hoyes, K. P., and Porter, J. B. (1993). Subcellular distribution of desferrioxamine and hydroxypyridin-4-one chelators in K562 cells affects chelation of intracellular iron pools. *British Journal of Haematology* **85**(2), 393-400.
- Huebner, E. A., and Strittmatter, S. M. (2009). Axon regeneration in the peripheral and central nervous systems. *Results Probl Cell Differ* **48**, 339-51.
- Iannotti, C., Ping Zhang, Y., Shields, C. B., Han, Y., Burke, D. A., and Xu, X. M. (2004). A neuroprotective role of glial cell line-derived neurotrophic factor following moderate spinal cord contusion injury. *Exp Neurol* **189**(2), 317-32.
- Iannotti, C. A., Clark, M., Horn, K. P., van Rooijen, N., Silver, J., and Steinmetz, M. P. (2011). A combination immunomodulatory treatment promotes neuroprotection and locomotor recovery after contusion SCI. *Exp Neurol* **230**(1), 3-15.
- Ikeda, Y., Tajima, S., Yoshida, S., Yamano, N., Kihira, Y., Ishizawa, K., Aihara, K., Tomita, S., Tsuchiya, K., and Tamaki, T. (2011). Deferoxamine promotes angiogenesis via the activation of vascular endothelial cell function. *Atherosclerosis* **215**(2), 339-47.

- Jaakkola, P., Mole, D. R., Tian, Y.-M., Wilson, M. I., Gielbert, J., Gaskell, S. J., Kriegsheim, A. v., Hebestreit, H. F., Mukherji, M., Schofield, C. J., Maxwell, P. H., Pugh, C. W., and Ratcliffe, P. J. (2001). Targeting of HIF- α to the von Hippel-Lindau Ubiquitylation Complex by O₂-Regulated Prolyl Hydroxylation. *Science* **292**(5516), 468-472.
- Jaerve, A., Bosse, F., and Müller, H. W. (2012a). SDF-1/CXCL12: its role in spinal cord injury. *Int J Biochem Cell Biol* **44**(3), 452-6.
- Jaerve, A., Schira, J., and Müller, H. W. (2012b). Concise review: the potential of stromal cell-derived factor 1 and its receptors to promote stem cell functions in spinal cord repair. *Stem Cells Transl Med* **1**(10), 732-9.
- Jaerve, A., Schiwy, N., Schmitz, C., and Mueller, H. W. (2011). Differential effect of aging on axon sprouting and regenerative growth in spinal cord injury. *Exp Neurol* **231**(2), 284-94.
- Jaffe, E. A., Hoyer, L. W., and Nachman, R. L. (1973). Synthesis of antihemophilic factor antigen by cultured human endothelial cells. *J Clin Invest* **52**(11), 2757-64.
- Jankowska, E., Lundberg, A., Roberts, W. J., and Stuart, D. (1974). A long propriospinal system with direct effect on motoneurons and on interneurons in the cat lumbosacral cord. *Exp Brain Res* **21**(2), 169-94.
- Jeong, M. A., Plunet, W., Streijger, F., Lee, J. H., Plemel, J. R., Park, S., Lam, C. K., Liu, J., and Tetzlaff, W. (2011). Intermittent fasting improves functional recovery after rat thoracic contusion spinal cord injury. *J Neurotrauma* **28**(3), 479-92.
- Jia, Z., Zhu, H., Li, J., Wang, X., Misra, H., and Li, Y. (2012). Oxidative stress in spinal cord injury and antioxidant-based intervention. *Spinal Cord* **50**(4), 264-74.
- Jones, L. L., Oudega, M., Bunge, M. B., and Tuszynski, M. H. (2001). Neurotrophic factors, cellular bridges and gene therapy for spinal cord injury. *J Physiol* **533**(Pt 1), 83-9.
- Jones, L. L., and Tuszynski, M. H. (2001). Chronic intrathecal infusions after spinal cord injury cause scarring and compression. *Microsc Res Tech* **54**(5), 317-24.
- Jones, T. B., McDaniel, E. E., and Popovich, P. G. (2005). Inflammatory-mediated injury and repair in the traumatically injured spinal cord. *Curr Pharm Des* **11**(10), 1223-36.
- Joosten, E. A., Veldhuis, W. B., and Hamers, F. P. (2004). Collagen containing neonatal astrocytes stimulates regrowth of injured fibers and promotes modest locomotor recovery after spinal cord injury. *J Neurosci Res* **77**(1), 127-42.
- Jordan, L. M. (1998). Initiation of locomotion in mammals. *Ann N Y Acad Sci* **860**, 83-93.
- Kanagal, S. G., and Muir, G. D. (2008). The differential effects of cervical and thoracic dorsal funiculus lesions in rats. *Behav Brain Res* **187**(2), 379-86.
- Kanagal, S. G., and Muir, G. D. (2009). Task-dependent compensation after pyramidal tract and dorsolateral spinal lesions in rats. *Exp Neurol* **216**(1), 193-206.
- Kaneko, S., Iwanami, A., Nakamura, M., Kishino, A., Kikuchi, K., Shibata, S., Okano, H. J., Ikegami, T., Moriya, A., Konishi, O., Nakayama, C., Kumagai, K., Kimura, T., Sato, Y., Goshima, Y., Taniguchi, M., Ito, M., He, Z., Toyama, Y., and Okano, H. (2006). A selective Sema3A inhibitor enhances regenerative responses and functional recovery of the injured spinal cord. *Nat Med* **12**(12), 1380-9.

- Karuppagounder, S. S., and Ratan, R. R. (2012). Hypoxia-inducible factor prolyl hydroxylase inhibition: robust new target or another big bust for stroke therapeutics? *J Cereb Blood Flow Metab* **32**(7), 1347-61.
- Kawano, H., Kimura-Kuroda, J., Komuta, Y., Yoshioka, N., Li, H. P., Kawamura, K., Li, Y., and Raisman, G. (2012). Role of the lesion scar in the response to damage and repair of the central nervous system. *Cell Tissue Res* **349**(1), 169-80.
- Keberle, H. (1964). The biochemistry of desferrioxamine and its relation to iron metabolism *Ann N Y Acad Sci* **119**, 758-68.
- Kennedy, P. R. (1990). Corticospinal, rubrospinal and rubro-olivary projections: a unifying hypothesis. *Trends Neurosci* **13**(12), 474-9.
- Kicic, A., Chua, A. C., and Baker, E. (2001). Effect of iron chelators on proliferation and iron uptake in hepatoma cells. *Cancer* **92**(12), 3093-110.
- Kiehn, O. (2006). Locomotor circuits in the mammalian spinal cord. *Annu Rev Neurosci* **29**, 279-306.
- Kim, D., Schallert, T., Liu, Y., Browarak, T., Nayeri, N., Tessler, A., Fischer, and Murray, M. (2001). Transplantation of genetically modified fibroblasts expressing BDNF in adult rats with a subtotal hemisection improves specific motor and sensory functions. *Neurorehabil Neural Repair* **15**(2), 141-50.
- Kivirikko, K. I., Myllyla, R., and Pihlajaniemi, T. (1989). Protein hydroxylation: prolyl 4-hydroxylase, an enzyme with four cosubstrates and a multifunctional subunit. *FASEB J* **3**(5), 1609-17.
- Klapka, N., Hermanns, S., and Müller, H. W. (2002). Interactions between glia and extracellular matrix and their role for axonal growth. In "Glial interfaces in the nervous system." (H. Aldskogius, and J. Fraher, Eds.). IOS Press, Amsterdam.
- Klapka, N., Hermanns, S., Straten, G., Masanneck, C., Duis, S., Hamers, F. P., Müller, D., Zuschmitter, W., and Müller, H. W. (2005). Suppression of fibrous scarring in spinal cord injury of rat promotes long-distance regeneration of corticospinal tract axons, rescue of primary motoneurons in somatosensory cortex and significant functional recovery. *Eur J Neurosci* **22**(12), 3047-58.
- Klapka, N., and Müller, H. W. (2006). Collagen matrix in spinal cord injury. *J Neurotrauma* **23**(3-4), 422-35.
- Kojima, A., and Tator, C. H. (2002). Intrathecal administration of epidermal growth factor and fibroblast growth factor 2 promotes ependymal proliferation and functional recovery after spinal cord injury in adult rats. *J Neurotrauma* **19**(2), 223-38.
- Koopmans, G. C., Deumens, R., Honig, W. M., Hamers, F. P., Steinbusch, H. W., and Joosten, E. A. (2005). The assessment of locomotor function in spinal cord injured rats: the importance of objective analysis of coordination. *J Neurotrauma* **22**(2), 214-25.
- Küchler, M., Fouad, K., Weinmann, O., Schwab, M. E., and Raineteau, O. (2002). Red nucleus projections to distinct motor neuron pools in the rat spinal cord. *J Comp Neurol* **448**(4), 349-59.

- Kumar, K., Kelly, M., and Pirlot, T. (2001). Continuous intrathecal morphine treatment for chronic pain of nonmalignant etiology: long-term benefits and efficacy. *Surg Neurol* **55**(2), 79-86; discussion 86-8.
- Kunkel-Bagden, E., Dai, H. N., and Bregman, B. S. (1993). Methods to assess the development and recovery of locomotor function after spinal cord injury in rats. *Exp Neurol* **119**(2), 153-64.
- Kwon, B. K., Tetzlaff, W., Grauer, J. N., Beiner, J., and Vaccaro, A. R. (2004). Pathophysiology and pharmacologic treatment of acute spinal cord injury. *Spine J* **4**(4), 451-64.
- Lankhorst, A. J., Verzijl, M. R., and Hamers, F. P. T. (1999). Experimental spinal cord contusion injury: Comparison of different outcome parameters. *Neuroscience Research Communications* **24**(3), 135-148.
- Leal-Filho, M. B. (2011). Spinal cord injury: From inflammation to glial scar. *Surg Neurol Int* **2**, 112.
- Lee, D. W., Andersen, J. K., and Kaur, D. (2006). Iron dysregulation and neurodegeneration: the molecular connection. *Mol Interv* **6**(2), 89-97.
- Lee, J. Y., Keep, R. F., He, Y., Sagher, O., Hua, Y., and Xi, G. (2010). Hemoglobin and iron handling in brain after subarachnoid hemorrhage and the effect of deferoxamine on early brain injury. *J Cereb Blood Flow Metab* **30**(11), 1793-803.
- Lemon, R. N. (2008). Descending pathways in motor control. *Annu Rev Neurosci* **31**, 195-218.
- Leung, D. W., Cachianes, G., Kuang, W. J., Goeddel, D. V., and Ferrara, N. (1989). Vascular endothelial growth factor is a secreted angiogenic mitogen. *Science* **246**(4935), 1306-9.
- Lewén, A., Matz, P., and Chan, P. H. (2000). Free radical pathways in CNS injury. *J Neurotrauma* **17**(10), 871-90.
- Li, J., and Lepski, G. (2013). Cell transplantation for spinal cord injury: a systematic review. *Biomed Res Int* **2013**, 786475.
- Li, M., and Ransohoff, R. M. (2008). Multiple roles of chemokine CXCL12 in the central nervous system: a migration from immunology to neurobiology. *Prog Neurobiol* **84**(2), 116-31.
- Li, S., and Stys, P. K. (2000). Mechanisms of ionotropic glutamate receptor-mediated excitotoxicity in isolated spinal cord white matter. *J Neurosci* **20**(3), 1190-8.
- Li, Y., Field, P. M., and Raisman, G. (1997). Repair of adult rat corticospinal tract by transplants of olfactory ensheathing cells. *Science* **277**(5334), 2000-2.
- Li, Y., and Raisman, G. (1995). Sprouts from cut corticospinal axons persist in the presence of astrocytic scarring in long-term lesions of the adult rat spinal cord. *Exp Neurol* **134**(1), 102-11.
- Liesi, P., and Kauppila, T. (2002). Induction of type IV collagen and other basement-membrane-associated proteins after spinal cord injury of the adult rat may participate in formation of the glial scar. *Exp Neurol* **173**(1), 31-45.

- Linden, T., Katschinski, D. M., Eckhardt, K., Scheid, A., Pagel, H., and Wenger, R. H. (2003). The antimycotic ciclopirox olamine induces HIF-1 α stability, VEGF expression, and angiogenesis. *FASEB J* **17**(6), 761-3.
- Liu, D., Liu, J., Sun, D., Alcock, N. W., and Wen, J. (2003). Spinal cord injury increases iron levels: catalytic production of hydroxyl radicals. *Free Radic Biol Med* **34**(1), 64-71.
- Liu, J., Tang, T., and Yang, H. (2011). Protective effect of deferoxamine on experimental spinal cord injury in rat. *Injury* **42**(8), 742-5.
- Liu, Y., Belayev, L., Zhao, W., Busto, R., Belayev, A., and Ginsberg, M. D. (2001). Neuroprotective effect of treatment with human albumin in permanent focal cerebral ischemia: histopathology and cortical perfusion studies. *Eur J Pharmacol* **428**(2), 193-201.
- Lloyd, J. B., Cable, H., and Rice-Evans, C. (1991). Evidence that desferrioxamine cannot enter cells by passive diffusion. *Biochem Pharmacol* **41**(9), 1361-3.
- Long, D. A., Ghosh, K., Moore, A. N., Dixon, C. E., and Dash, P. K. (1996). Deferoxamine improves spatial memory performance following experimental brain injury in rats. *Brain Res* **717**(1-2), 109-17.
- Loy, D. N., Crawford, C. H., Darnall, J. B., Burke, D. A., Onifer, S. M., and Whittemore, S. R. (2002). Temporal progression of angiogenesis and basal lamina deposition after contusive spinal cord injury in the adult rat. *J Comp Neurol* **445**(4), 308-24.
- Lu, D., Goussev, A., Chen, J., Pannu, P., Li, Y., Mahmood, A., and Chopp, M. (2004). Atorvastatin reduces neurological deficit and increases synaptogenesis, angiogenesis, and neuronal survival in rats subjected to traumatic brain injury. *J Neurotrauma* **21**(1), 21-32.
- Lu, P., and Tuszynski, M. H. (2008). Growth factors and combinatorial therapies for CNS regeneration. *Exp Neurol* **209**(2), 313-20.
- MackKay-Lyons, M. (2002). Central Pattern Generation of Locomotion: A Review of the Evidence. *Physical Therapy* **82**(1), 69-83.
- Magnuson, D. S., Lovett, R., Coffee, C., Gray, R., Han, Y., Zhang, Y. P., and Burke, D. A. (2005). Functional consequences of lumbar spinal cord contusion injuries in the adult rat. *J Neurotrauma* **22**(5), 529-43.
- Maier, I. C., and Schwab, M. E. (2006). Sprouting, regeneration and circuit formation in the injured spinal cord: factors and activity. *Philos Trans R Soc Lond B Biol Sci* **361**(1473), 1611-34.
- Majczynski, H., and Slawinska, U. (2007). Locomotor recovery after thoracic spinal cord lesions in cats, rats and humans. *Acta Neurobiol Exp (Wars)* **67**(3), 235-57.
- Mann, C. M., and Kwon, B. K. (2007). An Update on the Pathophysiology of Acute Spinal Cord Injury. *Seminars in Spine Surgery* **19**(4), 272-279.
- Martin, J. (2012). "Neuroanatomy Text and Atlas, Fourth Edition." McGraw-Hill Education.

- Massey, J. M., Hubscher, C. H., Wagoner, M. R., Decker, J. A., Amps, J., Silver, J., and Onifer, S. M. (2006). Chondroitinase ABC digestion of the perineuronal net promotes functional collateral sprouting in the cuneate nucleus after cervical spinal cord injury. *J Neurosci* **26**(16), 4406-14.
- Mauter, A. E., Weinzierl, M. R., Donovan, F., and Noble, L. J. (2000). Vascular events after spinal cord injury: contribution to secondary pathogenesis. *Phys Ther* **80**(7), 673-87.
- McKerracher, L., David, S., Jackson, D. L., Kottis, V., Dunn, R. J., and Braun, P. E. (1994). Identification of myelin-associated glycoprotein as a major myelin-derived inhibitor of neurite growth. *Neuron* **13**(4), 805-811.
- McKerracher, L., and Higuchi, H. (2006). Targeting Rho to stimulate repair after spinal cord injury. *J Neurotrauma* **23**(3-4), 309-17.
- McTigue, D. M., Horner, P. J., Stokes, B. T., and Gage, F. H. (1998). Neurotrophin-3 and brain-derived neurotrophic factor induce oligodendrocyte proliferation and myelination of regenerating axons in the contused adult rat spinal cord. *J Neurosci* **18**(14), 5354-65.
- Medina, J. M., and Taberner, A. (2002). Astrocyte-synthesized oleic acid behaves as a neurotrophic factor for neurons. *J Physiol Paris* **96**(3-4), 265-71.
- Metz, G. A., Dietz, V., Schwab, M. E., and van de Meent, H. (1998). The effects of unilateral pyramidal tract section on hindlimb motor performance in the rat. *Behav Brain Res* **96**(1-2), 37-46.
- Metz, G. A., Merkler, D., Dietz, V., Schwab, M. E., and Fouad, K. (2000). Efficient testing of motor function in spinal cord injured rats. *Brain Res* **883**(2), 165-77.
- Metz, G. A., and Whishaw, I. Q. (2002). Cortical and subcortical lesions impair skilled walking in the ladder rung walking test: a new task to evaluate fore- and hindlimb stepping, placing, and co-ordination. *J Neurosci Methods* **115**(2), 169-79.
- Metz, G. A., and Whishaw, I. Q. (2009). The ladder rung walking task: a scoring system and its practical application. *J Vis Exp*(28).
- Miller, J. T., Bartley, J. H., Wimborne, H. J., Walker, A. L., Hess, D. C., Hill, W. D., and Carroll, J. E. (2005). The neuroblast and angioblast chemotactic factor SDF-1 (CXCL12) expression is briefly up regulated by reactive astrocytes in brain following neonatal hypoxic-ischemic injury. *BMC Neurosci* **6**, 63.
- Miller, S., and Burg, J. (1973). The Function of Long Propriospinal Pathways in the Co-Ordination of Quadrupedal Stepping in the Cat. In "Control of Posture and Locomotion" (R. B. Stein, K. G. Pearson, R. S. Smith, and J. B. Redford, Eds.), Vol. 7, pp. 561-577. Springer US.
- Misra, P., Lebeche, D., Ly, H., Schwarzkopf, M., Diaz, G., Hajjar, R. J., Schechter, A. D., and Frangioni, J. V. (2008). Quantitation of CXCR4 expression in myocardial infarction using 99mTc-labeled SDF-1alpha. *J Nucl Med* **49**(6), 963-9.
- Moos, T., and Morgan, E. H. (2004). The metabolism of neuronal iron and its pathogenic role in neurological disease: review. *Ann N Y Acad Sci* **1012**, 14-26.

- Moreau-Fauvarque, C., Kumanogoh, A., Camand, E., Jaillard, C., Barbin, G., Boquet, I., Love, C., Jones, E. Y., Kikutani, H., Lubetzki, C., Dusart, I., and Chedotal, A. (2003). The transmembrane semaphorin Sema4D/CD100, an inhibitor of axonal growth, is expressed on oligodendrocytes and upregulated after CNS lesion. *J Neurosci* **23**(27), 9229-39.
- Morgenstern, D. A., Asher, R. A., and Fawcett, J. W. (2002). Chondroitin sulphate proteoglycans in the CNS injury response. *Prog Brain Res* **137**, 313-32.
- Muir, G. D., and Webb, A. A. (2000). Mini-review: assessment of behavioural recovery following spinal cord injury in rats. *Eur J Neurosci* **12**(9), 3079-86.
- Muir, G. D., Webb, A. A., Kanagal, S., and Taylor, L. (2007). Dorsolateral cervical spinal injury differentially affects forelimb and hindlimb action in rats. *Eur J Neurosci* **25**(5), 1501-10.
- Muir, G. D., and Whishaw, I. Q. (1999). Complete locomotor recovery following corticospinal tract lesions: measurement of ground reaction forces during overground locomotion in rats. *Behav Brain Res* **103**(1), 45-53.
- Muir, G. D., and Whishaw, I. Q. (2000). Red nucleus lesions impair overground locomotion in rats: a kinetic analysis. *Eur J Neurosci* **12**(3), 1113-22.
- Mukhopadhyay, G., Doherty, P., Walsh, F. S., Crocker, P. R., and Filbin, M. T. (1994). A novel role for myelin-associated glycoprotein as an inhibitor of axonal regeneration. *Neuron* **13**(3), 757-67.
- Mumenthaler, M., Schliack, H., and Stöhr, M. (2003). "Läsionen peripherer Nerven und radikuläre Syndrome." Thieme Verlag.
- Nagasawa, T., Hirota, S., Tachibana, K., Takakura, N., Nishikawa, S., Kitamura, Y., Yoshida, N., Kikutani, H., and Kishimoto, T. (1996). Defects of B-cell lymphopoiesis and bone-marrow myelopoiesis in mice lacking the CXC chemokine PBSF/SDF-1. *Nature* **382**(6592), 635-8.
- Nakamura, T., Keep, R. F., Hua, Y., Schallert, T., Hoff, J. T., and Xi, G. (2004). Deferoxamine-induced attenuation of brain edema and neurological deficits in a rat model of intracerebral hemorrhage. *J Neurosurg* **100**(4), 672-8.
- Nathan, P. W., Smith, M. C., and Deacon, P. (1990). The corticospinal tracts in man. Course and location of fibres at different segmental levels. *Brain* **113** (Pt 2), 303-24.
- Nishino, A., Suzuki, M., Ohtani, H., Motohashi, O., Umezawa, K., Nagura, H., and Yoshimoto, T. (1993). Thrombin may contribute to the pathophysiology of central nervous system injury. *J Neurotrauma* **10**(2), 167-79.
- Novartis (2012). Desferal (deferoxamine mesylate) for injection prescribing information.
- Nowicki, M., Kosacka, J., Spanel-Borowski, K., and Borlak, J. (2009). Deferoxamine-induced neurite outgrowth and synapse formation in postnatal rat dorsal root ganglion (DRG) cell cultures. *Eur J Cell Biol* **88**(10), 551-62.
- Oberlin, E., Amara, A., Bachelier, F., Bessia, C., Virelizier, J. L., Arenzana-Seisdedos, F., Schwartz, O., Heard, J. M., Clark-Lewis, I., Legler, D. F., Loetscher, M., Baggiolini, M., and Moser, B. (1996). The CXC chemokine SDF-1 is the ligand for LESTR/fusin and prevents infection by T-cell-line-adapted HIV-1. *Nature* **382**(6594), 833-5.

- Obermair, F. J., Schroter, A., and Thallmair, M. (2008). Endogenous neural progenitor cells as therapeutic target after spinal cord injury. *Physiology (Bethesda)* **23**, 296-304.
- Olivieri, N. F., and Brittenham, G. M. (1997). Iron-chelating therapy and the treatment of thalassemia. *Blood* **89**(3), 739-61.
- Opatz, J., Kury, P., Schiwy, N., Jarve, A., Estrada, V., Brazda, N., Bosse, F., and Müller, H. W. (2009). SDF-1 stimulates neurite growth on inhibitory CNS myelin. *Mol Cell Neurosci* **40**(2), 293-300.
- Oudega, M. (2010). Spinal Cord Injury and Repair: Role of Blood Vessel Loss and Endogenous Angiogenesis. In "Advances in Wound Care: Volume 1", pp. 335-340. 0 vols. Mary Ann Liebert, Inc., publishers.
- Oudega, M. (2012). Molecular and cellular mechanisms underlying the role of blood vessels in spinal cord injury and repair. *Cell Tissue Res* **349**(1), 269-88.
- Palesch, Y. Y., Hill, M. D., Ryckborst, K. J., Tamariz, D., and Ginsberg, M. D. (2006). The ALIAS Pilot Trial: a dose-escalation and safety study of albumin therapy for acute ischemic stroke--II: neurologic outcome and efficacy analysis. *Stroke* **37**(8), 2107-14.
- Palmer, C., Roberts, R. L., and Bero, C. (1994). Deferoxamine posttreatment reduces ischemic brain injury in neonatal rats. *Stroke* **25**(5), 1039-45.
- Paterniti, I., Mazzon, E., Emanuela, E., Paola, R. D., Galuppo, M., Bramanti, P., and Cuzzocrea, S. (2010). Modulation of inflammatory response after spinal cord trauma with deferoxamine, an iron chelator. *Free Radic Res* **44**(6), 694-709.
- Paxinos, G., and Watson, C. (2005). "The rat brain in stereotaxic coordinates : [the new coronal set - 161 diagrams]." 5. ed. Elsevier Acad. Press, Amsterdam [u.a.].
- Pekny, M., and Nilsson, M. (2005). Astrocyte activation and reactive gliosis. *Glia* **50**(4), 427-34.
- Peters Jr, T. (1975). 3 - Serum Albumin. In "The Plasma Proteins (Second Edition)" (F. W. Putnam, Ed.), pp. 133-181. Academic Press.
- Petrat, F., de Groot, H., Sustmann, R., and Rauen, U. (2002). The chelatable iron pool in living cells: a methodically defined quantity. *Biol Chem* **383**(3-4), 489-502.
- Pihlajaniemi, T., Myllyla, R., and Kivirikko, K. I. (1991). Prolyl 4-hydroxylase and its role in collagen synthesis. *J Hepatol* **13 Suppl 3**, S2-7.
- Porter, J. B., and Huehns, E. R. (1989). The toxic effects of desferrioxamine. *Baillieres Clin Haematol* **2**(2), 459-74.
- Prajapati, K. D., Sharma, S. S., and Roy, N. (2011). Current perspectives on potential role of albumin in neuroprotection. *Rev Neurosci* **22**(3), 355-63.
- Prinjha, R., Moore, S. E., Vinson, M., Blake, S., Morrow, R., Christie, G., Michalovich, D., Simmons, D. L., and Walsh, F. S. (2000). Inhibitor of neurite outgrowth in humans. *Nature* **403**(6768), 383-4.
- Raineteau, O., Fouad, K., Bareyre, F. M., and Schwab, M. E. (2002). Reorganization of descending motor tracts in the rat spinal cord. *Eur J Neurosci* **16**(9), 1761-71.

- Raisman, G. (2004). Olfactory ensheathing cells and repair of brain and spinal cord injuries. *Cloning Stem Cells* **6**(4), 364-8.
- Raivich, G., Bohatschek, M., Da Costa, C., Iwata, O., Galiano, M., Hristova, M., Nateri, A. S., Makwana, M., Riera-Sans, L., Wolfer, D. P., Lipp, H. P., Aguzzi, A., Wagner, E. F., and Behrens, A. (2004). The AP-1 transcription factor c-Jun is required for efficient axonal regeneration. *Neuron* **43**(1), 57-67.
- Ramón y Cajal, S. (1928). "Degeneration and regeneration of the nervous system." Oxford University Press [u.a.], London.
- Rathore, K. I., Kerr, B. J., Redensek, A., Lopez-Vales, R., Jeong, S. Y., Ponka, P., and David, S. (2008). Ceruloplasmin protects injured spinal cord from iron-mediated oxidative damage. *J Neurosci* **28**(48), 12736-47.
- Redondo-Castro, E., Torres-Espin, A., Garcia-Alias, G., and Navarro, X. (2013). Quantitative assessment of locomotion and interlimb coordination in rats after different spinal cord injuries. *J Neurosci Methods* **213**(2), 165-178.
- Reed, W. R., Shum-Siu, A., Onifer, S. M., and Magnuson, D. S. (2006). Inter-enlargement pathways in the ventrolateral funiculus of the adult rat spinal cord. *Neuroscience* **142**(4), 1195-207.
- Reina, M. A., De Leon Casasola, O., Lopez, A., De Andres, J. A., Mora, M., and Fernandez, A. (2002). The origin of the spinal subdural space: ultrastructure findings. *Anesth Analg* **94**(4), 991-5, table of contents.
- Risling, M., Fried, K., Linda, H., Carlstedt, T., and Cullheim, S. (1993). Regrowth of motor axons following spinal cord lesions: distribution of laminin and collagen in the CNS scar tissue. *Brain Res Bull* **30**(3-4), 405-14.
- Rolls, A., Shechter, R., and Schwartz, M. (2009). The bright side of the glial scar in CNS repair. *Nat Rev Neurosci* **10**(3), 235-41.
- Rossi, F., Buffo, A., and Strata, P. (2001). Regulation of intrinsic regenerative properties and axonal plasticity in cerebellar Purkinje cells. *Restor Neurol Neurosci* **19**(1-2), 85-94.
- Rossignol, S., and Frigon, A. (2011). Recovery of locomotion after spinal cord injury: some facts and mechanisms. *Annu Rev Neurosci* **34**, 413-40.
- Rothman, R. J., Serroni, A., and Farber, J. L. (1992). Cellular pool of transient ferric iron, chelatable by deferoxamine and distinct from ferritin, that is involved in oxidative cell injury. *Mol Pharmacol* **42**(4), 703-10.
- Ryu, J. K., Davalos, D., and Akassoglou, K. (2009). Fibrinogen signal transduction in the nervous system. *J Thromb Haemost* **7 Suppl 1**, 151-4.
- Sakura, S., Hashimoto, K., Bollen, A. W., Ciriales, R., and Drasner, K. (1996). Intrathecal catheterization in the rat. Improved technique for morphologic analysis of drug-induced injury. *Anesthesiology* **85**(5), 1184-9.
- Samuni, Y., Coffin, D., DeLuca, A. M., DeGraff, W. G., Venson, D. J., Ambudkar, I., Chevion, M., and Mitchell, J. B. (1999). The Use of Zn-Desferrioxamine for Radioprotection in Mice, Tissue Culture, and Isolated DNA. *Cancer Research* **59**(2), 405-409.

- Sanchez-Martin, L., Estecha, A., Samaniego, R., Sanchez-Ramon, S., Vega, M. A., and Sanchez-Mateos, P. (2011). The chemokine CXCL12 regulates monocyte-macrophage differentiation and RUNX3 expression. *Blood* **117**(1), 88-97.
- Santos-Benito, F. F., and Ramon-Cueto, A. (2003). Olfactory ensheathing glia transplantation: a therapy to promote repair in the mammalian central nervous system. *Anat Rec B New Anat* **271**(1), 77-85.
- Saval, A., and Chiodo, A. E. (2010). Intrathecal baclofen for spasticity management: a comparative analysis of spasticity of spinal vs cortical origin. *J Spinal Cord Med* **33**(1), 16-21.
- Schachtrup, C., Ryu, J. K., Helmrick, M. J., Vagena, E., Galanakis, D. K., Degen, J. L., Margolis, R. U., and Akassoglou, K. (2010). Fibrinogen triggers astrocyte scar formation by promoting the availability of active TGF-beta after vascular damage. *J Neurosci* **30**(17), 5843-54.
- Schira, J., Gasis, M., Estrada, V., Hendricks, M., Schmitz, C., Trapp, T., Kruse, F., Kogler, G., Wernet, P., Hartung, H. P., and Müller, H. W. (2012). Significant clinical, neuropathological and behavioural recovery from acute spinal cord trauma by transplantation of a well-defined somatic stem cell from human umbilical cord blood. *Brain* **135**(Pt 2), 431-46.
- Schiwy, N., Brazda, N., and Müller, H. W. (2009). Enhanced regenerative axon growth of multiple fibre populations in traumatic spinal cord injury following scar-suppressing treatment. *Eur J Neurosci* **30**(8), 1544-53.
- Schrimsher, G. W., and Reier, P. J. (1993). Forelimb motor performance following dorsal column, dorsolateral funiculi, or ventrolateral funiculi lesions of the cervical spinal cord in the rat. *Exp Neurol* **120**(2), 264-76.
- Schucht, P., Raineteau, O., Schwab, M. E., and Fouad, K. (2002). Anatomical correlates of locomotor recovery following dorsal and ventral lesions of the rat spinal cord. *Exp Neurol* **176**(1), 143-53.
- Schwab, J. M., Beschorner, R., Nguyen, T. D., Meyermann, R., and Schluesener, H. J. (2001). Differential cellular accumulation of connective tissue growth factor defines a subset of reactive astrocytes, invading fibroblasts, and endothelial cells following central nervous system injury in rats and humans. *J Neurotrauma* **18**(4), 377-88.
- Schwab, J. M., Brechtel, K., Mueller, C. A., Failli, V., Kaps, H. P., Tuli, S. K., and Schluesener, H. J. (2006). Experimental strategies to promote spinal cord regeneration--an integrative perspective. *Prog Neurobiol* **78**(2), 91-116.
- Schwab, M. E., and Bartholdi, D. (1996). Degeneration and regeneration of axons in the lesioned spinal cord. *Physiol Rev* **76**(2), 319-70.
- Seiffers, R., Allchorne, A. J., and Woolf, C. J. (2006). The transcription factor ATF-3 promotes neurite outgrowth. *Mol Cell Neurosci* **32**(1-2), 143-54.
- Shearer, M. C., and Fawcett, J. W. (2001). The astrocyte/meningeal cell interface--a barrier to successful nerve regeneration? *Cell Tissue Res* **305**(2), 267-73.
- Shellswell, G. B., Restall, D. J., Duance, V. C., and Bailey, A. J. (1979). Identification and differential distribution of collagen types in the central and peripheral nervous systems. *FEBS Lett* **106**(2), 305-8.

- Sierro, F., Biben, C., Martinez-Munoz, L., Mellado, M., Ransohoff, R. M., Li, M., Woehl, B., Leung, H., Groom, J., Batten, M., Harvey, R. P., Martinez, A. C., Mackay, C. R., and Mackay, F. (2007). Disrupted cardiac development but normal hematopoiesis in mice deficient in the second CXCL12/SDF-1 receptor, CXCR7. *Proc Natl Acad Sci U S A* **104**(37), 14759-64.
- Silver, J., and Miller, J. H. (2004). Regeneration beyond the glial scar. *Nat Rev Neurosci* **5**(2), 146-56.
- Simonart, T., Degraef, C., Andrei, G., Mosselmans, R., Hermans, P., Van Vooren, J.-P., Noel, J.-C., Boelaert, J. R., Snoeck, R., and Heenen, M. (2000). Iron Chelators Inhibit the Growth and Induce the Apoptosis of Kaposi's Sarcoma Cells and of their Putative Endothelial Precursors **115**(5), 893-900.
- Sinis, N., Di Scipio, F., Schonle, P., Werdin, F., Kraus, A., Koopmanns, G., Masanneck, C., Hermanns, S., Danker, T., Guenther, E., Haerle, M., Schaller, H. E., Geuna, S., and Mueller, H. W. (2009). Local administration of DFO-loaded lipid particles improves recovery after end-to-end reconstruction of rat median nerve. *Restor Neurol Neurosci* **27**(6), 651-62.
- Soderblom, C., Luo, X., Blumenthal, E., Bray, E., Lyapichev, K., Ramos, J., Krishnan, V., Lai-Hsu, C., Park, K. K., Tsoufas, P., and Lee, J. K. (2013). Perivascular fibroblasts form the fibrotic scar after contusive spinal cord injury. *J Neurosci* **33**(34), 13882-7.
- Steward, O., Zheng, B., and Tessier-Lavigne, M. (2003). False resurrections: distinguishing regenerated from spared axons in the injured central nervous system. *J Comp Neurol* **459**(1), 1-8.
- Stichel, C. C., Hermanns, S., Luhmann, H. J., Lausberg, F., Niermann, H., D'Urso, D., Servos, G., Hartwig, H. G., and Müller, H. W. (1999a). Inhibition of collagen IV deposition promotes regeneration of injured CNS axons. *Eur J Neurosci* **11**(2), 632-46.
- Stichel, C. C., and Müller, H. W. (1994). Relationship between injury-induced astrogliosis, laminin expression and axonal sprouting in the adult rat brain. *J Neurocytol* **23**(10), 615-30.
- Stichel, C. C., and Müller, H. W. (1998a). The CNS lesion scar: new vistas on an old regeneration barrier. *Cell Tissue Res* **294**(1), 1-9.
- Stichel, C. C., and Müller, H. W. (1998b). Experimental strategies to promote axonal regeneration after traumatic central nervous system injury. *Prog Neurobiol* **56**(2), 119-48.
- Stichel, C. C., Niermann, H., D'Urso, D., Lausberg, F., Hermanns, S., and Müller, H. W. (1999b). Basal membrane-depleted scar in lesioned CNS: characteristics and relationships with regenerating axons. *Neuroscience* **93**(1), 321-33.
- Stoll, G., and Müller, H. W. (1999). Nerve injury, axonal degeneration and neural regeneration: basic insights. *Brain Pathol* **9**(2), 313-25.
- Taberner, A., Lavado, E. M., Granda, B., Velasco, A., and Medina, J. M. (2001). Neuronal differentiation is triggered by oleic acid synthesized and released by astrocytes. *J Neurochem* **79**(3), 606-16.

- Tabernerero, A., Medina, A., Sanchez-Abarca, L. I., Lavado, E., and Medina, J. M. (1999). The effect of albumin on astrocyte energy metabolism is not brought about through the control of cytosolic Ca²⁺ concentrations but by free-fatty acid sequestration. *Glia* **25**(1), 1-9.
- Tabernerero, A., Velasco, A., Granda, B., Lavado, E. M., and Medina, J. M. (2002). Transcytosis of albumin in astrocytes activates the sterol regulatory element-binding protein-1, which promotes the synthesis of the neurotrophic factor oleic acid. *J Biol Chem* **277**(6), 4240-6.
- Tator, C. H. (1995). Update on the pathophysiology and pathology of acute spinal cord injury. *Brain Pathol* **5**(4), 407-13.
- Tator, C. H., and Fehlings, M. G. (1991). Review of the secondary injury theory of acute spinal cord trauma with emphasis on vascular mechanisms. *J Neurosurg* **75**(1), 15-26.
- Thallmair, M., Metz, G. A., Z'Graggen, W. J., Raineteau, O., Kartje, G. L., and Schwab, M. E. (1998). Neurite growth inhibitors restrict plasticity and functional recovery following corticospinal tract lesions. *Nat Neurosci* **1**(2), 124-31.
- Timpl, R., and Brown, J. C. (1996). Supramolecular assembly of basement membranes. *Bioessays* **18**(2), 123-32.
- Tobin, G. R., Chvapil, M., and Gildenberg, P. L. (1979). Collagen biosynthesis in healing spinal cord wounds. *Surg Forum* **30**, 454-6.
- Tonge, D. A., Golding, J. P., Edbladh, M., Kroon, M., Ekstrom, P. E., and Edstrom, A. (1997). Effects of extracellular matrix components on axonal outgrowth from peripheral nerves of adult animals in vitro. *Exp Neurol* **146**(1), 81-90.
- Tysseling, V. M., Mithal, D., Sahni, V., Birch, D., Jung, H., Belmadani, A., Miller, R. J., and Kessler, J. A. (2011). SDF1 in the dorsal corticospinal tract promotes CXCR4+ cell migration after spinal cord injury. *J Neuroinflammation* **8**, 16.
- Van Meeteren, N. L., Eggers, R., Lankhorst, A. J., Gispen, W. H., and Hamers, F. P. (2003). Locomotor recovery after spinal cord contusion injury in rats is improved by spontaneous exercise. *J Neurotrauma* **20**(10), 1029-37.
- Vargas, M. E., and Barres, B. A. (2007). Why is Wallerian degeneration in the CNS so slow? *Annu Rev Neurosci* **30**, 153-79.
- Waller, A. (1850). Experiments on the Section of the Glossopharyngeal and Hypoglossal Nerves of the Frog, and Observations of the Alterations Produced Thereby in the Structure of Their Primitive Fibres. *Philosophical Transactions of the Royal Society of London* **140**(ArticleType: research-article / Full publication date: 1850 /), 423-429.
- Wang, K. C., Koprivica, V., Kim, J. A., Sivasankaran, R., Guo, Y., Neve, R. L., and He, Z. (2002). Oligodendrocyte-myelin glycoprotein is a Nogo receptor ligand that inhibits neurite outgrowth. *Nature* **417**(6892), 941-4.
- Wang, L., Zhang, Z., Wang, Y., Zhang, R., and Chopp, M. (2004). Treatment of stroke with erythropoietin enhances neurogenesis and angiogenesis and improves neurological function in rats. *Stroke* **35**(7), 1732-7.

- Watson, C. (2009). "The spinal cord : a Christopher and Dana Reeve Foundation text and atlas." Academic Press, London.
- Webb, A. A., and Muir, G. D. (2002). Compensatory locomotor adjustments of rats with cervical or thoracic spinal cord hemisections. *J Neurotrauma* **19**(2), 239-56.
- Webb, A. A., and Muir, G. D. (2003). Unilateral dorsal column and rubrospinal tract injuries affect overground locomotion in the unrestrained rat. *Eur J Neurosci* **18**(2), 412-22.
- Weidner, N., Ner, A., Salimi, N., and Tuszynski, M. H. (2001). Spontaneous corticospinal axonal plasticity and functional recovery after adult central nervous system injury. *Proc Natl Acad Sci U S A* **98**(6), 3513-8.
- Weinmann, O., Schnell, L., Ghosh, A., Montani, L., Wiessner, C., Wannier, T., Rouiller, E., Mir, A., and Schwab, M. E. (2006). Intrathecally infused antibodies against Nogo-A penetrate the CNS and downregulate the endogenous neurite growth inhibitor Nogo-A. *Mol Cell Neurosci* **32**(1-2), 161-73.
- Whishaw, I. Q., Gorny, B., and Sarna, J. (1998). Paw and limb use in skilled and spontaneous reaching after pyramidal tract, red nucleus and combined lesions in the rat: behavioral and anatomical dissociations. *Behav Brain Res* **93**(1-2), 167-83.
- Whishaw, I. Q., Pellis, S. M., Gorny, B., Kolb, B., and Tetzlaff, W. (1993). Proximal and distal impairments in rat forelimb use in reaching follow unilateral pyramidal tract lesions. *Behav Brain Res* **56**(1), 59-76.
- Whishaw, I. Q., Tomie, J. A., and Ladowsky, R. L. (1990). Red nucleus lesions do not affect limb preference or use, but exacerbate the effects of motor cortex lesions on grasping in the rat. *Behav Brain Res* **40**(2), 131-44.
- Widenfalk, J., Lipson, A., Jubran, M., Hofstetter, C., Ebendal, T., Cao, Y., and Olson, L. (2003). Vascular endothelial growth factor improves functional outcome and decreases secondary degeneration in experimental spinal cord contusion injury. *Neuroscience* **120**(4), 951-60.
- Xiong, Y., Lu, D., Qu, C., Goussev, A., Schallert, T., Mahmood, A., and Chopp, M. (2008). Effects of erythropoietin on reducing brain damage and improving functional outcome after traumatic brain injury in mice. *J Neurosurg* **109**(3), 510-21.
- Xiong, Y., Mahmood, A., and Chopp, M. (2010). Neurorestorative treatments for traumatic brain injury. *Discov Med* **10**(54), 434-42.
- Yang, H. W., and Lemon, R. N. (2003). An electron microscopic examination of the corticospinal projection to the cervical spinal cord in the rat: lack of evidence for cortico-motoneuronal synapses. *Exp Brain Res* **149**(4), 458-69.
- Yiu, G., and He, Z. (2006). Glial inhibition of CNS axon regeneration. *Nat Rev Neurosci* **7**(8), 617-27.
- Yu, J., Guo, Y., Sun, M., Li, B., Zhang, Y., and Li, C. (2009). Iron is a potential key mediator of glutamate excitotoxicity in spinal cord motor neurons. *Brain Res* **1257**, 102-7.
- Yurchenco, P. D., and Schittny, J. C. (1990). Molecular architecture of basement membranes. *FASEB J* **4**(6), 1577-90.

- Z'Graggen, W. J., Metz, G. A., Kartje, G. L., Thallmair, M., and Schwab, M. E. (1998). Functional recovery and enhanced corticofugal plasticity after unilateral pyramidal tract lesion and blockade of myelin-associated neurite growth inhibitors in adult rats. *J Neurosci* **18**(12), 4744-57.
- Zendedel, A., Nobakht, M., Bakhtiyari, M., Beyer, C., Kipp, M., Baazm, M., and Joghataie, M. T. (2012). Stromal cell-derived factor-1 alpha (SDF-1alpha) improves neural recovery after spinal cord contusion in rats. *Brain Res*.
- Zhang, S. X., Huang, F., Gates, M., White, J., and Holmberg, E. G. (2010). Extensive scarring induced by chronic intrathecal tubing augmented cord tissue damage and worsened functional recovery after rat spinal cord injury. *J Neurosci Methods* **191**(2), 201-7.
- Zhang, Z., and Guth, L. (1997). Experimental spinal cord injury: Wallerian degeneration in the dorsal column is followed by revascularization, glial proliferation, and nerve regeneration. *Exp Neurol* **147**(1), 159-71.
- Zou, Y. R., Kottmann, A. H., Kuroda, M., Taniuchi, I., and Littman, D. R. (1998). Function of the chemokine receptor CXCR4 in haematopoiesis and in cerebellar development. *Nature* **393**(6685), 595-9.
- Zuniga, R. E., Perera, S., and Abram, S. E. (2002). Intrathecal baclofen: a useful agent in the treatment of well-established complex regional pain syndrome. *Reg Anesth Pain Med* **27**(1), 90-3.

6 Abbreviations

5-HT	5-hydroxytryptamine (serotonin)
ATF-3	activating transcription factor-3
BBB	Basso, Beattie, Bresnahan locomotor score
BDA	biotinylated dextran amine
BDNF	brain-derived neurotrophic factor
BM	basement membrane
BMS	Basso Mouse Scale
BPY	2,2'-bipyridine
BPY-DCA	2,2'-bipyridine-5,5'-dicarboxylic acid
BSA	bovine serum albumin
8-Br-cAMP	8-bromoadenosine 3',5'-cyclic monophosphate
CGRP	calcitonin gene-related peptide
ChABC	chondroitinase ABC
CNS	central nervous system
Coll IV	collagen type IV
CPG	central pattern generator
CSPG	chondroitin sulphate proteoglycan
CST	corticospinal tract
CTB	Cholera toxin B subunit
CTGF	connective tissue growth factor
d	day
DAPI	4',6-Diamidino-2-phenylindole
DFO	deferoxamine mesylate
dk	donkey
DLF	dorsolateral funiculus
dpl	days post-lesion
DPX	xylool-containing mounting fluid
DRG	dorsal root ganglion
DS	donkey serum
DSHB	Developmental Studies Hybridoma Bank
ECM	extracellular matrix
ER	endoplasmic reticulum
EtOH	ethanol
FL	forelimb

G	gauge
g	gram
GAP-43	growth-associated protein-43
GFAP	glial fibrillary acid protein
gt	goat
h	hour
HIF	hypoxia inducible factor
HL	hindlimb
ID	inner diameter
IgG	immunglobuline gamma
i.p.	intraperitoneal
M	molar
MAG	myelin-associated glycoprotein
min	minute
ml	millilitre
ms	mouse
MW	molecular weight
NT-3	neurotrophin-3
OD	outer diameter
OEG	olfactory ensheathing glia
OMgp	oligodendrocyte-myelin glycoprotein
PB	phosphate buffer
PBS	phosphate-buffered saline
PE	polyethylene
PFA	paraformaldehyde
PNS	peripheral nervous system
PS	propriospinal
PU	polyurethane
RAGs	regeneration associated genes
rb	rabbit
RI	regularity index
ReST	reticulospinal tract
RST	rubrospinal tract
RT	room temperature
s.c.	subcutaneous
SCI	spinal cord injury
SDF-1 α	stromal cell-derived growth factor-1 alpha

SEM	standard error of the mean
SIH	salicylaldehyde isonicotinoyl hydrazone
SWK	Scouten wire knife
TGF- β	transforming growth factor- β
Th	thoracic level
TH	tyrosine hydroxylase
Tris	tris(hydroxymethyl)-aminomethane
VEGF	vascular endothelial growth factor
vWF	von Willebrand factor
wpl	weeks post-lesion

7 Danksagung

An dieser Stelle möchte ich mich bei allen herzlich bedanken, die zum Gelingen dieser Arbeit beigetragen haben.

Besonderer Dank gilt Herrn Prof. Dr. Hans Werner Müller für die Bereitstellung und Betreuung dieses für mich äußerst interessanten Themas, sowie für seine hervorragende und uneingeschränkte Unterstützung, die wesentlich zum Erfolg dieser Arbeit beigetragen hat.

Frau Prof. Dr. Christine Rose danke ich herzlich für die Bereitschaft, meine Doktorarbeit zu begutachten.

Ein großes Dankeschön geht auch an alle meine Kollegen im Labor für Molekulare Neurobiologie, ohne deren uneingeschränkten Unterstützung und den zahlreichen anregenden Diskussionen der erfolgreiche Abschluss meiner Doktorarbeit nicht möglich gewesen wäre. Insbesondere möchte ich mich herzlich bei Dr. Veronica Estrada für ihre unermüdliche Hilfsbereitschaft, ihren wertvollen Anregungen und Tipps, sowie für die freundschaftliche Zusammenarbeit bedanken. Dr. Nicole Brazda danke ich besonders für die ausführliche Einführung in die Thematik, wodurch sie mir eine solide Grundlage für meine Doktorarbeit gegeben hat. Christine Schmitz und Julia Domke danke ich für ihren Arbeitseinsatz und ihre Hilfe bei den Experimenten. Ohne sie wäre die Verhaltensstudie nicht realisierbar gewesen. Allen Kollegen danke ich für die tolle und hilfsbereite Arbeitsatmosphäre, die mir besonders in stressigen Zeiten half nicht meine Freude am wissenschaftlichen Arbeiten zu verlieren.

Bei Dr. Barbara Grimpe möchte ich mich herzlich bedanken für ihre uneingeschränkte Unterstützung, ihren wertvollen Anregungen, und für die Zeit, die sie sich immer wieder genommen hat um gemeinsam verschiedene Sachverhalte zu erörtern und zu diskutieren.

Dem Graduiertenkolleg GRK 1033 „Molecular Targets of the Aging Process and Strategies for the Prevention of Aging“ danke ich für die finanzielle Unterstützung und die Ermöglichung, meine Forschungsergebnisse auf diversen internationalen Konferenzen zu präsentieren. Den Institutionen iGRAD und Selma-Meyer-Mentoring der HHU Düsseldorf verdanke ich ein herausragendes Qualifizierungsprogramm.

Mein größter Dank gilt meiner Familie und meinen Freunden, die mir zu jeder Zeit Halt und Unterstützung gegeben haben.

Eidesstattliche Erklärung:

Ich versichere an Eides Statt, dass die Dissertation von mir selbständig und ohne unzulässige fremde Hilfe unter Beachtung der „Grundsätze zur Sicherung guter wissenschaftlicher Praxis an der Heinrich-Heine-Universität Düsseldorf“ erstellt worden ist. Diese Dissertation hat in gleicher oder ähnlicher Form noch keiner anderen Prüfungsbehörde vorgelegen. Ich habe bisher keine erfolglosen Promotionsversuche unternommen.

Düsseldorf, den 14. Juli 2014

Brigitte König